Topological Approaches to Chromatic Number and Box Complex Analysis of Partition Graphs

Behnaz Refahi

Thesis submitted in partial fulfillment of the requirements for the degree of
Master of Science [1]

Mathematics and Statistics
Faculty of Science
University of Ottawa

[1]The program is a joint program with Carleton University, administered by the Ottawa-Carleton Institute of Mathematics and Statistics

Author's declaration for electronic submission of a thesis

I hereby declare that I am the sole author of this thesis. This is a true copy of the thesis, including any required final revisions, as accepted by my examiners. I understand that my thesis may be made electronically available to the public.

Online submission in 2023

Abstract

Determining the chromatic number of the partition graph $\mathcal{P}(3^3)$ poses a considerable challenge. We can bound it to $4 \leq \chi(\mathcal{P}(3^3)) \leq 6$, with exhaustive search confirming $\chi(\mathcal{P}(3^3)) = 6$. A potential mathematical proof strategy for this equality involves identifying a $\mathbb{Z}_2$-invariant S^4 with non-trivial homology in the box complex of the partition graph $\mathcal{P}(3^3)$, namely $\mathrm{B}_{\mathrm{edge}}\big(\mathcal{P}(3^3)\big)$, and applying the Borsuk-Ulam theorem to compute its $\mathbb{Z}_2$-index. This provides a robust topological lower bound for the chromatic number of $\mathcal{P}(3^3)$, termed the Lovász bound. We have verified the absence of such an S^4 within certain sections of $\mathrm{B}_{\mathrm{edge}}\big(\mathcal{P}(3^3)\big)$. We also validated this approach through a case study on the Petersen graph.

This thesis offers a thorough examination of various topological lower bounds for a graph's chromatic number, complete with proofs and examples. We demonstrate instances where these lower bounds converge to a single value and others where they diverge significantly from a graph's actual chromatic number.

We also classify all vertex pairs, triples, and quadruples of $\mathcal{P}(3^3)$ into unique equivalence classes, facilitating the derivation of all maximal complete bipartite subgraphs. This classification informs the construction of all simplices of $\mathrm{B}_{\mathrm{edge}}\big(\mathcal{P}(3^3)\big)$. Following a detailed and technical exploration, we uncover both the maximal size of the pairwise intersections of its maximal simplices and their underlying structure.

Our study proposes an algorithm for building the box complex of the partition graph $\mathcal{P}(3^3)$ using our method of identifying maximal complete bipartite subgraphs. This reduces time complexity to $O(n^3)$, marking a substantial enhancement over brute-force techniques.

Lastly, we apply discrete Morse theory to construct a simplicial complex homotopy equivalent to the box complex of $\mathcal{P}(3^3)$, using two methods: elementary collapses and the determination of a discrete Morse function on the box complex. This process reduces the dimension of the box complex from 35 to 12, streamlining future calculations of the $\mathbb{Z}_2$-index and the Lovász bound.

Acknowledgement

"It is only with the heart that one can see rightly; what is essential is invisible to the eye."

— Antoine de Saint-Exupéry, The Little Prince

First and foremost, I would like to express my deepest gratitude to my supervisors, Maia Fraser and Mike Newman. Their expert guidance, critical insights, and invaluable counsel have been instrumental throughout the course of this research journey, profoundly shaping my thesis. I am also immensely grateful for their generous financial support, without which this project would not have been possible.

To my beloved Mom and Dad, though separated by physical distance, your emotional proximity has been a constant source of strength for me. Your unwavering faith in my abilities and unyielding support have made this academic journey less daunting, and for that, I am profoundly grateful.

To my sweet sister, Golara, your gentle nature has been a soothing balm, helping me to alleviate the stress that comes with academic pursuits. Your optimism and cheerfulness have been my refuge during challenging times, and I am immensely thankful for your presence in my life.

I would also like to extend my heartfelt thanks to my Women in Math comrades, Alex, Adèle, and Jane. Your company has enriched my academic journey, providing a unique lens through which I could view science, life, and people. Our insightful conversations and shared experiences have helped me grow as a researcher and as a person.

To my dear friend, Maiko, your constant presence in my life is a gift that I deeply cherish. I will always remember our insightful conversations, whether they were about life's intricacies or the enigma of mathematics. I am profoundly grateful for every shared moment and cherished memory.

My sincere gratitude goes to my friends Lord and Xiao, whose academic support during my toughest times was an absolute godsend. Your valuable guidance and

generous assistance have lightened my academic burdens and allowed me to persevere. I am truly thankful for your friendship and academic camaraderie.

Additionally, I want to pay tribute to a dearly missed friend, Alma, whose life was tragically cut short. We could have built a treasury of memories, uplifting each other through the highs and lows of life. The moments we shared were precious, and even though you are not here, I will hold onto your friendship forever.

I reserve my deepest gratitude for my beloved husband, Ehsan. Your unfaltering love, support, and understanding have been invaluable to me. Your remarkable ability to empathize with my emotions, coupled with your willingness to journey each step with me, has resonated profoundly within me. Your care and affection have been the backbone of my strength and perseverance, and for that, I am eternally grateful.

To conclude, I count myself immensely fortunate to have been surrounded by such supportive and loving individuals throughout this journey. The connections and bonds we have built are priceless, and I eagerly look forward to sharing more life moments and academic milestones with you all.

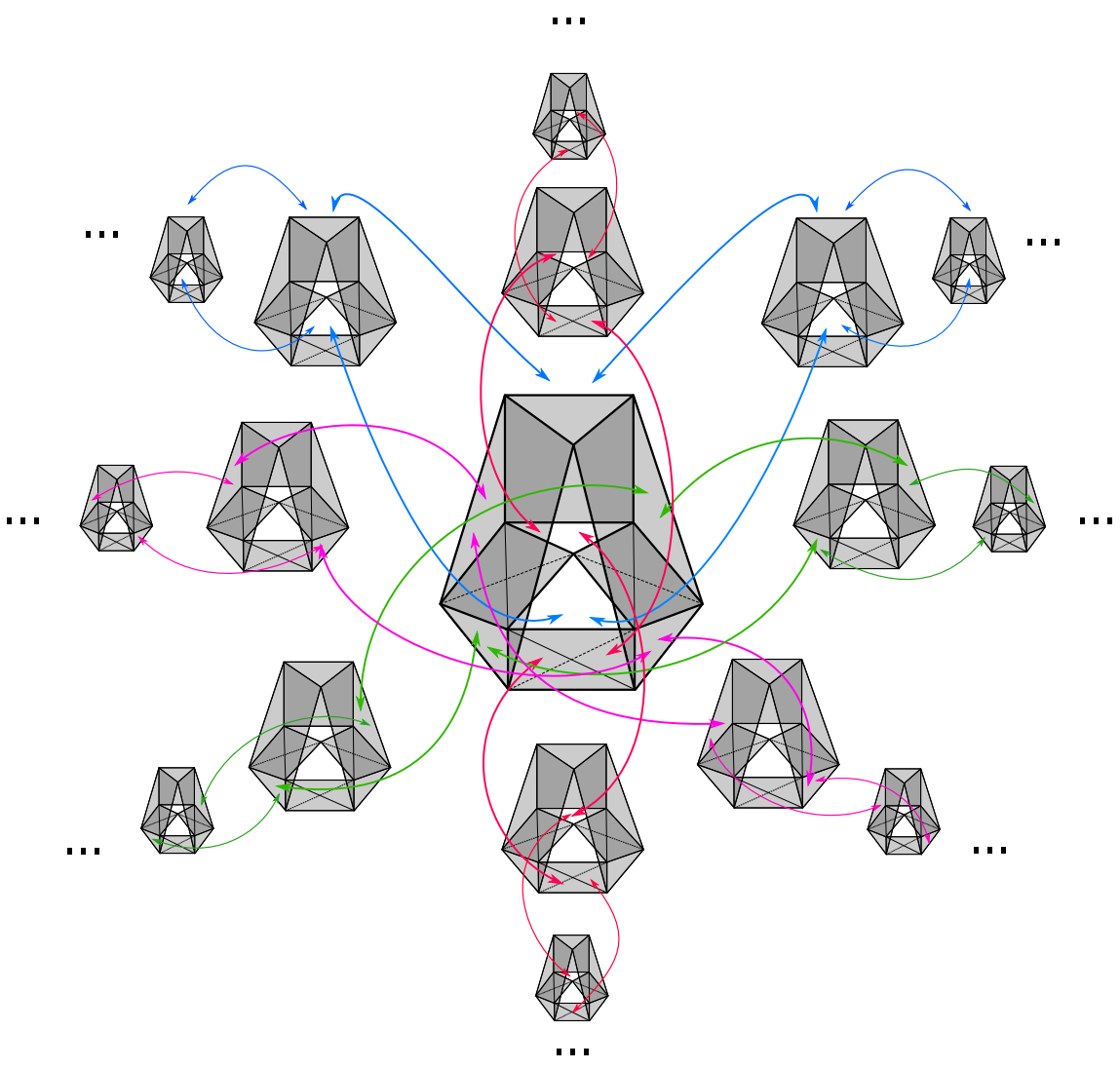

Contents

List of Figures

List of Tables

Introduction

"Imagination is more important than knowledge. For knowledge is limited, whereas imagination embraces the entire world, stimulating progress, giving birth to evolution. It is, strictly speaking, a real factor in scientific research."

— Albert Einstein

Graph theory, a central branch of discrete mathematics, is an indispensable tool to model and resolve complex problems from diverse fields such as engineering and computer science [17]. A pivotal concept within this discipline is the chromatic number of a graph. Defined as the minimum number of colours required to colour the vertices of the graph such that no two adjacent vertices share the same colour. It gives rise to intriguing theoretical questions, for example, the renowned Four Colour Theorem [18].

In addition to its theoretical relevance, the concept of the chromatic number has practical implications. These extend to addressing real-world problems like exam or task scheduling [19], frequency assignment in telecommunication systems [21], and register allocation in compiler optimization [22]. However, calculating the chromatic number of an arbitrary graph is an NP-complete problem [20]. This complexity underscores the need for efficient algorithms and heuristics. Therefore, our thesis embarks on a unique path of employing topological methods to resolve a chromatic number question in graph theory.

The synergistic interplay between topology and graph theory opens avenues for innovative problem-solving. Examples of this collaboration are 'Topological Graph Theory' and 'Network Topology' [23]. The former focuses on embedding graphs in surfaces and studies the properties of graphs invariant under topological transformations, like the Four Colour Theorem [18]. The latter, applied in computer science and network engineering, considers the layout of network elements (nodes and links), drawing from graph theory and topology.

In this thesis, we probe into the interaction between topology and graph theory in a unique context which is from the paper Topological Lower Bound for the Chromatic

Number: A Hierarchy by J. Matoušek, G. M.Ziegler in [3]. We build a simplicial complex from a given graph in a specific manner and study it to determine a lower bound for the chromatic number of the graph.

In his 1978 paper [2], Lovász utilized topological methods premised on the Borsuk-Ulam theorem to demonstrate that the chromatic number of the Kneser graph $\mathrm{KG}\binom{[n]}{k}$ is $n-2k+2$, denoted by

$$\chi(\mathrm{KG}\binom{[n]}{k}) = n-2k+2.$$

Several topological lower bounds for the chromatic number of a graph G have been proposed, including those by Sarkaria, Dol'nikov-Kříž, Bárány, and Lovász himself. In 2003, Matoušek and Ziegler introduced a hierarchical arrangement of these lower bounds, known as the Hierarchy theorem. In this thesis, we use this theorem to obtain a lower bound for $\chi(\mathrm{KG}\binom{[n]}{k})$, and a supplementary lemma to establish an upper bound that matches the lower bound, thus proving the above equation with a methodology distinct from that of Lovász. This also illustrates that there are instances where all the lower bounds in the hierarchy theorem can converge to a single value.

Additionally, we calculate the Lovász bound for odd cycles and bipartite graphs, illustrating scenarios where this lower bound matches the actual chromatic number of the graph. Furthermore, our study illustrates that these lower bounds can also significantly diverge from the actual chromatic number of a graph. This is demonstrated by calculating the Lovász bound for a graph devoid of a 4-cycle.

The Lovász bound is the strongest of the lower bounds in the hierarchy theorem, and involves the $\mathbb{Z}_2$-index of a particular type of simplicial complex called *box complex* of a graph G denoted by $\mathrm{B}_{\mathrm{edge}}(G)$. Simplices of $\mathrm{B}_{\mathrm{edge}}(G)$ are subsets of edge sets of complete bipartite subgraphs of G, where the edges are oriented from the left side to the right side. These complexes are essential in the theorem because the $\mathbb{Z}_2$-index can only be applied to $\mathbb{Z}_2$-spaces, and box complexes are suitable $\mathbb{Z}_2$-spaces.

In this thesis, we conduct a comprehensive study of the *partition graph* $\mathcal{P}(3^3)$, which is a special type of the general partition graph $\mathcal{P}(g^g)$ for $g=3$. Every vertex of a partition graph $\mathcal{P}(g^g)$ is a partition of $\{1,2,...,g^2\}$ into g cells of size g. Two vertices u and v are adjacent if the intersection of each cell of u with each cell of v is nonempty.

In the upcoming sections, we will explore 4-clique structures within $\mathcal{P}(3^3)$. Furthermore, Proposition 2.1.3 establishes an upper bound of 6 for the chromatic number of this graph. Consequently, we can constrain the chromatic number of $\mathcal{P}(3^3)$ to the range of 4 to 6: $4 \leq \chi(\mathcal{P}(3^3)) \leq 6$. Through exhaustive search, it has been shown that $\chi(\mathcal{P}(3^3)) = 6$. Given that the Lovász bound serves as the strongest among the topological lower bounds provided by the hierarchy theorem, one feasible strategy to establish $\chi(\mathcal{P}(3^3)) = 6$ is to demonstrate that the Lovász bound equals 6. This can be approached by identifying a $\mathbb{Z}_2$-invariant S^4 with non-trivial homology in the

box complex $\mathrm{B}_{\text{edge}}(\mathcal{P}(3^3))$ and applying the Borsuk-Ulam theorem. Although we have been unable to identify such an S^4 in the box complex using current methods, we show that certain portions of the box complex preclude the existence of any $\mathbb{Z}_2$-invariant S^4 with non-trivial homology.

In this thesis, we successfully applied the proposed approach to the Petersen graph. By calculating the box complex of the Petersen graph and simplifying it to a homotopy equivalent simplicial complex, we computed its $\mathbb{Z}_2$-index. This computation yielded a Lovász bound of 3, matching the chromatic number of the Petersen graph.

Our primary objective is to gain a deeper insight into $\chi(\mathcal{P}(g^g))$ by leveraging the Hierarchy theorem. We will specifically concentrate on the case where $g = 3$. To apply the Hierarchy theorem, we must construct $\mathrm{B}_{\text{edge}}(G)$, which is the box complex of $\mathcal{P}(3^3)$. To accomplish this, it is necessary to identify the complete bipartite subgraphs within the graph $\mathcal{P}(3^3)$. As a prerequisite, we undertake a comprehensive study of the general properties of $\mathcal{P}(3^3)$, noting that this graph exhibits vertex-transitivity, edge-transitivity, and arc-transitivity. This understanding proves highly beneficial in facilitating further analyses of this graph.

Additionally, we categorized all vertex pairs, triples, and quadruples of the $\mathcal{P}(3^3)$ graph into distinct equivalence classes. We also derive all maximal complete bipartite subgraphs of $\mathcal{P}(3^3)$ solely from pairs of vertices. By leveraging our categorization of vertex pairs, triples, and quadruples, as well as incorporating new lemmas, we demonstrate that the bipartite subgraphs obtained from the vertex pairs are in fact the only maximal bipartite subgraphs of the graph. This approach allows us to categorize all the maximal complete bipartite subgraphs of $\mathcal{P}(3^3)$ into equivalence classes, providing valuable insights into the structure of the graph.

Given that each simplex of the box complex $\mathrm{B}_{\text{edge}}(\mathcal{P}(3^3))$ represents an edge subset of a complete bipartite subgraph of $\mathcal{P}(3^3)$, with the edges ordered from left to right, we utilize the classification of all maximal complete bipartite subgraphs to identify all the maximal simplices of $\mathrm{B}_{\text{edge}}(\mathcal{P}(3^3))$ and their antipodes. Following this, we delve into the structure of pairwise intersections of the simplices within $\mathrm{B}_{\text{edge}}(\mathcal{P}(3^3))$. Through this investigation, we uncover the maximal size of the pairwise intersections of the simplices.

A brute force algorithm to construct the box complex of a general graph would be of time complexity of roughly $O(n^4 \cdot 4^n)$. Thus, it is computationally expensive for large graphs and may not scale well to practical use cases. In this thesis, we propose an algorithm that constructs the box complex of the partition graph $\mathcal{P}(3^3)$. By utilizing the approach to identifying the maximal complete bipartite subgraphs within the graph $\mathcal{P}(3^3)$, our program significantly reduces the time complexity to $O(n^3)$. This represents a substantial improvement over a brute-force approach, resulting in improved processing speed.

In order to make the box complex of $\mathcal{P}(3^3)$ more analyzable, we resort to dis-

crete Morse theory. The original Morse theory, formulated by Marston Morse in the 1920s and 1930s, offers a powerful mechanism for examining the topology of smooth manifolds by scrutinizing the critical points of real-valued functions on these spaces. This approach has significantly shaped various mathematical disciplines, including algebraic topology, differential geometry, and mathematical physics. The core ideas of Morse theory were later expanded into a discrete context by Robin Forman in the late 1990s, sparking the inception of discrete Morse theory. This theory adapts Morse theory concepts for use in discrete contexts such as cell complexes, offering an efficient, elegant way to explore the topology of these complexes.

In discrete Morse theory, the continuous functions applied in the original Morse theory are replaced by assigning a numerical value to each cell of the complex, thus turning all processes discrete. This reformulation illustrates the potential for developing a robust theory within combinatorial spaces that echoes the intricacies of smooth theory, without necessitating continuity. Discrete Morse theory has found successful applications across various fields of applied mathematics and computer science, including topological data analysis [12, 13], geometry [10], denoising [16], mesh compression [15] image processing and computer graphics [14, 11].

Using this theory, we construct a simplicial complex homotopy equivalent to the box complex of $\mathcal{P}(3^3)$ in two ways: by using the elementary collapses, and by finding a discrete Morse function on the box complex. This dimension reduction reduces the dimension of the box complex from 35 to 12, which simplifies the future calculation of the $\mathbb{Z}_2$-index and thus the Lovász bound. Additionally, the reduction yields a more tractable object for further analysis.

Chapter 1

Box Complex

"Alice: This is impossible.
The mad hatter: Only if you believe it is."
— Alice in Wonderland, 2010 film

The study of combinatorial topology offers a rich interplay between various mathematical domains such as algebra, topology, and combinatorics. The box complex which is a type of simplicial complex derived from a graph, is one of the tools that embodies this interplay.

The content presented in this chapter primarily follows the research and findings articulated in the paper referenced as [3]. Our goal in this chapter is to interpret, elaborate, and present these sophisticated concepts in a comprehensible manner to the reader. We also state and prove some of our results.

In the initial section, we revisit several key mathematical concepts including the Kneser graph, simplicial complexes, along with $\mathbb{Z}_2$-spaces and the $\mathbb{Z}_2$-index. These concepts are foundational and integral to understanding box complexes, and the explorations that we will undertake in subsequent sections are rooted in these fundamental ideas.

Moving forward, the concept of neighbourhood complexes is introduced and explored, as presented in the source paper. This discussion serves as a stepping stone towards the understanding of box complexes. Different types of box complexes are introduced, all of which are based on the definitions and examples provided in the source paper. The relationships among these complexes are also explored, elucidating the rich interconnectedness inherent within them.

A crucial element of this chapter, and indeed in the paper [3], is the Hierarchy Theorem. This theorem is a significant result that correlates the box complexes of

a graph to the chromatic number of the same graph. An in-depth examination of this theorem is provided, along with comprehensive proofs of lower bounds on the chromatic number, including the Lovász, Dol'nikov-Kříž, and Bárány Bounds, all of which are derived from the original paper.

In the concluding section of the chapter, we will shift our focus onto the distinctive properties of the box complex when applied to specific types of graphs. We will concentrate our examination on even and odd cycles, as well as bipartite graphs. This analysis provides insight into the way certain graphical structures manifest in the properties of their corresponding box complexes.

1.1 Preliminaries

In this section, the background needed for this research is provided.

Kneser graphs

Let X be a finite set and $\mathcal{F} \subseteq 2^X$ a system of subsets of X. The *Kneser graph* $\mathrm{KG}(\mathcal{F})$ has vertex set $\mathcal{F}$, and the edges are all pairs of disjoint sets in $\mathcal{F}$. For convenience, we assume that $X = [n] := 1, 2, ..., n$, unless stated otherwise.

A proper **k**-*colouring* of a graph is a labelling of the graph's vertices with k colours such that no two vertices sharing the same edge have the same colour. The smallest number of colours needed to colour a graph G is called its *chromatic number* and is often denoted $\chi(G)$. A graph that can be assigned a (proper) k-colouring is k-colourable.

Kneser conjecture, first proved by Lovász in 1978, states that the chromatic number of a Kneser graph $\mathrm{KG}\binom{[n]}{k}$ is $n - 2k + 2$, for $n \geq 2k > 0$, where $\binom{[n]}{k}$ denotes the family of all $k-$element subsets of $[n]$. Here we prove a weaker statement than the Kneser conjecture.

Proposition 1.1.1. There exists a $n-2k+2$ colouring of the Kneser graph $\mathrm{KG}\binom{[n]}{k}$ or equivalently, this amount is an upper bound for the chromatic number of this graph:

$$\chi(\mathrm{KG}\binom{[n]}{k}) \leq n - 2k + 2.$$

Proof: Let c_i be all the subsets of $[n]$ which contain i as their smallest number. Consider the sets $c_1, c_2, ..., c_{n-2k+1}$, then, assign one colour to each c_i. Since the sets included in each c_i are not disjoint, the corresponding vertices are not adjacent. So far we have used $n-2k+1$ colours. All remaining sets are subsets of $\{n-2k+2, \cdots, n\}$ which is of cardinality $2k-1$. So, none of these sets are disjoint. Hence, we can assign one colour to all these sets. ∎

It is easy to see that every finite graph $G = (V, E)$ can be represented as a Kneser graph of some set system. A simple and natural representation is this: Let $\bar{E} := \binom{V}{2} \backslash E$ denote the set of non-edges of G, and for every $v \in V$, set $F_v := \{\bar{e} \in \bar{E} : v \in \bar{e}\}$. The Kneser graph of $\{F_v : v \in V\}$ is isomorphic to G; the only problem is that the sets F_v need not be all distinct (For example, for $G = K_n$, we have $F_v = \emptyset$ for all v). To remedy this, one can define $F'_v := F_v \cup \{v\}$, obtaining distinct sets.

Example. Consider the graph G as the following, we see how it can be represented as a Kneser graph.

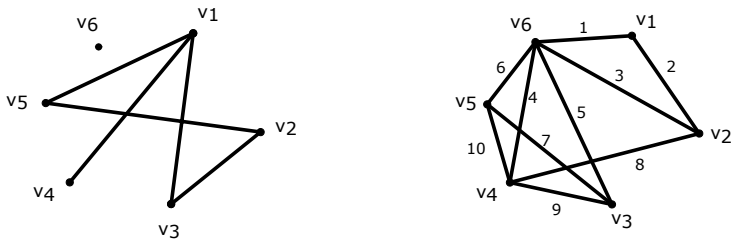

Figure 1.1: Graph G at left and graph $\bar{G}$ at right

The vertices of Kneser graph are as follows,

$$F'_{v_1} = \{1, 2, v_1\} \qquad F'_{v_2} = \{2, 3, 8, v_2\}$$
$$F'_{v_3} = \{5, 7, 9, v_3\} \qquad F'_{v_4} = \{9, 8, 6, 10, v_4\}$$
$$F'_{v_5} = \{4, 7, 10, v_5\} \qquad F_{v_6} = \{1, 3, 5, 6, 4, v_6\}$$

The Kneser graph of the above sets is as follows,

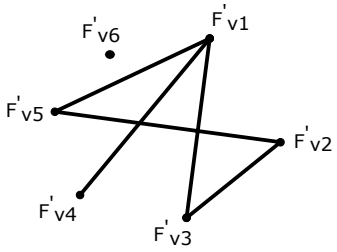

Figure 1.2: Kneser form of the graph G

Geometric simplicial complexes

In geometry, points $v_0, v_1, ..., v_k$ are *affinely dependent* in $\mathbb{R}^d$ if there are real numbers $\alpha_0, \alpha_1, ..., \alpha_k$, not all of them 0, such that $\sum_{i=0}^{k} \alpha_i v_i = 0$ and $\sum_{i=0}^{k} \alpha_i = 0$. Otherwise,

$v_0, v_1, ..., v_k$ are called affinely independent. A set of points in a Euclidean space is defined to be convex if it contains the line segments connecting each pair of its points. The *convex hull* of a given set X is defined as the intersection of all convex sets containing X and we denote it by $\text{conv}(X)$.

A *simplex* σ is the convex hull of a finite affinely independent set A in $\mathbb{R}^d$. The points of A are called the *vertices* of σ. The dimension of σ is $\dim(\sigma) = |A| - 1$. Thus every k-simplex (k-dimensional simplex) has $k+1$ vertices. This concept generalizes the notion of a triangle or tetrahedron to arbitrary dimensions. The convex hull of an arbitrary subset of vertices of a simplex σ is a *face* of σ. Thus every face is itself a simplex. A nonempty family Σ of simplices is a *simplicial complex* if the following two conditions hold:

1. Each face of any simplex $\sigma \in \Sigma$ is also a simplex of Σ.
2. The intersection $\sigma_1 \cap \sigma_2$ of any two simplices $\sigma_1,\ \sigma_2 \in \Sigma$ is a face of both σ_1 and σ_2.

The dimension of a simplicial complex is the largest dimension of a simplex: $\dim \Sigma := \max\{\dim \sigma : \sigma \in \Sigma\}$. We consider only finite simplicial complexes. The vertex set of Σ, denoted by $V(\Sigma)$, is the union of the vertex sets of all simplices of Σ.

Abstract simplicial complexes

Let V be a set, an abstract simplicial complex K is a hereditary set system $K \subseteq 2^V$ of subsets of V; that is, we require that $F \in K$ and $G \subseteq F$ implies $G \in K$ (in particular, $\emptyset \in K$ whenever $K \neq \emptyset$). The sets in K are its *simplices*. The vertex set of K is defined as $V(K) = \cup K$, the union of all simplices of K. The elements of the vertex set are called the *vertices* of the complex. Similar to the geometric version the dimension of a simplex S in K is defined as $\dim(S) = |S| - 1$: simplicies consisting of a single element are zero-dimensional, simplices consisting of two elements are one-dimensional, etc. The dimension of the complex K is defined as the maximum dimension of any of its simplices, or infinity if there is no finite bound on the dimension of the simplices. A subcomplex of K is an abstract simplicial complex L such that every face of L belongs to K; that is, $L \subseteq K$. A *face* of a simplex S is a non-empty subset $S' \subseteq S$. We call $f : K \to L$ a simplicial map if $f(S) \in L$ for all $S \in K$. Two abstract simplicial complexes K and L are isomorphic if there is a bijective simplicial map $f : V(K) \to V(L)$ such that $S \in K$ if and only if $f(S) \in L$.

Given a geometric simplicial complex Σ, we can construct an abstract simplicial complex K by throwing away all simplicies and retaining only their sets of vertices; this is called the *vertex scheme* of Σ. In this case, we say Σ is a geometric realization of K and also of any abstract simplicial complex isomorphic to K, and we write $\Sigma = \| K \|$. Note that a geometric simplicial complex has a topology as a subset of $\mathbb{R}^d$ and it can be shown that all geometric realizations of an abstract simplicial complex

K are homeomorphic as topological spaces. Although there is not a unique geometric simplicial complex $\| K \|$ associated to K, there is therefore a unique topological space $\| K \|$ that has the structure of a geometric simplicial complex and whose vertex scheme is isomorphic to K. Properly speaking this is the meaning of $\| \cdot \|$. Constructing geometric realizations is feasible if the dimension of the ambient space is sufficiently high.

The following theorem ensures each abstract simplicial complex has a geometric realization.

Theorem 1.1.2. [4, Theorem 1.6.1] Every finite d-dimensional simplicial complex K has a geometric realization in $\mathbb{R}^{2d+1}$.

However, most of the time the geometric realization can be embedded in a lesser dimensional space. The geometric realization of K can be convex or not, while, the geometric realization of a simplex is always convex. Sometimes we just write "simplicial complex" when referring to an abstract or geometric simplicial complex when the usage is clear from the context.

For a partially ordered set $(X, \preceq)$, the *order complex* $\Delta(X, \preceq)$ has X as the vertex set and all chains as simplices; that is, a simplex has the form $\{x_1, x_2, ..., x_k\} \subseteq X$ with $x_1 \prec x_2 \prec ... \prec x_k$. In particular, if $\mathcal{F}$ is a set system, we write $\Delta\mathcal{F}$ for $\Delta(\mathcal{F}\backslash\{\emptyset\}, \subseteq)$. If K is a simplicial complex, then ΔK is the *first barycentric subdivision of* K, also denoted by $\mathrm{sd}\, K$ (The empty simplex $\emptyset$ is not a vertex of the barycentric subdivision).

The (twofold) *deleted join* of the simplicial complex K, denoted by K_Δ^{*2}, has vertex set $V(K) \times [2]$ (two copies of $V(K)$) and the simplices are

$$\{S_1 \uplus S_2 : S_1, S_2 \in K, S_1 \cap S_2 = \emptyset\}$$

where we use the shorthand $S_1 \uplus S_2 := (S_1 \times \{1\}) \cup (S_2 \times \{2\})$.

Example 1.1.3. Take a simple triangle as an example of the simplicial complex K. This triangle has 3 vertices, call them a, b, and c, and 3 edges, call them ab, bc, and ac.

The (twofold) deleted join of this triangle, K_Δ^{*2}, will have a vertex set consisting of two copies of the vertices a, b, and c, and we label them a', b', c', a'', b'', c''.

Next, we need to construct the simplices. Remember that simplices in K_Δ^{*2} are formed by taking disjoint sets of simplices from the original complex, K, one from each copy. For example, a valid 2-simplex would be formed by combining the vertex a from copy 1 with the edge bc from copy 2, resulting in the 2-simplex $\{a', b'', c''\}$. Following this process, two examples of the 2-simplices are $\{a', b'', c''\}$, $\{b', a'', c''\}$. In the same manner, we can continue to build 1-simplices (edges) for the complex K_Δ^{*2}.

Definition 1.1.4. Let $\mathcal{F}$ be a set system with ground set X. Let $\mathrm{K}(\mathcal{F})$ be a simplicial complex with vertex set X and

$$\mathrm{K}(\mathcal{F}) := \{S \subseteq X : F \nsubseteq S \text{ for all } F \in \mathcal{F}\}$$

As an example consider the ground set $X = \{1, 2, 3\}$ and $\mathcal{F} = \{\{1\}, \{1, 2\}\}$, then $\mathrm{K} = \{\{2\}, \{3\}, \{2, 3\}\}$.

$\mathbb{Z}_2$-space and $\mathbb{Z}_2$-index

A $\mathbb{Z}_2$ *-space* is a pair (T, ν), where T is a topological space and $\nu : T \to T$, called the $\mathbb{Z}_2$*-action*, is a homeomorphism such that $\nu^2 = \nu \circ \nu = id_T$. Two elements $t \in T$ and $\nu(t) \in T$ are called *antipodal*. If (T_1, ν_1) and (T_2, ν_2) are $\mathbb{Z}_2$-spaces, a $\mathbb{Z}_2$*-map* between them is a continuous mapping $f : T_1 \to T_2$ such that $f \circ \nu_1 = \nu_2 \circ f$. The sphere S^n is considered as a $\mathbb{Z}_2$-space with the antipodal mapping $x \mapsto -x$. The $\mathbb{Z}_2$- *index* of a $\mathbb{Z}_2$-space (T, ν) is

$$\mathrm{ind}(T, \nu) := \min\{n \geq 0 : \text{there is a } \mathbb{Z}_2\text{-map } (T, \nu) \to S^n\} \in \{0, 1, 2, ...\} \cup \{\infty\}$$

(The $\mathbb{Z}_2$-action ν is omitted from the notation if it is clear from the context). For example, in the Borsuk-Ulam section, we see $\mathrm{ind}\, S^n = n$.

Proposition 1.1.5. If $\mathrm{ind}(T_1, \nu_1) > \mathrm{ind}(T_2, \nu_2)$, then there is no $\mathbb{Z}_2$-map $T_1 \to T_2$. In other words, if there exists a $\mathbb{Z}_2$-map $T_1 \to T_2$, then $\mathrm{ind}(T_1, \nu_1) \leq \mathrm{ind}(T_2, \nu_2)$.

Proof: Suppose there is a $\mathbb{Z}_2$-map $h : T_1 \to T_2$, then we have the following diagram,

$$\begin{array}{ccc} T_1 & \xrightarrow{h} & T_2 \\ {\scriptstyle \nu_1}\downarrow & & \downarrow{\scriptstyle \nu_2} \\ T_1 & \xrightarrow{h} & T_2 \end{array}$$

the equation $\nu_2 \circ h = h \circ \nu_1$ holds for this diagram. Let $p : S^n \to S^n$ be the continuous antipodal map $p(x) = -x$. Assume $\mathrm{ind}(T_1, \nu_1) = m$, $\mathrm{ind}(T_2, \nu_2) = n$, and $m > n$. So, there exists $\mathbb{Z}_2$-map $g : T_2 \to S^n$ and we have the following diagram,

$$\begin{array}{ccc} T_2 & \xrightarrow{g} & S^n \\ {\scriptstyle \nu_2}\downarrow & & \downarrow{\scriptstyle p} \\ T_2 & \xrightarrow{g} & S^n \end{array}$$

Since $\mathrm{ind}(T_1, \nu_1) = m$, there is no $\mathbb{Z}_2$-map $f : T_1 \to S^n$ such that the equation $f \circ \nu_1 = p \circ f$ holds. Using the two diagrams we can make the following diagram,

$$\begin{array}{ccccc} T_1 & \xrightarrow{h} & T_2 & \xrightarrow{g} & S^n \\ {\scriptstyle \nu_1}\downarrow & & {\scriptstyle \nu_2}\downarrow & & \downarrow{\scriptstyle p} \\ T_1 & \xrightarrow{h} & T_2 & \xrightarrow{g} & S^n \end{array}$$

So the equation $p \circ (g \circ h) = (g \circ h) \circ \nu_1$ holds which means $g \circ h : T_1 \to S^n$ is a $\mathbb{Z}_2$-map, this is a contradiction. ∎

Borsuk-Ulam Theorem

The Borsuk-Ulam theorem is a foundational result in the field of algebraic topology. In its most common form, for a sphere in n-dimensional Euclidean space, the Borsuk-Ulam theorem states that for any continuous function f from the n-sphere to n-dimensional Euclidean space, there exists a pair of antipodal points with the same value on f. These are points that are diametrically opposite to each other on the sphere and are mapped to the same point by the function f. One of the intriguing interpretations of this theorem is that at any given time, there are two antipodal places on earth with identical temperature and air pressure.

There are various equivalent versions of this theorem, some of which are crucial for this research. While proving any of the versions of the Borsuk–Ulam theorem is far from trivial and requires some technical apparatus, checking the equivalence of all these statements is significantly less daunting. For a comprehensive proof of this theorem and additional versions, refer to [4].

Theorem 1.1.6. [4, Theorem 2.1.1] For every $n \geq 0$, the following statements are equivalent and true:

1. For every continuous mapping $f : S^n \to \mathbb{R}^n$, there exists a point $x \in S^n$ with $f(x) = f(-x)$, (This is the most common interpretation).
2. For every antipodal mapping $f : S^n \to \mathbb{R}^n$ (that is, f is continuous and $f(-x) = -f(x)$ for all $x \in S^n$) there exists a point $x \in S^n$ satisfying $f(x) = 0$.
3. There is no antipodal mapping $f : S^n \to S^{n-1}$.
4. There is no continuous mapping $f : B^n \to S^{n-1}$ that is antipodal on the boundary, i.e., satisfies $f(-x) = -f(x)$ for all $x \in S^{n-1} = \partial B^n$.

Proof: $(\mathbf{1}) \to (\mathbf{2})$: Since there exists the point $x \in S^n$ such that $f(x) = f(-x)$ and f is an antipodal mapping, then,

$$f(x) = f(-x) = -f(x)$$

So, $f(x) = 0$.

$(\mathbf{2}) \to (\mathbf{1})$: Suppose $f : S^n \to \mathbb{R}^n$ is a continuous mapping. Define function $g : S^n \to \mathbb{R}^n$ as $g(x) := f(x) - f(-x)$. Then,

$$g(-x) = f(-x) - f(x) = -(f(x) - f(-x)) = -g(x)$$

Hence, function g is a continuous antipodal mapping. So, there exists a point $x \in S^n$ such that $g(x) = 0$ and $f(x) = f(-x)$.

(**2**) $\rightarrow$ (**3**) : An antipodal mapping $S^n \rightarrow S^{n-1} \subseteq \mathbb{R}^n$ is a nowhere zero antipodal mapping $S^n \rightarrow \mathbb{R}^n$ (because 0 is not antipodal to any other point in $\mathbb{R}^n$ and is not included in S^{n-1}).

(**3**) $\rightarrow$ (**2**) : Assume that $f : S^n \rightarrow \mathbb{R}^n$ is a continuous nowhere zero antipodal mapping. Then, the antipodal mapping $g : S^n \rightarrow S^{n-1}$ given by $g(x) = f(x)/\|f(x)\|$ contradicts.

(**3**) $\rightarrow$ (**4**) : We can easily prove it by observing that the projection $\pi : (x_1, \ldots, x_{n+1}) \mapsto (x_1, \ldots, x_n)$ is a homeomorphism between the upper hemisphere U of S^n and the closed ball B^n.

Let $g : B^n \rightarrow S^{n-1}$ be a mapping as in (4). We can define a mapping $f : S^n \rightarrow S^n - 1$ by setting $f(x) = g(\pi(x))$ for $x \in U$, and $f(-x) = -g(\pi(x))$ for $x \in U$. This specifies f on the whole of S^n, it is consistent because g is antipodal on the equator of S^n, and the resulting f is continuous since it is continuous on both of the closed hemispheres.

(**4**) $\rightarrow$ (**3**) : Let $f : S^n \rightarrow S^{n-1}$ be an antipodal mapping as in (3). Then, we can define a mapping $g : B^n \rightarrow S^{n-1}$ that is antipodal on ∂B^n by $g(x) = f(\pi^{-1}(x))$ using the function π introduced above. ∎

Corollary 1.1.7. Let S^n be the $n-$dimensional sphere. Then $\text{ind}(S^n) = n$.

Proof: The proof follows directly from the third statement of the Borsuk-Ulam Theorem (see Theorem 1.1.6). This statement guarantees that the smallest integer m for which a $\mathbb{Z}_2$-map exists from S^n to S^m is equal to n. Consequently, we can conclude that $\text{ind}(S^n) = n$ ∎

Simplicial $\mathbb{Z}_2$-complexes

Definition 1.1.8. A *simplicial $\mathbb{Z}_2$-complex* is a simplicial complex K with a simplicial map ν of K into itself such that ν is a $\mathbb{Z}_2$-action on K.

For the deleted join K^{*2}_{Δ}, we have the $\mathbb{Z}_2$-action by "swapping the two copies of $V(K)$", formally $(v, 1) \mapsto (v, 2)$ and $(v, 2) \mapsto (v, 1)$.

Proposition 1.1.9. Suppose K is a simplicial $\mathbb{Z}_2$-complex whose $\mathbb{Z}_2$-action is not free (that is, has a fixed point), then $\text{ind}\, K = \infty$.

Proof: Suppose x is a fixed point of $\nu : K \rightarrow K$ which means $\nu(x) = x$ and

$f : K \to S^n$ is a $\mathbb{Z}_2$-map. So, we can form the following diagram,

$$\begin{array}{ccc} K & \xrightarrow{f} & S^n \\ {\scriptstyle \nu}\downarrow & & \downarrow{\scriptstyle p} \\ K & \xrightarrow{f} & S^n \end{array}$$

The diagram is commutative, $p \circ f = f \circ \nu$. For the special fixed point $x \in K$ we have $p(f(x)) = f(\nu(x)) = f(x)$. So, $f(x)$ is a fixed point for p, which is a contradiction because $p(x) = -x$ for all $x \in S^n$. Hence, there is no such a number n for which $f : K \to S^n$ be a $\mathbb{Z}_2$-map. We can conclude that $\operatorname{ind} K = \infty$. ∎

The following theorem, originally stated in [3], establishes an upper bound on the $\mathbb{Z}_2-$index of $\mathbb{Z}_2$-simplicial complexes. In this section, we provide a detailed proof to support this theorem.

Proposition 1.1.10. [3] For any simplicial $\mathbb{Z}_2$-complex K whose $\mathbb{Z}_2$-action is free, we have the following hierarchy,

$$\dim K \geq \operatorname{ind} K \tag{1.1.1}$$

Proof:

The goal is to construct a $\mathbb{Z}_2$-map $g : \|K\| \to S^n$ for a $\mathbb{Z}_2$-simplicial complex K with $\dim(K) = n$. We will use induction on n to build this map.

For the base case of our induction, we start with n = 0. In this scenario, $\|K\|$ consists of 0-dimensional simplices, i.e., points. We can define a $\mathbb{Z}_2$-map from $\|K\|$ to S^0 (which is composed of two points) by pairing each point in $\|K\|$ with a point in S^0, in a manner that respects the $\mathbb{Z}_2$-action.

For the induction step, assume that we have constructed a $\mathbb{Z}_2$-map $g_k : \|K_k\| \to S^k$ for all $k < n$. We denote by $\|K_k\|$ the k-skeleton of K, i.e., the subspace of K spanned by simplices of dimension at most k. We already have a $\mathbb{Z}_2$-map $g_{n-1} : \|K_{n-1}\| \to S^{n-1}$.

The n-sphere S^n can be thought of as being formed by gluing together two n-balls (B^{n+} and B^{n-}) along their boundary, which is an $(n-1)$-sphere S^{n-1}. Our goal is to extend g_{n-1} to a $\mathbb{Z}_2$-map $g_n : \|K\| \to S^n$.

We begin by letting g_n coincide with g_{n-1} on $\|K_{n-1}\|$. Now, consider an n-simplex s in K, and its antipodal simplex $\tilde{s}$ under the $\mathbb{Z}_2$-action. We extend the definition of g_n to the interiors of s and $\tilde{s}$ by mapping them to B^{n+} and B^{n-} respectively. This construction respects the $\mathbb{Z}_2$-action because s and $\tilde{s}$ are mapped to opposite hemispheres of S^n. ∎

1.2 Neighbourhood Complexes

For a graph G and any subset $A \subseteq V(G)$, let

$$\mathrm{CN}(A) := \{v \in V(G) : \{a, v\} \in E(G) \text{ for all } a \in A\} \subseteq V \setminus A \tag{1.2.1}$$

be the set of all *common neighbours* of A. By $\mathrm{CN}(\emptyset)$ we mean all the vertices of G.

For a graph G, we can build simplicial complexes. Two of them are introduced below:

Definition 1.2.1. [3] The *neighbourhood complex* of a graph G is a simplicial complex defined as

$$N(G) := \{S \subseteq V(G) : \mathrm{CN}(S) \neq \emptyset\}.$$

Therefore, the simplices of $N(G)$ are the vertex subsets that have at least one common neighbour.

Refer back to the order complex definition, denoted by Δ, discussed in Section 1.1. We now present another simplicial complex, defined as the order complex of the complete system of "closed sets" in $N(G)$, as established in [3]:

$$L(G) := \Delta\{A \subset V(G) : \mathrm{CN}(\mathrm{CN}(A)) = A\}.$$

Thus, the vertices of $L(G)$ are sides of inclusion-maximal complete bipartite subgraphs of G.

Example. Suppose

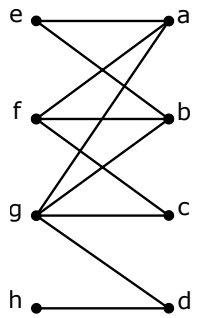

Figure 1.3: Graph G

Then, one can specify write the simplices of $N(G)$ and $L(G)$.

$N(G) = \{$vertices: $\{a\}, \{b\}, ..., \{h\}$,
edges: $\{a, b\}, \{a, c\}, \{a, d\}, \{b, c\}, \{b, d\}, \{c, d\}, \{e, f\}, \{e, g\}, \{f, g\}, \{g, h\}$

triangles: $\{a, b, c\}, \{e, f, g\}, \{a, c, d\}, \{a, b, d\}, \{b, c, d\}$
4-simplex: $\{a, b, c, d\}\}$

It is obvious that every non-isolated vertex of G is a vertex of $N(G)$.

$$L(G) = \Delta\{\{a, b, c\}, \{e, f, g\}, \{d\}, \{g, h\}, \{a, b, c, d\}, \{g\}\}$$

We can think of the $L(G)$ simplices as pairs. For example, the sets $\{a, b, c\}$ and $\{f, g\}$ are pairs because $\mathrm{CN}\{a, b, c\} = \{f, g\}$ and $\mathrm{CN}\{f, g\} = \{a, b, c\}$.

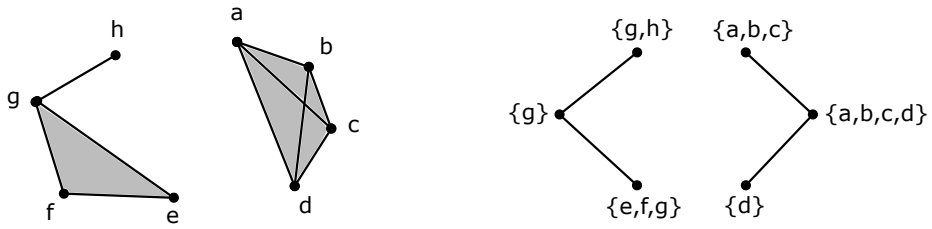

Figure 1.4: Complex $N(G)$ at left and complex $L(G)$ at right

After presenting the definition of the complexes $N(G)$ and $L(G)$ and discussing their characteristics through a concrete example, we now further investigate the relationship between these two complexes. We will elucidate the relationship between their vertices and simplices, especially how their structures intertwine with each other.

The following lemma establishes a fundamental connection between $N(G)$ and $L(G)$: the correspondence between the maximal simplices of $N(G)$ and the vertices of $L(G)$.

Lemma 1.2.2. Each maximal simplex of the complex $N(G)$ is a vertex of the complex $L(G)$.

Proof: Suppose S is a maximal simplex of $N(G)$ and $\mathrm{CN}(S) = S'$. The goal is to prove $\mathrm{CN}(S') = S$, then conclude S and S' are vertices of $L(G)$.

Since $\mathrm{CN}(S) = S'$, each $v \in S$ is adjacent to all the vertices of S'. So, $S \subseteq \mathrm{CN}(S')$. Suppose $v \in \mathrm{CN}(S')$ and $v \notin S$. As S is a maximal simplex of $N(G)$ and $\mathrm{CN}(S) = S'$, it means there is a maximal complete bipartite subgraph of G with sides S and S'. If $v \in \mathrm{CN}(S')$ and $v \notin S$ then the subgraph $S \cup \{v\}$ and S' make a bigger complete bipartite subgraph than the bipartite subgraph with sides S and S' which is a contradiction. ∎

The following lemma establishes a basic but essential property about the common neighbours function.

Lemma 1.2.3. Given a graph G and two subsets S and T of $V(G)$ such that $S \subseteq T$, it holds that $\mathrm{CN}(T) \subseteq \mathrm{CN}(S)$.

Proof: Let v be an arbitrary vertex in $\mathrm{CN}(T)$. By definition of $\mathrm{CN}(T)$, the vertex v is adjacent to every vertex in T. Since S is a subset of T, every vertex in S is also a vertex in T, and hence, v is adjacent to every vertex in S. This shows that v is in $\mathrm{CN}(S)$. As v was arbitrary, we have shown that every vertex in $\mathrm{CN}(T)$ is also in $\mathrm{CN}(S)$, which implies $\mathrm{CN}(T) \subseteq \mathrm{CN}(S)$. ∎

Lemma 1.2.4. Given a graph G and a subset S of $V(G)$, it is true that

$$\mathrm{CN}\big(\mathrm{CN}(\mathrm{CN}(S))\big) = \mathrm{CN}(S).$$

Proof: Since vertices of S are adjacent to all the vertices of $\mathrm{CN}(S)$, then $S \subseteq \mathrm{CN}(\mathrm{CN}(S))$. By Lemma 1.2.3, we have $\mathrm{CN}\big(\mathrm{CN}(\mathrm{CN}(S))\big) \subseteq \mathrm{CN}(S)$.

Now assume $x \in \mathrm{CN}(S)$. Then all the vertices of $\mathrm{CN}(\mathrm{CN}(S))$ are adjacent to x. Consequently, $s \in \mathrm{CN}\big(\mathrm{CN}(\mathrm{CN}(S))\big)$. So,

$$\mathrm{CN}(S) \subseteq \mathrm{CN}\big(\mathrm{CN}(\mathrm{CN}(S))\big).$$

∎

Propelled by the conclusions drawn from these lemmas, we are then able to prove the following proposition. This proposition lays out a significant conclusion about the intersection of maximal simplices of $N(G)$. This intersection, under the application of the CN function twice, remains invariant, resulting in being a vertex of $L(G)$.

Proposition 1.2.5. The intersection of the maximal simplices of $N(G)$ is a vertex in $L(G)$.

Proof: Let S and T be two maximal simplices of $N(G)$. By lemma 1.2.2 we know S and T are vertices of $L(G)$, so, $\mathrm{CN}(\mathrm{CN}(S)) = S$ and $\mathrm{CN}(\mathrm{CN}(T)) = T$. The goal is to prove $\mathrm{CN}(\mathrm{CN}(S \cap T)) = S \cap T$. Suppose $\mathrm{CN}(S \cap T) = S'$, it is obvious that $S \cap T \subseteq \mathrm{CN}(S')$. Assume $v \in \mathrm{CN}(S')$ but $v \notin S \cap T$. Then v is just adjacent to all the vertices of S'. Without loss of generality, suppose $v \notin S$. Since $\mathrm{CN}(\mathrm{CN}(S)) = S$, then $v \notin \mathrm{CN}(\mathrm{CN}(S))$. By the last argument, one can say

$$\mathrm{CN}(S) \subseteq \mathrm{CN}(S \cap T) \;\Rightarrow\; \mathrm{CN}(\mathrm{CN}(S \cap T)) \subseteq \mathrm{CN}(\mathrm{CN}(S)).$$

As we supposed $v \notin \mathrm{CN}(\mathrm{CN}(S))$ but $v \in \mathrm{CN}(\mathrm{CN}(S \cap T))$, there is a contraction. So, $\mathrm{CN}(\mathrm{CN}(S \cap T)) = S \cap T$. ∎

A retraction is a continuous mapping from a topological space into a subspace that preserves the position of all points in that subspace. The subspace is then called a retract of the original space. A deformation retraction is a mapping that captures the idea of continuously shrinking a space into a subspace.

Definition 1.2.6. Let X be a topological space and A a subspace of X. Then a continuous map $r : X \to A$ is a *retraction* if the restriction of r to A is the identity map on A; that is, $r(a) = a$ for all a in A.

A retraction in a discrete context gives us a way to "collapse" a larger structure onto a smaller one while preserving the structure of the smaller object. The condition $r(a) = a$ for all a in A is what gives us the "retraction" concept - it is saying that if we start with a point in A, applying the function r does not change it - it "retracts" back onto itself.

Given two continuous functions f and g from a topological space X to a topological space Y, a *homotopy* between f and g is a continuous function $H : X \times [0, 1] \to Y$ such that $H(x, 0) = f(x)$ and $H(x, 1) = g(x)$ for all x in X.

Definition 1.2.7. Let X and Y be topological spaces. A map $f : X \to Y$ is a *homotopy equivalence* if there exists a map $g : Y \to X$ such that $g \circ f$ is homotopic to the identity map id_X and $f \circ g$ is homotopic to the identity map id_Y.

Definition 1.2.8. A continuous map $F : X \times [0, 1] \to X$ is a *deformation retraction* of a space X onto a space A, if for every $x \in X$ and $a \in A$,

$$F(x, 0) = x, \quad F(x, 1) \in A, \quad F(a, 1) = a.$$

In other words, a deformation retraction is a homotopy between a retraction and the identity map on X. The subspace A is called a deformation retract of X.

If, in the definition of a deformation retraction, we add the requirement that $F(a, t) = a$ for all $a \in A$, F is called a *strong deformation retraction.* The following proposition originally was stated in [3]. While the statement can be found in the referenced work, for the sake of completeness and context, we provide a detailed proof here.

Proposition 1.2.9. L(G) is a strong deformation retract of N(G).

Proof: Define $r : N(G) \to L(G)$ by mapping each element x in $N(G)$ to the set of common neighbours of x, denoted by CN(x).

The aim is to show that r is well-defined, i.e., that for all $x \in N(G)$, the image $r(x)$ indeed belongs to $L(G)$. To see this, note that each member of $N(G)$ is a subset of the vertices of G which have at least one common neighbour. So, every subset $x \in N(G)$ lies within one side of a maximal bipartite subgraph of G, which we denote as y. Now, since $x \subseteq y$, we have $r(y) \subseteq r(x)$ by Lemma 1.2.3. However, $r(y)$ is one

side of a maximal bipartite subgraph. So we actually have equality: $r(x) = r(y)$. Because of the same reason, $\mathrm{CN}(\mathrm{CN}(r(y))) = r(y)$ and thus $r(y) \in L(G)$. Therefore, $r(x) \in L(G)$.

Consider any $x \in L(G)$. By the definition of $L(G)$, we have $r^2(x) = x$, indicating that $r^2 : N(G) \to L(G)$ is a retraction of $N(G)$ onto $L(G)$. Since r is a function concerning the discrete structure of $N(G)$ and $L(G)$, there is no need to check the continuity of r, we consider it a continuous function.

Now consider the geometric realization of the simplicial complexes of $N(G)$ and $L(G)$. We can exhibit a strong deformation retraction of $\|N(G)\|$ onto $\|L(G)\|$ using the homotopy $f : \|N(G)\| \times I \to \|N(G)\|$, where $I = [0, 1]$ and $f(x, t) = (1 - t)x + t \cdot r(x)$. This function is continuous because all the operations and the function r are continuous. This function satisfies the properties of a strong deformation retract, namely:

$$\begin{aligned} f(x, 0) &= x && \forall x \in \|N(G)\| \\ f(x, 1) &\in \|L(G)\| && \forall x \in \|N(G)\| \\ f(a, t) &= a && \forall a \in \|L(G)\|, \forall t \in I \end{aligned}$$

Hence, f provides a strong deformation retraction of $\|N(G)\|$ onto $\|L(G)\|$. ∎

1.3 Box Complexes

In the definition that follows, we present six different variations of box complexes. Four of these variations are defined with respect to the Kneser graph of a set $\mathcal{F}$, while the remaining two are directly defined for the set $\mathcal{F}$. As a reminder, the Kneser graph of a set $\mathcal{F}$, denoted $\mathrm{KG}(\mathcal{F})$, was introduced earlier in Section 1.1.

Definition 1.3.1. (Box complexes). Let $G = (V, E) = \mathrm{KG}(\mathcal{F})$ be a finite graph with no isolated vertices, and suppose that the ground set of $\mathcal{F}$ is $[n]$. The first two complexes are on the vertex set $V \times [2]$.

1. The box complex $\mathrm{B}(G)$ is

$$\begin{aligned} \mathrm{B}(G) := \{ & A' \uplus A'' : A', A'' \subseteq V,\ A' \cap A'' = \emptyset, \\ & G[A', A''] \text{ is complete},\ \mathrm{CN}(A'), \mathrm{CN}(A'') \neq \emptyset \}. \end{aligned}$$

   The simplices of $\mathrm{B}(G)$ correspond to complete bipartite subgraphs in G. We admit A' or A'' empty, but it is required that all vertices of the other side have a common neighbour.

A canonical simplicial $\mathbb{Z}_2$-action on $\mathrm{B}(G)$ is given by interchanging the two copies of $V(G)$; that is, $(v,1) \mapsto (v,2)$ and $(v,2) \mapsto (v,1)$, for $v \in V(G)$. This makes $\mathrm{B}(G)$ into a $\mathbb{Z}_2$-space.

2. A simpler definition, but a larger complex, is obtained as

$$\begin{aligned}\mathrm{B}_0(G) :=& \{A' \uplus A'' : A', A'' \subseteq V(G), \\ & A' \cap A'' = \emptyset,\ G[A', A''] \text{ is complete}\}\end{aligned}$$

This box complex contains $\mathrm{B}(G)$, here if one side is empty, the other can be anything.

3. The following definition of a box complex takes into account only the complete bipartite graphs with both sides nonempty:

$$\begin{aligned}\mathrm{B}_{chain}(G) :=& \Delta\{A' \uplus A'' : \emptyset \neq A', A'' \subset V, \\ & A' \cap A'' = \emptyset,\ G[A', A''] \text{ is complete}\}\end{aligned}$$

Here the vertices are the vertex set of complete bipartite subgraphs of G, and the simplices are chains of such sets under inclusion. Also $\mathrm{B}_{chain}(G)$ is included in $\Delta\,\mathrm{B}(G)$. A set of vertices can serve as the vertex set of different complete bipartite subgraphs, leading to different vertices and simplicies of $\mathrm{B}_{chain}(G)$.

4. The vertices of the next box complex are the directed edges of G; that is, ordered pairs (u,v) with $\{u,v\} \in E$.

$$\begin{aligned}\mathrm{B}_{edge}(G) :=& \{\overrightarrow{F} \subset A' \times A'' : \emptyset \neq A', A'' \subset V, \\ & A' \cap A'' = \emptyset, G[A', A''] \text{ is complete}\}\end{aligned}$$

Simplices of this box complex are subsets of edge sets of complete bipartite subgraphs of G, where the edges are oriented from the first side to the second side.

5. The simplicial complex $\Delta((2^{[n]})^{*2}_{\Delta} \setminus K^{*2}_{\Delta})$ will appear in theorem 1.4.1, as an intermediate step in Sarkaria's derivation of his lower bound. Now, we delve into $((2^{[n]})^{*2}_{\Delta} \setminus K^{*2}_{\Delta})$ more. Recall definition 1.1.4 about the simplicial complex $K = K(\mathcal{F})$. Then, K^{*2}_{Δ} is all the $B' \uplus B''$ such that $B', B'' \subseteq [n]$, $B' \cap B'' = \emptyset$, and $F \nsubseteq B',\ B''$ for all $F \in \mathcal{F}$. So, $\Delta((2^{[n]})^{*2}_{\Delta} \setminus K^{*2}_{\Delta})$ can be expressed as

$$\begin{aligned}\mathrm{B}^{\mathrm{KG}}_{Sark}(\mathcal{F}) :=& \Delta\{B' \uplus B'' : B', B'' \subseteq [n],\ B' \cap B'' = \emptyset \\ & \text{at least one of } B', B'' \text{contains a set of } \mathcal{F}\}.\end{aligned}$$

The vertex sets are pairs of disjoint subsets of the ground set of $\mathcal{F}$ that support a complete bipartite subgraph of the Kneser graph, with at least one side nonempty.

6. Finally, another Kneser box complex is

$$\mathrm{B}^{\mathrm{KG}}_{chain}(\mathcal{F}) := \Delta\{B' \uplus B'' : B', B'' \subseteq [n], B' \cap B'' = \emptyset \\ \text{both } B', B'' \text{ contain a set of } \mathcal{F}\}.$$

On each of these types of box complexes, we have the natural $\mathbb{Z}_2$-action that interchanges the sides of the bipartite subgraph.

Example 1.3.2. Let the graph G be the 5-cycle, $G = C_5$. In this example, we provided different box complexes for the graph C_5 with their geometrical object.

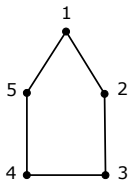

Figure 1.5: A C_5 graph

1. The simplicial complex of $\mathrm{B}(C_5)$:

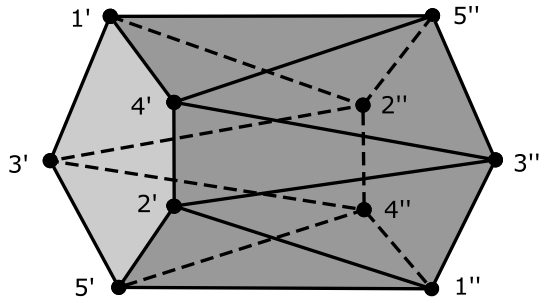

Figure 1.6: $\mathrm{B}(C_5)$

In this example, $\mathrm{B}(C_5)$ does not contain any tetrahedrons or the simplices of the form $\{1', 2', 3', 4', 5'\}$ or $\{1'', 2'', 3'', 4'', 5''\}$, in other words left and right-hand sides are removed.

To have a better understanding of the simplices of the box complex $\mathrm{B}(C_5)$ we take a closer look at the Figure 1.6. To write down the vertices we just need to pick a vertex from C_5 and do the $\uplus$ operation with empty set, also, the order matters because each pair (a C_5 vertex and empty set) makes a vertex at the left-hand side and another one at the right-hand side, the difference is just the order of the pair (for example $\emptyset \uplus \{1\}$ and $\{1\} \uplus \emptyset$ are two vertices at right and left-hand side respectively).

The edges of $\mathrm{B}(C_5)$ are of two kinds, the middle ones and the ones at the sides. To make the side edges we need to take two vertices of C_5 like v_1 and v_2 for which $\mathrm{CN}(v_1, v_2) \neq \emptyset$, then do $\uplus$ with empty set. Again, order matters because changing the order of a pair gives us another edge at the other side (like $\{1,3\} \uplus \emptyset$ is an edge at the left-hand side and $\emptyset \uplus \{1,3\}$ is an edge at the right-hand side). On the other hand, the middle edges are ordered pairs of the vertices v_1 and v_2 for which $\mathrm{CN}(v_1), \mathrm{CN}(v_2) \neq \emptyset$ and $G[\{v_1\}, \{v_2\}]$ is complete (in this case, since there is just one vertex in our set, having a common neighbour is equal to having a neighbour). But this time we do the $\uplus$ operation between the vertices and do not use empty set (for example $\{1\} \uplus \{2\}$ and $\{2\} \uplus \{1\}$ are two middle edges).

For the $2-$simplices or triangles we need to choose 3 vertices of C_5 like $\{v_1, v_2\}$ and $\{v_3\}$ with the property $\mathrm{CN}(\{v_1, v_2\}), \mathrm{CN}(\{v_3\}) \neq \emptyset$ and $G[\{v_1, v_2\}, \{v_3\}]$ is complete, then do the $\uplus$ operation for two sets with considering the pair as an ordered pair ($\{1,3\} \uplus \{2\}$ and $\{2\} \uplus \{1,3\}$ are two triangles).

To declare the vertices on the left side are different from the vertices on the right side we distinguish them with $'$ and $''$ in the figures. But for pointing out to them when talking about the simplices of the box complexes we do not use $'$ and $''$. For a simplex like $X \uplus Y$, the set X shows the left side vertices or the ones with ' and the set Y shows the right side vertices or the ones with ".

2. The simplicial complex of $\mathrm{B}_0(C_5)$:

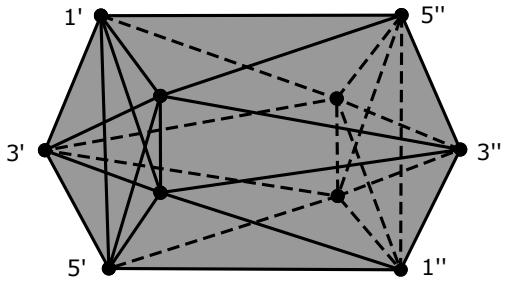

Figure 1.7: $\mathrm{B}_0(C_5)$

If we notice we see that the two left and right sides of $\mathrm{B}_0(G)$ are complete graphs. This box complex is a union of $\mathrm{B}(C_5)$ and some other simplices. The new simplices are the ones which make the sides complete. The reason for this difference is that in $\mathrm{B}_0(C_5)$ the constraint $\mathrm{CN}(A'), \mathrm{CN}(A'') \neq \emptyset$ does not exist, therefore $\mathrm{B}_0(C_5)$ has more simplices than $\mathrm{B}(C_5)$ (for example two of the new simplices are $\{1,5\} \uplus \emptyset$ and $\emptyset \uplus \{1,5\}$).

3. The simplicial complex of $\mathrm{B}_{chain}(C_5)$:

   The box complex $\mathrm{B}_{chain}(C_5)$ in Figure 1.8 is the barycentric subdivision of just the middle simplices of $\mathrm{B}(C_5)$, i.e., the simplicies of the form $\{i'\} \uplus \{j'', t''\}$, $\{j', t'\} \uplus \{i''\}$, or $\{i'\} \uplus \{j''\}$ and the reason is the sets A' and A'' are non-empty based on the definition of this box complex.

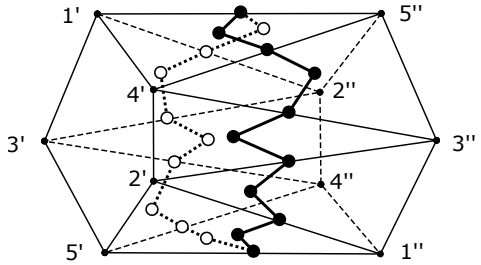

Figure 1.8: $\mathrm{B}_{chain}(C_5)$

4. The simplicial complex of $\mathrm{B}_{edge}(C_5)$:

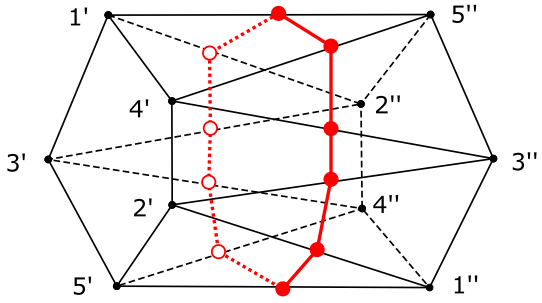

Figure 1.9: $\mathrm{B}_{edge}(C_5)$

   We can use the same set of sets we used for $\mathrm{B}_0(C_5)$ because the constraints on the sets are the same but instead of doing $\uplus$, here we do $\times$ (for example, in Figure 1.9, $\{(1,2)\} = \{1\} \times \{2\}$ is a vertex and $\{(1,2),(1,5)\} = \{1\} \times \{2,5\}$ is an edge).

5. To give an example on $\mathrm{B}_{Sark}(\mathcal{F})$ and $\mathrm{B}_{chain}(\mathcal{F})$ we need to work on a set $\mathcal{F}$. Consider the set $\mathcal{F} = \{\{1\},\{1,2\}\}$ and the ground set as $[n] = \{1,2,3\}$. The simplicial complex $K(\mathcal{F})$ is (look at definition 1.1.4),

$$K = K(\mathcal{F}) = \{\{2\},\{3\},\{2,3\}\}$$

   So it is just two vertices and the edge between them.

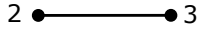

Figure 1.10: $K(\mathcal{F})$

Recalling the definition of deleted join,

$$K_{\Delta}^{*2} = \{S_1 \uplus S_2 : S_1, S_2 \in K, S_1 \cap S_2 = \emptyset\}$$

for vertices we follow the same procedure as before, take one singleton and do the operation $\uplus$ with empty set, like $\{2\} \uplus \emptyset$. For edges we take two different singletons and do the operation $\uplus$, like $\{2\} \uplus \{3\}$. So K_{Δ}^{*2} looks like

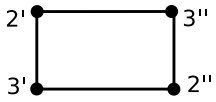

Figure 1.11: K_{Δ}^{*2}

The set $2^{[3]}$ consists of all subsets of $\{1, 2, 3\}$. So we can draw the simplicial complex $(2^{[3]})_{\Delta}^{*2}$ as

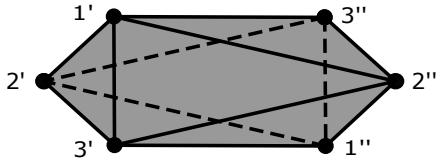

Figure 1.12: $(2^{[3]})_{\Delta}^{*2}$

This simplicial complex contains the triangles in the figure 11 but does not contain any higher dimensional simplex. Then, by removing K_{Δ}^{*2} from $(2^{[3]})_{\Delta}^{*2}$ we get

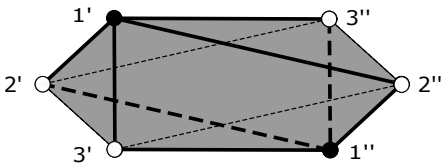

Figure 1.13: $(2^{[3]})_{\Delta}^{*2} \setminus K_{\Delta}^{*2}$

The order complex of the last partially ordered set is like bellow

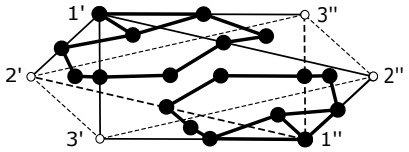

Figure 1.14: $\Delta((2^{[3]})^{*2}_{\Delta} \setminus K^{*2}_{\Delta})$ and $\mathrm{B}^{\mathrm{KG}}_{Sark}$

To find the box complex $\mathrm{B}^{\mathrm{KG}}_{Sark}$ we should look at its definition. This box complex is the order complex of a set, so first we need to find this set. Since $\{1\}$ and $\{1,2\}$ are the only members of $\mathcal{F}$ we can have any combination using one of these sets or any other set in $2^{[3]}$ which contains one of these two sets, with another set from $2^{[3]}$ as long as their intersection is empty (for example $\{1\} \uplus \{2\}$ and $\{2\} \uplus \{1,3\}$). Then, one can try to draw the box complex $\mathrm{B}^{\mathrm{KG}}_{Sark}$ and get the same figure as the above for $\Delta((2^{[3]})^{*2}_{\Delta} \setminus K^{*2}_{\Delta})$.

In this case for our example the box complex $\mathrm{B}^{\mathrm{KG}}_{chain}(\mathcal{F})$ is empty. Notice that the box complexes $\mathrm{B}^{\mathrm{KG}}_{Sark}$ and $\mathrm{B}^{\mathrm{KG}}_{chain}(\mathcal{F})$ are simplicial complexes but we take the order complex of a partially ordered set which is not always a simplicial complex because we are allowed to have a triangle without some edges or vertices.

We will study the index of these simplicial complexes later on. For this purpose, we need to know more about the index. Suppose K and K' are two $\mathbb{Z}_2$-spaces and $\operatorname{ind} K' = n$, also, $f : K \to K'$ is a simplicial $\mathbb{Z}_2$-map. Hence, there exists the $\mathbb{Z}_2$-map $\nu_1 : K' \to S^n$. So, the map $\nu_2 = \nu_1 \circ f$ is a $\mathbb{Z}_2$-map from K to S^n. Therefore, $\operatorname{ind} K \leq n$.

Lemma 1.3.3. Let K be a simplicial complex and (K, ν_1) be a $\mathbb{Z}_2$ space. Then, $\operatorname{ind} K = \operatorname{ind} \operatorname{sd} K$.

Proof: Since K is a $\mathbb{Z}_2$-space, each vertex in K has an antipodal vertex, as well as each simplex of K. Hence, the barycentric $\operatorname{sd} K$ is a $\mathbb{Z}_2$-space, by sending each new vertex that appears in $\operatorname{sd} K$ to its antipodal vertex in $\operatorname{sd} K$. One can set the inclusion $f : K \to \operatorname{sd} K$. It is obvious that f is a $\mathbb{Z}_2$-map and simplicial. As a result, $\operatorname{ind} K \leq \operatorname{ind} \operatorname{sd} K$.

Now suppose $\operatorname{ind} K = n$, so, there exists the $\mathbb{Z}_2$-map $g : K \to S^n$. Since S^n has a continuous structure, as long as there exists a $\mathbb{Z}_2$-map from K to S^n, there exists a $\mathbb{Z}_2$-map from $\operatorname{sd} K$ to S^n. Hence, $\operatorname{ind} \operatorname{sd} K \leq \operatorname{ind} K$. As a conclusion, $\operatorname{ind} \operatorname{sd} K = \operatorname{ind} K$. ∎

Here *susp* K denotes the *suspension* of a simplicial complex K (a "double cone" over K) as

$$\operatorname{susp} K := K \cup \{S \cup \{s\} : S \in K\} \cup \{S \cup \{n\} : S \in K\}$$

where s and n are two new vertices not belonging to $V(K)$.

The following proposition provides explicit simplicial $\mathbb{Z}_2$-maps among the various box complexes.

Proposition 1.3.4. For any finite graph $G = \mathrm{KG}(\mathcal{F})$ without isolated vertices, there are simplicial $\mathbb{Z}_2$-maps

$$\begin{aligned}
\mathrm{B}(G) &\to \mathrm{B}_0(G) && (M1)\\
\mathrm{sd}\,\mathrm{B}_{edge}(G) &\leftrightarrow \mathrm{B}_{chain}(G) && (M2)\\
\mathrm{B}_{chain}(G) &\to \mathrm{sd}\,\mathrm{B}(G) && (M3)\\
\mathrm{sd}\,\mathrm{B}_0(G) &\to \mathrm{susp}\,\mathrm{B}_{chain}(G) && (M4)\\
\mathrm{B}_{chain}(G) &\leftrightarrow \mathrm{B}^{\mathrm{KG}}_{chain}(\mathcal{F}) && (M5)\\
\mathrm{sd}\,\mathrm{B}_0(G) &\leftrightarrow \mathrm{B}^{\mathrm{KG}}_{Sark}(\mathcal{F}) && (M6)\\
\mathrm{sd}\,\mathrm{sd}\,\mathrm{B}(G) &\to \mathrm{B}_{chain}(G) && (M7)\\
\mathrm{sd}\,L(G) &\to \mathrm{B}_{chain}(G) && (M8)\\
\mathrm{sd}\,\mathrm{B}_{chain}(G) &\to \mathrm{sd}\,L(G). && (M9)
\end{aligned}$$

Proof: Here is a scheme of the proof, more details can be found in the reference [3].

(M1): It is an inclusion.

(M2): The map $\mathrm{sd}\,\mathrm{B}_{edge}(G) \to \mathrm{B}_{chain}(G)$ is defined on the vertices of $\mathrm{sd}\,\mathrm{B}_{edge}(G)$ by setting $\vec{F} \to h(\vec{F}) \uplus t(\vec{F})$, where $h(\vec{F})$ collects the tails and $t(\vec{F})$ collects the heads, of the directed edges in $\vec{F}$. For the other direction, we take the edges between the sides of each complete bipartite subgraph.

(M3): It can be seen as an inclusion.

(M4): The map is obtained by mapping the complete bipartite subgraphs (with one side empty) to the suspension points.

(M5): A $\mathbb{Z}_2$-map $\mathrm{B}^{\mathrm{KG}}_{chain}(\mathcal{F}) \to \mathrm{B}_{chain}(G)$ is defined on the vertices by

$$B' \uplus B'' \to \{F' \in \mathcal{F} : F' \subseteq B'\} \uplus \{F'' \in \mathcal{F} : F'' \subseteq B''\}.$$

A $\mathbb{Z}_2$-map $\mathrm{B}_{chain}(G) \to \mathrm{B}^{\mathrm{KG}}_{chain}(\mathcal{F})$ is obtained by mapping the vertices:

$$A' \uplus A'' \to (\cup A') \uplus (\cup A'').$$

(M6): The same formulas define $\mathbb{Z}_2$-maps $\mathrm{B}_0(G) \leftrightarrow \mathrm{B}^{\mathrm{KG}}_{Sark}(\mathcal{F})$.

(M7): The vertices of $\mathrm{sd}\,\mathrm{sd}\,\mathrm{B}(G)$ are like

$$\mathcal{A} = (A'_0 \uplus A''_0 \subset ... \subset ... \subset A'_k \uplus A''_k).$$

Let $\mu'(\mathcal{A})$ be the smallest nonempty set in the chain of sets $\mathcal{A}' := (A'_0 \subset ... \subset A'_k \subseteq \mathrm{CN}(A''_k) \subseteq ... \subseteq \mathrm{CN}(A''_0)$, and similarly for $\mu''(\mathcal{A}'')$. Then let the map be

$$\mathcal{A} \to \mu'(\mathcal{A}) \uplus \mu''(\mathcal{A}).$$

(M8): Define a $\mathbb{Z}_2$-map $f : \mathrm{sd}\, L(G) \to \mathrm{B}_{chain}(G)$ in a way that $f(\mathcal{A}) := A_0 \uplus \mathrm{CN}(A_k)$, where a vertex of $\mathrm{sd}\, L(G)$ is a chain $\mathcal{A} = (A_0 \subset A_1 \subset ... \subset A_k)$ of nonempty closed sets.

(M9): A vertex in $\mathrm{sd}\, \mathrm{B}_{chain}(G)$ is a chain $\mathcal{A} = (A'_0 \uplus A''_0 \subset ... \subset ... \subset A'_k \uplus A''_k)$ so we get the chain $\mathrm{CN}^2(A'_0) \subseteq ... \subseteq \mathrm{CN}^2(A'_k) \subseteq \mathrm{CN}(A''_k) \subseteq ... \subseteq \mathrm{CN}(A''_0)$. By omitting the repeated sets from this chain, we obtain a vertex of $\mathrm{sd}\, L(G)$. ∎

Now we can use this proposition to prove the following theorem. In this theorem, all the box complexes are divided into two groups based on their $\mathbb{Z}_2$-index.

Theorem 1.3.5. The following holds for the $\mathbb{Z}_2$-indices of the various box complexes:

$$\begin{aligned}\mathrm{ind}\, \mathrm{B}(G) = \mathrm{ind}\, \mathrm{B}^{\mathrm{KG}}_{chain}(\mathcal{F}) = \mathrm{ind}\, \mathrm{B}_{edge}(G) = \mathrm{ind}\, \mathrm{B}_{chain}(G) = \mathrm{ind}\, \mathrm{L}(G) \\ \leq \mathrm{ind}\, \mathrm{B}_0(G) = \mathrm{ind}\, \mathrm{B}^{\mathrm{KG}}_{Sark}(\mathcal{F}) \leq \mathrm{ind}\, \mathrm{B}(G) + 1.\end{aligned}$$

Proof: All the equalities and inequalities can be derived from the last proposition. For the last inequality we intend to use $(M4)$ from the last proposition which is about suspension, so we need to prove $\mathrm{ind}\, \mathrm{susp}\, K \leq \mathrm{ind}\, K + 1$ as well.

Suppose $\mathrm{ind}\, K = n$. Let $f : K \to S^n$ be the $\mathbb{Z}_2$-map. We make a new $\mathbb{Z}_2$-map $g : \mathrm{susp}\, \mathrm{K} \to \mathrm{susp}\, S^n$. Suppose $\nu : K \to K$ and $p : S^n \to S^n$ are $\mathbb{Z}_2$-actions of K and S^n respectively. It is easy to extend them to the $\mathbb{Z}_2$-maps $\nu' : \mathrm{susp}\, K \to \mathrm{susp}\, K$ and $p' : \mathrm{susp}\, S^n \to \mathrm{susp}\, S^n$ by mapping the new vertices to each other. Then the $\mathbb{Z}_2$-map g would be identity on K and maps the new vertices of $\mathrm{susp}\, K$ to the new vertices of $\mathrm{susp}\, S^n$ in such a way that makes it a $\mathbb{Z}_2$-map. Also, it can be seen easily that $\mathrm{susp}\, S^n = S^{n+1}$. We can get the homeomorphism by dividing the vectors of $\mathrm{susp}\, S^n$ by their norms. ∎

1.4 The Hierarchy Theorem

In the following theorem, we can find the comparison of all the considered lower bounds for $\chi(G)$. This is the main theorem of Matoušek and Ziegler's paper [3].

Theorem 1.4.1. (The Hierarchy Theorem). Let $G = (V, E) = \mathrm{KG}(\mathcal{F})$ be a finite (Kneser) graph with no isolated vertices, where $\mathcal{F} \subseteq 2^{[n]}$, and let $K = K(\mathcal{F}) =$

$\{S \subset [n] : F \nsubseteq S \text{ for all } F \in \mathcal{F}\}$. Then we have the following chain [1] of inequalities and equalities:

$\chi(G) \geq \operatorname{ind} \mathrm{B}(G) + 2 = \operatorname{ind} \mathrm{L}(G) + 2$	The Lovász bound
$\geq \operatorname{ind} \mathrm{B}_0(G) + 1 = \operatorname{ind} \Delta((2^{[n]})^{*2}_{\Delta} \backslash K^{*2}_{\Delta}) + 1$	
$\geq n - 1 - \operatorname{ind} K^{*2}_{\Delta}$	The Sarkaria bound
$\geq d$ if $K \subseteq \partial P$ for an $(\mathrm{n} - \mathrm{d}) -$ polytope P	The Bárány bound
$\chi(G) \geq n - 1 - \dim K^{*2}_{\Delta} = \mathrm{cd}_2(\mathcal{F})$	The Dol'nikov-Kříž bound

The remainder of Chapter 4 provides a proof of Theorem 1.4.1:

1.4.1 The Lovász Bound

We need to get familiar with some new concepts before providing the proof. A *cross polytope* is a convex hull

$$\operatorname{conv}\{e_1, -e_1, ..., e_n, -e_n\}$$

of the vectors of the standard orthogonal basis and their negatives. Alternatively, it is the unit ball of the l_1-norm: $\{x \in \mathbb{R}^n : \| x \| \leq 1\}$.

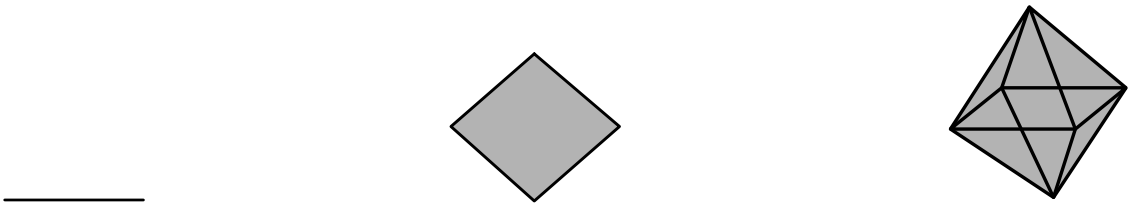

(a) $n = 1$ (b) $n = 2$ (c) $n = 3$

In reference [4] the boundary of an n-dimensional cross polytope is stated as $\Diamond^{n-1}$ which is a simplicial complex with a subset $F \subseteq V(\Diamond^{n-1})$ forming a simplex whenever there is no $i \in [n]$ such that both $i \in F$ and $-i \in F$.

In theorem 1.3.5 we saw the relation $\operatorname{ind} \mathrm{B}(G) \leq \operatorname{ind} \mathrm{B}_0(G)$. Here we state something stronger for the complete graph K_m. In reference, [3] it is stated that the box complex $\mathrm{B}_0(K_m)$ is isomorphic to the boundary complex of an $m-$dimensional cross polytope. So, the geometric realization of the simplicial complex $\mathrm{B}_0(K_m)$ is homeomorphic to an S^{m-1} and thus $\operatorname{ind} \mathrm{B}_0(K_m) = m - 1$.

Now, proving this statement. Suppose $\{1', 2', ..., m', 1'', 2'', ..., m''\}$ are the vertices of $\mathrm{B}_0(K_m)$. Since K_m is a complete graph, every vertex on the left-hand side is

[1] This is a chain of inequalities and equalities except at the end, where there is not a relation between the Bárány bound and the Dol'nikov-Kříž bound.

adjacent to all the vertices on the right-hand side except itself. Also, each pair of the vertices in K_m has a common neighbour, so, there is a copy of K_m at each side. Moreover, each vertex at $\Diamond^{m-1}$ is adjacent to all other vertices except its pair. Hence, the following isomorphism exists

$$f : \mathrm{B}_0(K_m) \to \Diamond^{m-1}$$
$$f(i') = i, f(i'') = -i$$

The function f and its inverse are obviously simplicial and bijective.

From the definition of box complexes, we know $\mathrm{B}(G) \subseteq \mathrm{B}_0(G)$. The box complex $\mathrm{B}(K_m)$ is isomorphic to $\Diamond^{m-1}$ with two opposite facets removed, with its antipodal $\mathbb{Z}_2$-action, because the only difference between $\mathrm{B}_0(K_m)$ and $\mathrm{B}(K_m)$ is that $\mathrm{B}_0(K_m)$ has two copies of K_m on its two sides and $\mathrm{B}(K_m)$ does not have.

Besides, every $m-$colouring of G can be regarded as a homomorphism of G into K_m so we can extend it to a homeomorphism of $\mathrm{B}(G)$ to $\mathrm{B}(K_m)$ in an obvious way, it induces a $\mathbb{Z}_2$-map of $\mathrm{B}(G)$ into S^{m-2}, and we obtain

$$\chi(G) \geq \operatorname{ind} \mathrm{B}(G) + 2.$$

Also, theorem 1.3.5 proved $\operatorname{ind} \mathrm{B}(G) = \operatorname{ind} \mathrm{L}(G)$.

Finding a lower bound for the chromatic number of the Petersen graph is a non-trivial application of the Lovász bound.

Example 1.4.2. In this example, we consider the Petersen graph denoted by P and depicted in Figure 1.16.

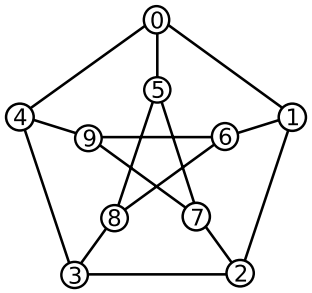

Figure 1.16: The Petersen graph

Our aim is to investigate the edge box complex of this graph, $\mathrm{B}_{\mathrm{edge}}(P)$. According to the definition of the box complex, the simplices of this simplicial complex correspond to the edge subsets of the complete bipartite subgraphs of the graph P. The maximal complete bipartite subgraphs of P are $K_{1,3}$, which consist of a vertex and its three neighbours. The intersection of two such subgraphs contains at most one edge. Consequently, in the box complex, the maximal simplices are triangles, and their intersections are either empty or consist of a single vertex.

We identify the two antipodal vertices $(6, 9)$ and $(9, 6)$ in the box complex $\mathrm{B}_{\mathrm{edge}}(P)$. It can be verified that these vertices are connected through the edges shown in Figure 1.17.

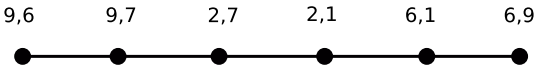

Figure 1.17: The connecting edges of tho antipodal points $(6, 9)$ and $(9, 6)$ in the box complex of Petersen graph

This set of edges is homotopy-equivalent to a one-dimensional ball B^1, and the two endpoints of this path, the antipodal vertices $(6, 9)$ and $(9, 6)$, form a $\mathbb{Z}_2$-invariant S^0. According to the fourth version of the Borsuk-Ulam theorem (Theorem 1.1.6), there does not exist a $\mathbb{Z}_2$-map from B^1 with $\mathbb{Z}_2$-invariant boundary to S^0. Therefore, there is no such map from the box complex $\mathrm{B}_{\mathrm{edge}}(P)$ to S^0, implying that the $\mathbb{Z}_2$-index of $\mathrm{B}_{\mathrm{edge}}(P)$ is greater than zero.

Given that the graph is not particularly large, we can compute the entire $\mathrm{B}_{\mathrm{edge}}(P)$. To better understand $\mathrm{B}_{\mathrm{edge}}(P)$, we can perform some simplifications. We can identify all vertices of each triangle, turning each triangle into a single vertex. Additionally, to represent the intersection of two triangles, we create an edge between the corresponding points, as shown in Figure 1.18.

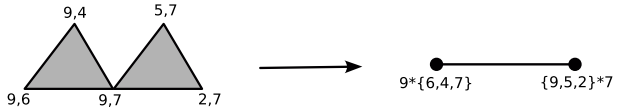

Figure 1.18: An example of the identifications on $\mathrm{B}_{\mathrm{edge}}(P)$

The resulting $\mathrm{B}_{\mathrm{edge}}(P)$ after these simplifications is depicted in Figure 1.19, with antipodals of black vertices shown in red.

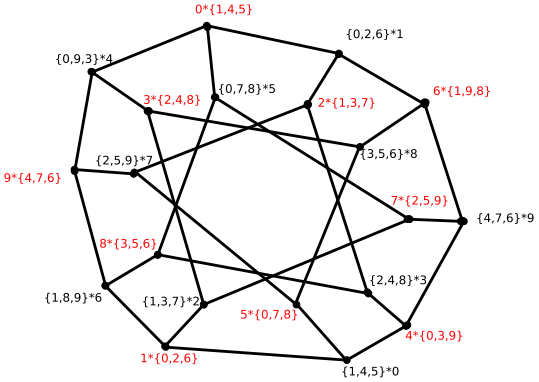

Figure 1.19: The edge box complex of the Petersen graph

We can further simplify this figure by identifying pairs of vertices, as shown in Figure 1.20.

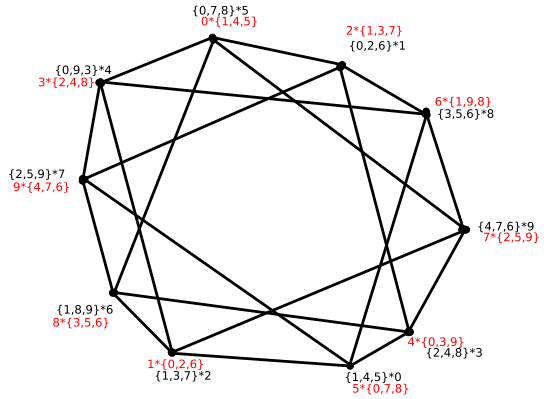

Figure 1.20: A simplified version of the edge box complex of Petersen graph

Both Figure 1.19 and Figure 1.20 are homotopy equivalent to $\mathrm{B}_{\mathrm{edge}}(P)$. It is evident that there is a $\mathbb{Z}_2$-map from this box complex to S^1. We can embed Figure 1.20 into $\mathbb{R}^2$ such that the origin is at its center, and each pair of antipodal points lie on a single line passing through the origin. Then, we can define a $\mathbb{Z}_2$-map as follows: consider all lines passing through the origin in each quadrant of the plane. For each point on these lines, map it to the corresponding point on S^1 lying in the same quadrant. Since the action of $\mathbb{Z}_2$ on S^1 corresponds to a reflection through the origin, this is a $\mathbb{Z}_2$-map.

In conclusion, the $\mathbb{Z}_2$-index of $\mathrm{B}_{\mathrm{edge}}(P)$ is equal to one, and the Lovász bound is equal to three. The inequality in the Hierarchy Theorem 1.4.1 verifies that $\chi(P) \geq 3$. In this example, the inequality holds as equality since the chromatic number of the Petersen graph is known to be three.

The Sarkaria bound. Since the proof is long we do not go into it here but refer the interested reader to chapter 5.7 of the reference [4].

1.4.2 The Dol'nikov-Kříž Bound

From the proposition 1.1.10 it can be seen easily that

$$n - 1 - \operatorname{ind} K_{\Delta}^{*2} \geq n - 1 - \dim K_{\Delta}^{*2}.$$

For a set system $\mathcal{F}$, let the 2-*colourability defect* $\mathrm{cd}_2(\mathcal{F})$ be the minimum size of a subset $Y \subseteq X$ such that the system of the sets of $\mathcal{F}$ that contain no points of Y is 2−colourable. In other words, we want to colour each point of X red, blue, or white in such a way that no set of $\mathcal{F}$ be completely red or completely blue but it can be

completely white, and $\mathrm{cd}_2(\mathcal{F})$ is the minimum number of white pints required for such a colouring.

To see the proof of $n-1-\dim K_\Delta^{*2} = \mathrm{cd}_2(\mathcal{F})$, suppose $\dim(K_\Delta^{*2}) = m$. It means dimension of the largest simplex S of K_Δ^{*2} is m, so, this simplex has $m+1$ vertices. Let V_1 and V_2 be the vertices of two sides of K_Δ^{*2} and vertices of the simplex S be the subset S_1 of V_1 and S_2 of V_2. By the definition of K there is no set of $\mathcal{F}$ included in S_1 or S_2. Hence, we can assign red to all vertices of S_1 and blue to all vertices of S_2. Then, we colour the rest of the $n-(m+1)$ vertices white, so, no set of $\mathcal{F}$ would be completely red or completely blue so it is a proper colouring.

Assume we colour an additional element x from X either in blue or red. Given that S_1 and S_2 are maximal sets of K, adding one extra element to them would result in a set from $\mathcal{F}$. If we choose to colour x blue, then the set $S_2 \cup \{x\}$ would be entirely blue, thus creating an all-blue set from $\mathcal{F}$. Similarly, if we decide to colour x red, we would yield an all-red set from $\mathcal{F}$, specifically $S_1 \cup \{x\}$.

1.4.3 The Bárány Bound

We need to prove that if the simplicial complex K is a part of the boundary of an $k-$dimensional convex polytope P, then $\mathrm{ind}(K_\Delta^{*2}) \leq k-1$. Before going into the details we need to get familiar with some new concepts and their properties.

If X and Y are topological spaces, the *join* $X * Y$ is the quotient of the product space $X \times Y \times [0,1]$ by the equivalence $\approx$, where $(x,y,0) \approx (x',y,0)$ and $(x,y,1) \approx (x,y',1)$ for all $x, x' \in X$ and $y, y' \in Y$.

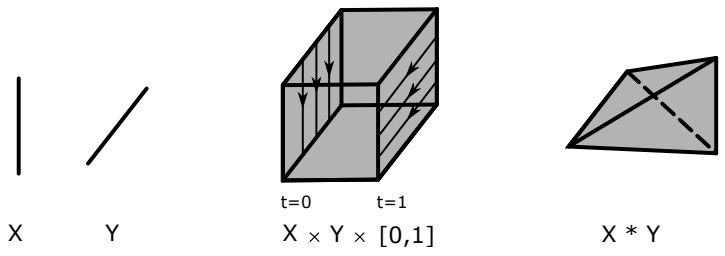

The following proposition and its proof from Matoušek's book [4] gives us a geometric understanding of join.

Proposition 1.4.3. (Geometric join). Suppose that X and Y are subspaces of some Euclidian space, and that $X \subseteq U$ and $Y \subseteq V$, where U and V are skew affine subspaces of some $\mathbb{R}^n$ (That is, $U \cap V = \emptyset$ and the affine hull of $U \cup V$ has dimension $\dim U + \dim V + 1$). Moreover, suppose that X and Y are bounded. Then the space

$$Z' := \{tx + (1-t)y : t \in [0,1], x \in X, y \in Y\} \subset \mathbb{R}^n$$

i.e., the union of all segments connecting a point of X to a point of Y, is homeomorphic to the join $X * Y$.

Proof: There is an obvious continuous map

$$f : X \times Y \times [0,1] \to Z'$$
$$(x, y, t) \to tx + (1-t)y.$$

We want to form $X * Y$ on the left-hand side. The map f descends to the quotient space because it takes the same value on the points which are identified. This gives us a continuous map as follows

$$g : (X \times Y \times [0,1])/\approx \to Z'.$$

In fact, g is a homeomorphism because it is bijection, continuous, and its inverse is continuous too. ∎

When K is a simplicial complex, $K^{*2} := \{S' \uplus S'' : S', S'' \in K\}$. If we look at the last picture as simplices, we get the same result but from a simplicial point of view. The explicit members of join $X * Y$ are as follows

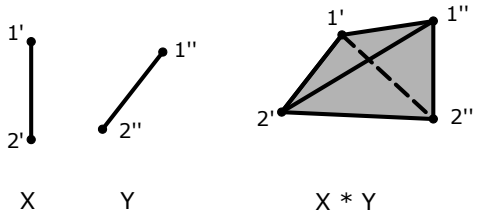

$$X * Y = \{\{1\} \uplus \{1\}, \{1\} \uplus \{2\}, \{2\} \uplus \{1\}, \{2\} \uplus \{2\}, \{1\} \uplus \{1,2\}, \{2\} \uplus \{1,2\},$$
$$\{1,2\} \uplus \{1\}, \{1,2\} \uplus \{2\}, \{1,2\} \uplus \{1,2\}\}$$

Also X^{*2}_{Δ} is as follows

$$X^{*2}_{\Delta} = \{\{1\} \uplus \{2\}, \{2\} \uplus \{1\}\}$$

and it looks like

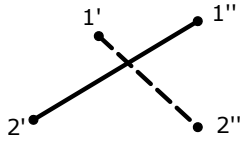

It is convenient to write a point in the join $X * Y$, which is formally an equivalence class $[(x, y, t)]$ as the "formal convex combination" $tx \oplus (1-t)y$.

Given two maps $f : X_1 \to X_2$ and $g : Y_1 \to Y_2$, the join of the maps is

$$f * g : X_1 * Y_1 \to X_2 * Y_2$$
$$tx \oplus (1-t)y \to tf(x) \oplus (1-t)g(y).$$

Now with the following steps and with the help of proposition 1.4.3 we can prove the claim $\| K \|^{*2} \simeq \| K^{*2} \|$.

1. Let U and V be skew affine subspaces in $\mathbb{R}^d$, and let $A \subset U$ and $B \subset V$ be affinely independent sets. Then, $A \cup B$ is affinely independent.

   Suppose $A \cup B$ is affinely dependent. So, there exists some nonzero coefficients α_i such that $\sum \alpha_i x_i = 0$ for all $x_i \in A \cup B$ and $\sum \alpha_i = 0$. Now separate x_i in A and B

   $$\sum \alpha_i x_i = \sum \alpha_i' x_i' + \sum \alpha_i'' x_i'' = 0$$

   where $x_i' \in A$ and $x_i'' \in B$. It means members of B are combinations of the members of A and vice versa. Hence,

   $$\sum \alpha_i' x_i' \ , \ \sum \alpha_i'' x_i'' \in U \cup V \ \Rightarrow \ \sum \alpha_i x_i \in U \cup V.$$

   On the other hand, $U \cap V = \emptyset$. So, the only possibility is that all x_i be in A or B. Without loss of generality, suppose $x_i \in A$ for all x_i. But A is affinely independent so we have a contradiction because we assumed $\sum \alpha_i x_i = 0$ and $\sum \alpha_i = 0$. As a result, $A \cup B$ is affinely independent.

2. The union of all segments connecting a point of $\text{conv}(A)$ to a point of $\text{conv}(B)$ is the simplex $\text{conv}(A \cup B)$.

   The goal is to prove $\text{conv}(\text{conv}(B) \cup \text{conv}(A)) = \text{conv}(A \cup B)$. Since $A \cup B \subseteq \text{conv}(A) \cup \text{conv}(B)$, it is obvious that

   $$\text{conv}(A \cup B) \subseteq \text{conv}(\text{conv}(B) \cup \text{conv}(A)).$$

   For the other direction, we have

   $$\text{conv}(A) \subseteq \text{conv}(A \cup B) \ , \ \text{conv}(B) \subseteq \text{conv}(A \cup B)$$
   $$\Rightarrow \text{conv}(A) \cup \text{conv}(B) \subseteq \text{conv}(A \cup B).$$

   Since $\text{conv}(\text{conv}(A \cup B)) = \text{conv}(A \cup B)$, we have

   $$\text{conv}(\text{conv}(A) \cup \text{conv}(B)) \subseteq \text{conv}(A \cup B).$$

3. Now we can use proposition 1.4.3 to prove that $\| K \| * \| L \| \simeq \| K * L \|$ for any two finite simplicial complexes K and L.

   Let $\| K \| \subseteq \mathbb{R}^{2k+1}$ and $\| L \| \subseteq \mathbb{R}^{2l+1}$ so we can take the subspaces $U \subseteq \mathbb{R}^{2k+2l+2}$ and $V \subseteq \mathbb{R}^{2k+2l+2}$ such that,

   $$\| K \| \subseteq U, \quad \| L \| \subseteq V, \quad U \cap V = \emptyset$$

   and the polytopes $\| K \|$ and $\| L \|$ be embeded in $\mathbb{R}^{2k+2l+2}$ such that they are affinely independent. By the first step, $\| K \| \cup \| L \|$ is affinely independent, so $\dim(\text{conv}(\| K \| \cup \| L \|)) = \dim(K) + \dim(L) + 1$.

   Now by the proposition, $\| K \| * \| L \|$ is homeomorphic to the union of all segments connecting a point of $\| K \|$ to a point of $\| L \|$. Take an arbitrary simplex of K as S_1 and an arbitrary simplex of L as S_2. We know simplices are convex hulls of their vertices, by the second step above we conclude all segments from S_1 to S_2 form the simplex $\text{conv}(S_1 \cup S_2)$ which is exactly the definition of $S_1 \uplus S_2$. Also, we know all the simplices of $K * L$ are of the form $S_1 \uplus S_2$, so there is a one-to-one relation between the simplices of both sides. Thus, if we take the identity map on the vertices, we get a simplicial and bijective map which is continuous from topological point of view.

As we said earlier K is part of a $k-$dimensional convex polytope P. The rest is from reference [3]. Using the homeomorphism $\| K^{*2} \| \to \| K \|^{*2}$ and a homeomorphism of the boundary of P with S^{k-1}, we obtain a $\mathbb{Z}_2$-map $h : \| K^{*2} \| \to S^{k-1} * S^{k-1}$. Moreover, if we restrict the left-hand side to $\| K^{*2}_{\Delta} \|$ we remove the simplices of K^{*2} which have the same vertices, then the image contains no point of the form (x, x, t) and it is of the form

$$(S^{k-1} * S^{k-1}) \backslash \{(x, x, t) : x \in S^{k-1}, t \in [0, 1]\}$$

but we rather work with the following set because it has the same index and it is more useful

$$Z := (S^{k-1} * S^{k-1}) \backslash \{(x, x, \frac{1}{2}) : x \in S^{k-1}\}.$$

This space is equipped with the $\mathbb{Z}_2$-action $(x, y, t) \to (x, y, 1 - t)$. This set certainly includes the previous one. So h is a $\mathbb{Z}_2$-map $\| K^{*2}_{\Delta} \| \to Z$. It suffices to show that $\text{ind}(Z) \leq k - 1$. Let S^{k-1} be represented as the unite sphere in $\mathbb{R}^k$. One can define the $\mathbb{Z}_2$-map $g : Z \to S^{k-1}$ by

$$g(x, y, t) := \frac{tx - (1 - t)y}{\| tx - (1 - t)y \|}.$$

If $tx - (1 - t)y = 0$ for unit vectors x, y, then $t = \frac{1}{2}$ and $x = y$. Also, this map gets the same value on the identified parts of the left side. Thus, the map is well defined,

and obviously continuous because before modding out the quotient space this map was $S^{k-1} \times S^{k-1} \times [0,1] \to S^{k-1}$ which is a continuous map. Clearly, g commutes with the respective $\mathbb{Z}_2$-actions. This concludes the proof.

1.5 Properties of the Box Complex in Special Graph Types

As previously discussed in Subsection 1.1, we introduced a special type of Kneser graph as $\mathrm{KG}\binom{[n]}{k}$. By applying the concept of the 2-colourability defect, cd_2, introduced in the Dol'nikov-Kříž Bound, and leveraging the results from Proposition 1.1.1, we can investigate the $\mathbb{Z}_2$-index of the Kneser graph $\mathrm{KG}\binom{[n]}{k}$. This will be detailed in the following proposition.

Proposition 1.5.1. Let G be the Kneser graph $\mathrm{KG}\binom{[n]}{k}$. Then $\mathrm{ind}(\mathrm{B}(G)) = n - 2k$ and $\chi(G) = n - 2k + 2$.

Proof: Let $\mathcal{F} \subseteq 2^{[n]}$ represent the set of vertices of the graph G. Each vertex corresponds to a k-subset of the n-set $[n]$. Recall 2-colourability defect from section 1.4.2. Our goal is to compute the 2-colourability defect, $\mathrm{cd}_2(\mathcal{F})$.

Consider a colouring scheme where we colour $k-1$ elements of $[n]$ in red and another $k-1$ elements in blue. The remaining elements of $[n]$, amounting to $n-2k+2$, are left uncoloured (or white). In this scenario, no set of $\mathcal{F}$ will be entirely red or entirely blue.

However, if we were to colour k elements in either red or blue, we would inevitably create a subset of size k that is monochromatic, which contradicts our objective. Thus, $k-1$ is the maximum number of elements that we can colour in one colour, either red or blue.

From this, we deduce that $\mathrm{cd}_2(\mathcal{F}) = n - 2k + 2$. According to the Hierarchy Theorem, the following inequality holds:

$$\chi(G) \geq \mathrm{ind}(\mathrm{B}(G)) + 2 \geq \mathrm{cd}_2(\mathcal{F}).$$

Furthermore, from Proposition 1.1.1, we have already established that $\chi(G) \leq n - 2k + 2$. Therefore

$$\begin{aligned} &n - 2k + 2 \leq \chi(G) \leq n - 2k + 2 \quad \text{and} \\ &n - 2k + 2 \leq \mathrm{ind}(\mathrm{B}(G)) + 2 \leq n - 2k + 2 \end{aligned}$$

which implies $\chi(G) = n - 2k + 2$ and $\mathrm{ind}(\mathrm{B}(G)) = n - 2k$. ∎

In [3], the authors presented a statement about the relationship between the absence of a 4-cycle in a graph and its $\mathbb{Z}_2$-index. Although the paper did not provide details

of the proof for this statement, we will elaborate on the proof here to elucidate the result concerning the $\mathbb{Z}_2$-index of graphs without a 4-cycle. For an alternative proof of this proposition, please refer to [7].

Proposition 1.5.2. [3] If the graph G does not include any 4-cycle C_4, then $\text{ind}(\text{B}(G)) \leq 1$.

Proof: To demonstrate the proposition, we aim to find a $\mathbb{Z}_2$-map from $\text{B}(G)$ to S^1. We construct this map in two steps. Firstly, we define a function f from $\text{sd}\,\text{B}(G)$ to a 1-dimensional subcomplex of $\text{B}(G)$. Secondly, we create a function from this 1-dimensional sub-complex to S^1.

The map f is applied on the vertices of $\text{sd}\,\text{B}(G)$, which are the simplices of $\text{B}(G)$. It's defined as follows:

$$f(A' \uplus A'') = \begin{cases} \emptyset \uplus \text{CN}(A') & |A'| \geq 2 \\ \text{CN}(A'') \uplus \emptyset & |A''| \geq 2 \\ A' \uplus A'' & \text{o.w} \end{cases} \tag{1.5.1}$$

In this function, f maps each simplex to a 1-dimensional or 0-dimensional simplex depending on its size. The intuition behind this function is to prepare for the subsequent mapping to S^1.

Consider a simplex $A' \uplus A''$ in $\text{B}(G)$. Then, (A', A'') forms a complete bipartite subgraph of G with A' on the left and A'' on the right. If both $|A'|$ and $|A''|$ are greater than or equal to 2, a cycle of length 4 would exist in this subgraph, contradicting our assumptions. Thus, at least one of $|A'|$ and $|A''|$ must be less than 2.

This argument ensures that if $|A'| \geq 2$ (or equivalently $|A''| \geq 2$), the number of common neighbours of A' (or A'' respectively) doesn't exceed 1. As a result, the image of $\text{sd}\,\text{B}(G)$ under the function f contains no simplex larger than 1-dimensional.

Also, $f(\text{sd}\,\text{B}(G))$ is a $\mathbb{Z}_2$-space, mapping $\emptyset \uplus \text{CN}(A')$ to $\text{CN}(A') \uplus \emptyset$ and swapping $A' \uplus A''$ and $A'' \uplus A'$, confirming that f is a $\mathbb{Z}_2$-map.

Next, we define a $\mathbb{Z}_2$-map g from $f(\text{sd}\,\text{B}(G))$ to S^1 embedded in $\mathbb{R}^2$, as follows:

$$g(A' \uplus A'') = \begin{cases} (1,0) & A' = \emptyset \\ (-1,0) & A'' = \emptyset \\ (0,1) \text{ or } (0,-1) & \text{o.w} \end{cases}$$

Note that if we choose $g(A' \uplus A'') = (0,1)$ then $g(A'' \uplus A') = (0,-1)$ and vise versa. This definition ensures that g maps the 1-dimensional subcomplex of $f(\text{sd}\,\text{B}(G))$ to S^1 and is a $\mathbb{Z}_2$-map.

The composite function $g \circ f$ is hence a $\mathbb{Z}_2$-map from $\text{sd}\,\text{B}(G)$ to S^1, implying that $\text{ind}\,\text{sd}\,\text{B}(G) \leq 1$. Therefore, by Lemma 1.3.3 (which states that the index of a simplicial complex is equal to the index of its barycentric subdivision), we conclude

that $\operatorname{ind} \mathrm{B}(G) \leq 1$. ∎

This proposition demonstrates that there are instances where the lower bounds outlined in the hierarchy theorem 1.4.1 can significantly deviate from the actual chromatic number of a graph. Since odd cycles do not include any 4-cycle, it can be concluded when G is an odd cycle we have $\operatorname{ind}(\mathrm{B}(G)) \leq 1$. The following proposition further refines our understanding of the $\operatorname{ind}(\mathrm{B}(G))$ for odd cycles.

Proposition 1.5.3. If G is an odd cycle, then $\operatorname{ind}(\mathrm{B}(G)) = 1$.

Proof: Let G be an odd cycle with $2n+1$ vertices. The vertices of $\mathrm{B}(G)$ are of the form $\{v\} \uplus \emptyset$ and $\emptyset \uplus \{v\}$ for each vertex v in $V(G)$, yielding a total of $2(2n+1)$ vertices.

Observe that the following sets enumerate all possible subsets of $V(G)$ sharing a common neighbour.

$$\{1,3\},\{3,5\},\{5,7\},...,\{2n+1,2\},\{2,4\},\{4,6\},...,\{2n,1\} \tag{1.5.2}$$

Each of these sets shares a common neighbour, and by the definition of $\mathrm{B}(G)$ in 1.3.1, they can form the components A' and A'' in the simplices of the form $A' \uplus \emptyset$ and $\emptyset \uplus A''$. These simplices are edges and, due to the order of the elements and order of the sets in (1.5.2), they form a cycle of $2n+1$ vertices. This is essentially a relabeling of G, and these cycles form either side of the box complex $\mathrm{B}(G)$.

Further, $\mathrm{B}(G)$ contains triangles of the form $A' \uplus A''$, where A' or A'' are as listed in (1.5.3). The triangles are

$$\{n, n+2\} \times \{n+1\} \quad , \quad \{n+1\} \times \{n, n+2\}. \tag{1.5.3}$$

These triangles interconnect, forming a hollow cylinder. The triangle $\{n, n+2\} \times \{n+1\}$ is attached to triangle $\{n\} \times \{n-1, n+1\}$ through the edge $\{n\} \times \{n+1\}$ and is attached to $\{n+2\} \times \{n+1, n+3\}$ through the edge $\{n+2\} \times \{n+1\}$. Since they are of dimension 2 and connect the left and right-hand sides, $\mathrm{B}(G)$ is a connected space. Figure 1.6 is an example of this box complex.

Since G does not contain a 4-cycle, $\operatorname{ind}(\mathrm{B}(G)) \leq 1$ (by Proposition 1.5.2). Also, $\mathrm{B}(G)$ is connected, so there is no $\mathbb{Z}_2$-map from this space to S^0, thus $\operatorname{ind}(\mathrm{B}(G)) = 1$. ∎

It is true that the chromatic number of a bipartite graph G is 2 and by the hierarchy theorem $\operatorname{ind}(\mathrm{B}(G)) \leq 0$ (i.e. $\operatorname{ind}(\mathrm{B}(G)) = 0$). Now, we want to confirm the index by finding the proper $\mathbb{Z}_2$-maps.

Lemma 1.5.4. If G is a bipartite graph, then $\mathrm{B}(G)$, $\mathrm{B}_{chain}(G)$, and $\mathrm{B}_{edge}(G)$ each admit a $\mathbb{Z}_2$-map to S^0.

Proof: Let $G = (A, B)$ be a bipartite graph, and let $s = s' \uplus s''$ be a simplex in $\mathrm{B}(G)$. By definition, $G[s', s'']$ must be complete. This imposes constraints on s' and s''.

Suppose $s', s'' \neq \emptyset$. Firstly, if $a, b \in s'$ where $a \in A$ and $b \in B$, then $s' \uplus s''$ cannot be a simplex of $\mathrm{B}(G)$ because s'' contains some elements from A or B or both of them, and there is no edge between a and the other elements of A, and no edge between b and other elements of B. So, $G[s', s'']$ cannot be complete. Secondly, if $s', s'' \subseteq A$ or $s', s'' \subseteq B$, $s' \uplus s''$ is also not a simplex of $\mathrm{B}(G)$ for the same reason.

If one of s' or s'' is empty, then complete $G[s', s'']$ happens when the non-empty side has a common neighbour. Again since it is a bipartite graph, a set of vertices from two sides cannot have a common neighbour and thus the nonempty side is a subset of just one side.

This leaves only the case where s' is a subset of A and s'' is a subset of B (or vice versa).

Let K and L be subcomplexes of $\mathrm{B}(G)$ defined as follows: a simplex $c = c' \uplus c''$ belongs to K if $c' \subseteq A$ and $c'' \subseteq B$, and to L if $c' \subseteq B$ and $c'' \subseteq A$. By the above reasoning, every simplex of $\mathrm{B}(G)$ belongs to either K or L, and $\mathrm{B}(G)$ is the disjoint union of K and L.

We define a $\mathbb{Z}_2$-action $\nu : \mathrm{B}(G) \to \mathrm{B}(G)$ with $\nu(K) = L$ and $\nu(L) = K$, and a simplicial map $f : \mathrm{B}(G) \to S^0 \subset \mathbb{R}$ by

$$f(K) = 1 \quad , \quad f(L) = -1 \tag{1.5.4}$$

which is a $\mathbb{Z}_2$-map since $f \circ \nu = \nu \circ f$.

Observing that the conditions in the definition of $\mathrm{B}(G)$ are also satisfied for $\mathrm{B}_{chain}(G)$ and $\mathrm{B}_{edge}(G)$, we find that $\mathrm{B}_{chain}(G)$ and $\mathrm{B}_{edge}(G)$ also decompose into two sub-complexes. A similar function to f therefore provides a $\mathbb{Z}_2$-map from $\mathrm{B}_{chain}(G)$ and $\mathrm{B}_{edge}(G)$ to S^0. ∎

We know even cycles and trees are bipartite subgraphs, hence by Lemma 1.5.4 the following corollary holds:

Corollary 1.5.5. If G is an even cycle or a tree, then $\mathrm{ind}(\mathrm{B}(G)) = 0$.

This proof also presents the simplicial complex structure of the box complex $\mathrm{B}(G)$ which is helpful to infer some structures of $\mathrm{B}_{edge}(G)$ and $\mathrm{B}_{chain}(G)$ as well. This information is useful in the next proposition.

Proposition 1.5.6. Let G be a bipartite subgraph of $\mathcal{P}(3^3)$. Then the box complexes $\mathrm{B}(G)$, $\mathrm{B}_{edge}(G)$, and $\mathrm{B}_{chain}(G)$ do not contain a S^n for $n \geq 1$ invariant to the $\mathbb{Z}_2$-action.

Proof: Recall from the proof of the previous lemma, each of $\mathrm{B}(G)$, $\mathrm{B}_{chain}(G)$, and $\mathrm{B}_{edge}(G)$ is expressed as a disjoint union of subcomplexes, denoted as K and

L. Moreover, these subcomplexes exhibit a $\mathbb{Z}_2$-action ν such that $\nu(K) = L$ and $\nu(L) = K$.

Suppose there exists an S^n for some $n \geq 1$ within the box complex. As S^n is connected, it must be fully contained in one of the disjoint components (either K or L). However, this creates a contradiction. Since the box complex and the S^n are both supposed to be $\mathbb{Z}_2$-equivariant, this would imply that all antipodal points on S^n would need to exist within the same component. This is impossible, as the $\mathbb{Z}_2$-action maps points from one component to the antipodal points in the other component. Thus, an S^n invariant to the $\mathbb{Z}_2$-action cannot exist in the box complex. ∎

Upon examining the definition of $\mathrm{B}_0(G)$, one observes that it requires $G[A', A'']$ to be complete. However, the previous lemma and Proposition 1.5.6 do not hold for this specific box complex. An illustrative example can be drawn from a simple bipartite graph G consisting of two vertices, a, b, connected by a single edge. Then $\mathrm{B}_0(G)$ is the simplicial complex in Figure 1.21.

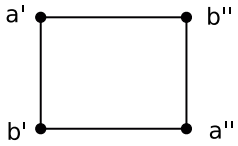

Figure 1.21: The box complex $\mathrm{B}_0(G)$ of a graph with two vertices and one edge

The box complex $\mathrm{B}_0(G)$ depicted above is a connected simplicial complex that is homeomorphic to S^1. Importantly, it cannot be mapped to S^0 via a $\mathbb{Z}_2$-map.

To demonstrate why, suppose a mapping function f exists. The only feasible way for f to continuously map $\mathrm{B}_0(G)$ to S^0 would be to map all elements to a single point in S^0. However, such a function would fail to commute with the $\mathbb{Z}_2$-actions on the domain and target spaces, violating a fundamental requirement for a $\mathbb{Z}_2$-map. Therefore, no $\mathbb{Z}_2$-map from $\mathrm{B}_0(G)$ to S^0 can exist.

Chapter 2

Partition Graph

"You wouldn't have the dream if you didn't already have what it takes to make it happen."

— Marie Forleo, Everything Is Figureoutable

In this chapter, we embark on an exploration of a unique family of graphs, termed as *partition graphs*, symbolized as $\mathcal{P}(g^g)$. This investigation delves into the complexity of these structures, beginning with simple elements and gradually escalating towards more complicated constructs.

Initially, we consider the partition graph $\mathcal{P}(2^2)$. Computing the chromatic number of this graph is a straightforward task. However, the complexity amplifies significantly when we move on to the partition graph $\mathcal{P}(3^3)$. As the size of the graph escalates exponentially, the task of finding the chromatic number becomes increasingly challenging.

Our approach to this challenge involves the utilization of the hierarchy theorem (Theorem 1.4.1). This theorem provides a potential strategy to bound the chromatic number of the graph G from below using topological tools. Among various lower bounds in this theorem, the Lovász bound proves to be the most potent. This bound is expressed in terms of the $\mathbb{Z}_2$-index of the box complex of the graph G.

We have previously established that almost all box complexes share a similar $\mathbb{Z}_2$-index (Theorem 1.3.5). In light of this, our research primarily focuses on the edge box complex of the partition graph, designated as $\mathrm{B}_{\mathrm{edge}}\big(\mathcal{P}(3^3)\big)$, due to its simpler structure compared to other box complexes. However, the computation and exploration of the topological characteristics of this object are far from simple; they demand the application of sophisticated topological methods. Some pertinent topological analyses related to this complex will be provided in subsequent chapters of this work.

Following the introduction and analysis of the basic features of the partition graph $\mathcal{P}(3^3)$, we aim to construct certain simplices of $\mathrm{B}_{\mathrm{edge}}\big(\mathcal{P}(3^3)\big)$. The construction of the remaining simplices of $\mathrm{B}_{\mathrm{edge}}\big(\mathcal{P}(3^3)\big)$ demands a further, more detailed analysis, which we undertake in subsequent chapters.

Through exhaustive search, it has been determined that $\chi(\mathcal{P}(3^3)) = 6$. In this chapter, we use mathematical tools to prove the known fact $\chi(\mathcal{P}(3^3)) \leq 6$. We also provide the groundwork for exploring the opposite inequality, $\chi(\mathcal{P}(3^3)) \geq 6$, by examining the box complex $\mathrm{B}_{\mathrm{edge}}\big(\mathcal{P}(3^3)\big)$. If a researcher aims to demonstrate $\operatorname{ind}\mathrm{B}_{\mathrm{edge}}\big(\mathcal{P}(3^3)\big) \geq 4$, a potential pathway is to uncover a "hollow" $\mathbb{Z}_2$-equivariant S^4 within $\mathrm{B}_{\mathrm{edge}}\big(\mathcal{P}(3^3)\big)$. Finding such an S^4 would confirm the non-existence of a $\mathbb{Z}_2$-map from $\mathrm{B}_{\mathrm{edge}}\big(\mathcal{P}(3^3)\big)$ to S^3, as outlined by the Borsuk-Ulam Theorem 1.1.6.

In the final section of this chapter, we prove the non-existence of an S^4 within the portion of $\mathrm{B}_{\mathrm{edge}}\big(\mathcal{P}(3^3)\big)$ we construct herein. By doing so, we lay the groundwork for further exploration and deeper understanding of the fascinating world of partition graphs.

2.1 Definition and Properties

We now focus on the core subject of this chapter: partition graphs. These are the intricate structures for which we aim to construct the box complex. We then further deepening our understanding of the complex nature of partition graphs by studying some of their general known properties.

In this text, permutation and combination are denoted as:

$$ {}^{m}P_k = \frac{m!}{(m-k)!} \quad , \quad \binom{m}{k} = {}^{m}C_k = \frac{m!}{k!(m-k)!}. $$

Definition 2.1.1. Every vertex of a *partition graph* $\mathcal{P}(g^g)$ is a partition of $\{1, 2, ..., g^2\}$ into g cells of size g. Two vertices u and v are adjacent if the intersection of each cell of u with each cell of v is nonempty.

Example 2.1.2. Suppose $g = 2$ and $G = \mathcal{P}(2^2)$. then the vertices of this graph are

$$ V(G) = \Big\{\big\{\{1,2\},\{3,4\}\big\}, \big\{\{1,3\},\{2,4\}\big\}, \big\{\{1,4\},\{2,3\}\big\}\Big\} $$

which are all adjacent, generating a triangle.

The following proposition provides an upper bound for the chromatic number of a partition graph:

Proposition 2.1.3. Let $G = \mathcal{P}(g^g)$ be a partition graph. Then

$$ \chi(\mathcal{P}(g^g)) \leq \binom{g+1}{2} $$

Proof: Fix a $g+1$ set $c \subseteq \{1, 2, ..., g^2\}$. For $i, j \in c, (i \neq j)$ let the set S_{ij} consists of all vertices which have i and j in one cell. Consider two arbitrary vertices u and v in S_{ij}. We shall call the cell with i and j in u and v respectively l and l'. Obviously $l \cap l' \neq \varnothing$. The cell l has $g-2$ more elements except i and j, also there are $g-1$ more cells in v except l'. So, by the pigeon hole theorem there is a cell in v which has empty intersection with l. Hence, u and v are not adjacent and as a result, S_{ij} is an independent set, i.e. there is no adjacent vertices in S_{ij}. So, we can assign one colour to each S_{ij}.

Now suppose x is an arbitrary vertex of $\mathcal{P}(g^g)$. Since x is a partition of $\{1, 2, ..., g^2\}$ into g cells of size g, there must exist $i, j \in c$ such that i, j are in one cell of x. It means $x \in S_{ij}$ and the independent set S_{ij} covers all the vertices of $\mathcal{P}(g^g)$, (For the overlap elements of some S_{ij} we can consider the colour assigned to any of the S_{ij}).

There are $\binom{g+1}{2}$ different S_{ij}, if we assign one colour to each S_{ij}, we have a proper colouring for $\mathcal{P}(g^g)$. Since the chromatic number is the minimum of all proper colourings, the inequality is true

$$\chi(\mathcal{P}(g^g)) \leq \binom{g+1}{2}.$$

∎

Proposition 2.1.4. Let $\mathcal{P}(g^g)$ be any partition graph. For every vertex v of $\mathcal{P}(g^g)$, there exists a corresponding vertex in a Kneser graph. This corresponding vertex is characterized by a set which encompasses all pairwise elements of the cells of v. Hence, every partition graph $\mathcal{P}(g^g)$ can be viewed as a Kneser graph.

Proof: Assume v to be a vertex of the partition graph, so it contains g cells, each of size g. The corresponding vertex in the Kneser graph, denoted as v', is defined as the set of all pairs chosen from the elements of each cell in v. As in standard Kneser graphs, two vertices are adjacent if and only if their corresponding sets are disjoint.

Consider two vertices u and v in $\mathcal{P}(g^g)$ that are adjacent. This adjacency implies that every cell in u intersects with each cell in v. Given the size of each cell is g and there are g cells in the set of each vertex, there is precisely one element from each cell of v present in each cell of u. Let's denote the corresponding vertices in the Kneser graph as u' and v'. Every pair selected from any cell of u contains two elements from two different cells of v. Thus, we cannot find any identical elements in u' and v'. Consequently, u' and v' are disjoint and therefore adjacent in the Kneser graph.

Now consider u' and v' as two arbitrary adjacent vertices of the Kneser graph. Their adjacency implies disjointness, which means there are no identical pair selections from any cell of u and any cell of v. Therefore, all the elements of each cell of u are dispersed among all cells of v, contributing just one element to each cell of v. As

a result, every cell of u intersects with every cell of v, which implies that u and v are adjacent in the partition graph. ∎

Proposition 2.1.5. The number of vertices in $\mathcal{P}(g^g)$ is given by

$$\frac{\binom{g^2}{g}\binom{g^2-g}{g}...\binom{g}{g}}{g!}. \tag{2.1.1}$$

Proof: The vertices of $\mathcal{P}(g^g)$ are composed of g disjoint cells, each of size g. There are $\binom{g^2}{g}$ choices for the first cell, $\binom{g^2-g}{g}$ choices for the second, and so forth until $\binom{g}{g}$ choices remain for the last cell.

This product gives the total count of g-cell sets satisfying two criteria: (i) each set covers the main set $1, ..., g^2$, and (ii) the cells in each set are disjoint. However, the count does not account for the condition that the order of cells within a vertex is irrelevant.

Given g disjoint cells, there are $g!$ different orderings to form a set. However, per the irrelevance of order, these variations represent the same vertex in $\mathcal{P}(g^g)$. Thus, we must divide the product $\binom{g^2}{g}\binom{g^2-g}{g}...\binom{g}{g}$ by $g!$ to get the exact vertex count. ∎

Proposition 2.1.6. The degree of each vertex of $\mathcal{P}(g^g)$ is equal to $(g!)^{g-1}$.

Proof: Consider an arbitrary vertex $v = \{c_1, c_2, \ldots, c_g\}$. As each cell of vertex v must have a nonempty intersection with each cell of an adjacent vertex, each cell of v contributes exactly one element to every cell of the adjacent vertex. For each cell c_i, there are $g!$ possible ways to distribute its elements among the cells of the adjacent vertex. Since there are g cells in v, the total number of combinations is $(g!)^g$. However, the order of the cells in the vertices is irrelevant. Therefore, we divide this number by $g!$. Consequently, the total number of adjacent vertices to vertex v is equal to $(g!)^{g-1}$.

Since this argument applies to an arbitrary vertex, the result holds for all vertices. We conclude that the degree of the vertices in the partition graph $\mathcal{P}(g^g)$ is equal to $(g!)^{g-1}$. ∎

Having familiarized ourselves with several recognized properties of a general partition graph, our attention now turns to particular instances of this graph. We aim to investigate their box complexes and establish the lower bounds of their chromatic numbers by applying Theorem 1.4.1. As we will see in Example 2.1.7, we can determine the lower bounds of the partition graph $\mathcal{P}(2^2)$ in a straightforward manner. However, the complexity escalates significantly when we progress to the partition graph $\mathcal{P}(3)$, which we will discuss in Example 2.1.8.

Example 2.1.7. Recall the graph $G = \mathcal{P}(2^2)$ from Example 2.1.2. The ground set of the vertices of the corresponding Kneser graph to $G = \mathcal{P}(2^2)$ is

$$X = \big\{\{1,2\},\{1,3\},\{1,4\},\{2,3\},\{2,4\},\{3,4\}\big\}$$

with 6 members. The set of the vertices of Kneser graph is

$$\mathcal{F} = \Big\{\big\{\{1,2\},\{3,4\}\big\},\big\{\{1,3\},\{2,4\}\big\},\big\{\{1,4\},\{2,3\}\big\}\Big\}$$

The following is the study of the chromatic number lower bounds of G:

The Lovász bound: The box complex $B(G)$ is homeomorphic to S^1, so, $\mathrm{ind}(B(G)) = 1$. In addition, the box complex $B_0(G)$ is homeomorphic to S^2, so, $\mathrm{ind}(B_0(G)) = 2$. Hence, the Lovász bound is 3.

Dol'nikov-Kříž Bound: The maximum cardinality of sets within K (as defined in Definition 1.1.4) is three. These sets follow one of two patterns: either all elements in a set include i, or none do, for each i in the set $1, 2, 3, 4$. Consequently, there exist $2 \times 4 = 8$ maximum cardinality sets in K.

Consider a maximal simplex of K^{*2}_{Δ}, for instance,

$$\big\{\{1,2\},\{1,3\},\{2,3\}\big\} \uplus \big\{\{1,4\},\{2,4\},\{3,4\}\big\}.$$

From this, we deduce that $\dim(K^{*2}_{\Delta}) = 5$ and calculate $\mathrm{cd}_2(\mathcal{F}) = n - 1 - \dim K^{*2}_{\Delta} = 6 - 1 - 5 = 0$. We find that this bound is not particularly informative.

The Bárány bound: The simplicial complex K has six vertices and eight maximal simplices, each formed by a triangle. Consider a cross polytope P in $\mathbb{R}^3$, which possesses six vertices located at the unit vectors and their corresponding antipodal points. We assign the vertices of K to match the vertices of P. The triangular faces of P are treated as the maximal simplices of K. With this arrangement, K is a subcomplex of the boundary complex of P, symbolized as $K \subseteq \delta P$. Thus the Bárány bound is $d = 3$.

The Sarkaria bound: Since Bárány bound and Lovász bound are 3, then Sarkaria bound is also 3.

Driven by curiosity, we used the data visualization application Gephi to visualize the partition graph $\mathcal{P}(3^3)$, shown in Figure 2.1. This image underlines the considerable size and complexity of the graph. However, it also highlights the limitations of relying solely on visualization for understanding such structures, underscoring the necessity of detailed mathematical analysis.

Example 2.1.8. Suppose $g = 3$ and $G = \mathcal{P}(3^3)$ is the partition graph. The vertices of $\mathcal{P}(3^3)$ are partitions of $\{1, 2, ..., 9\}$ into 3 cells of size 3.

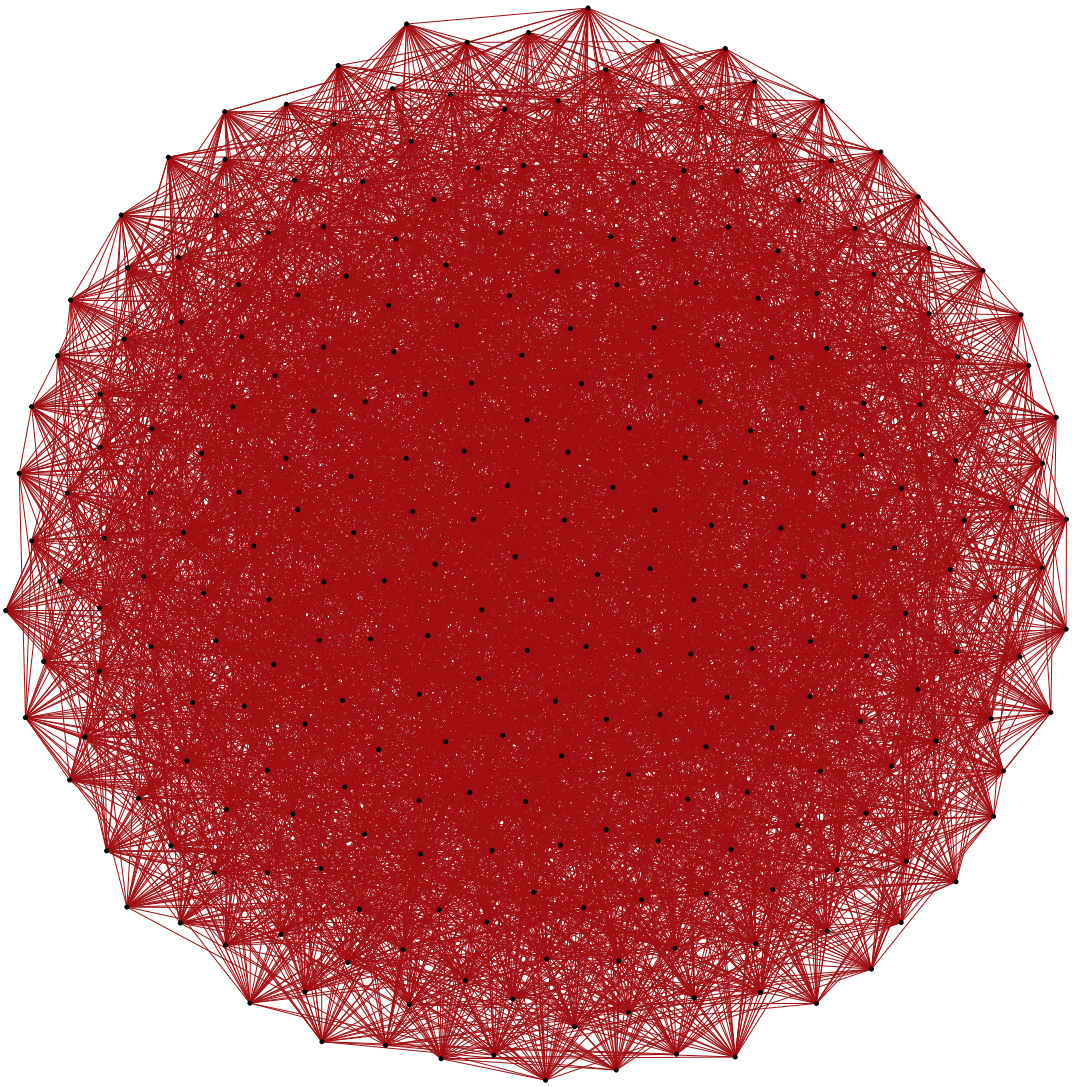

Figure 2.1: The partition graph $\mathcal{P}(3^3)$

In the following, we see examples of three vertices

$$V(\mathcal{P}(3^3)) = \Big\{\big\{\{1,2,3\},\{4,5,6\},\{7,8,9\}\big\},\big\{\{1,4,7\},\{2,5,8\},\{3,6,9\}\big\},\\ \big\{\{1,2,4\},\{3,5,6\},\{7,8,9\}\big\},...\Big\} \tag{2.1.2}$$

Denote the first three stated vertices in (2.1.2) as A, B, and C. In this configuration, A is connected to B but not to C, while B and C share no adjacency.

Let X be the ground set of elements forming the vertices of the Kneser graph $\mathrm{KG}(\mathcal{F}) = \mathcal{P}(3^3)$, then $|X| = \binom{9}{2} = 36$. Utilizing equation (2.1.1), we can derive the cardinality of $\mathcal{F}$:

$$|V(\mathcal{P}(3^3))| = |\mathcal{F}| = \frac{\binom{9}{3}\binom{6}{3}\binom{3}{3}}{3!} = 280. \tag{2.1.3}$$

The Dol'nikov-Kříž bound: Our goal is to color all elements of X with blue, red, or white such that no set in $\mathcal{F}$ is entirely red or blue, although complete whiteness is permissible. The elements of X are subsets of $\{1, 2, \cdots, 9\}$ with size 2. Assigning red to the sets containing only odd numbers, blue to the sets with only even numbers, and either blue or red to the mixed sets yields a proper coloring.

Why is this coloring considered proper? Essentially, we want to know why no set from $\mathcal{F}$ is completely red or blue. A set from $\mathcal{F}$ (or a vertex of the Kneser graph) consists of all pairs of elements across all cells of a given vertex of $\mathcal{P}(3^3)$. The union of all cells for every vertex of $\mathcal{P}(3^3)$ equals $c = \{1, 2, ..., 9\}$, and the cells of a vertex are disjoint sets of size 3. With 4 even and 5 odd numbers in the set c, the pigeonhole principle guarantees that at least one cell contains at least two odd numbers, and another cell contains at least two even numbers in every vertex of $\mathcal{P}(3^3)$. Consequently, each set in $\mathcal{F}$ will always contain one set with only odd numbers and one set with only even numbers. Thus, we can conclude that

$$\mathrm{cd}_2(\mathcal{P}(3^3)) = 0.$$

However, as we observe, this lower bound does not provide substantial information about the chromatic number.

The following proposition demonstrates that the clique number in this graph is not very large.

Proposition 2.1.9. The largest clique in $\mathcal{P}(3^3)$ is of size four.

Proof: Suppose the vertices u, v, x are adjacent in $\mathcal{P}(3^3)$. We aim to find another vertex adjacent to all of them. Let $n \in \{1, 2, \ldots, 9\}$ be an arbitrary element. This element is in a cell of vertex u along with two other elements, and it forms a cell with two other elements in vertex v, as well as in vertex x. These elements are all distinct

because u, v, and x are adjacent. Consequently, the element n cannot be placed into one cell with six other elements to make a new vertex adjacent to all the vertices u, v, x. However, there are two other elements we can utilize to form a cell with the element n in the new vertex. This approach allows us to find a 4-clique in $\mathcal{P}(3^3)$. It is not possible to add another vertex adjacent to all the vertices of a 4-clique because now the element n cannot form a cell with eight other elements, leaving no additional elements to create a cell. ∎

With a similar argument, we have the following proposition:

Proposition 2.1.10. Every edge and every triangle of $\mathcal{P}(3^3)$ are included in exactly one 4-clique.

Proof: Let v and w be two adjacent vertices in $\mathcal{P}(3^3)$. Let $n \in \{1, 2, \cdots, 9\}$, and s be a common neighbour of v and w. In order to place n in a cell of s, we need to identify and insert a pair of elements from the set $\{1, 2, \cdots, 9\}$ alongside n, such that they are neither together nor with n in any cells of v and w. Since v and w are adjacent, there are two elements from the set $\{1, 2, \cdots, 9\}$ that are with n in one cell of v, and two other elements in a cell of w. Consequently, the number of choices for elements in the same cell as n is reduced to four, specifically the elements not present with n in the cells of v and w. There are six possible pairs of elements out of these four elements. However, four of these pairs already exist in the cells of v and w without n. Therefore, only two pairs of elements are available that do not already exist in the cells of v and w, which can be used to place next to n and construct the vertex s.

In Proposition 2.1.9, we observed the existence of a 4-clique. This means a pair of adjacent vertices have two common neighbours within this 4-clique. Here, we demonstrated that this pair of vertices cannot have more than two common neighbours. Consequently, their only common neighbours are exclusive to the 4-clique. We can conclude that each edge and each triangle are included in only one 4-clique. ∎

2.2 Sub-structures of $\mathbf{B_{edge}}\big(\mathcal{P}(3^3)\big)$

According to the definition of the edge box complex outlined in 1.3.1, the simplices of $\mathrm{B}_{\mathrm{edge}}\big(\mathcal{P}(3^3)\big)$ consist of subsets taken from edge sets of complete bipartite subgraphs found within $\mathcal{P}(3^3)$. Our first step in this exploration is to identify these complete bipartite subgraphs embedded within $\mathcal{P}(3^3)$. This task, however, is not a simple one; it demands a complex analysis, which we provide in the forthcoming chapters. Nevertheless, there exist two families of complete bipartite subgraphs of $\mathrm{B}_{\mathrm{edge}}\big(\mathcal{P}(3^3)\big)$ that

prove to be more manageable to our examination. In this section, we will introduce these families and delve into a comprehensive analysis of their unique characteristics.

Definition 2.2.1. Some definitions of the objects that appear in this text multiple times:

1. *neighbourhood subgraph*: the bipartite graph formed by a vertex i, all of its neighbours in $\mathcal{P}(3^3)$, and the edges between them, often denoted as $K_{1,36} = (i, \mathrm{CN}(i))$.

2. *neighbourhood simplex*: part of $\mathrm{B}_{\mathrm{edge}}\big(\mathcal{P}(3^3)\big)$ derived from a neighbourhood subgraph of the vertex i, often denoted as $S_{1,36} = \{i\} \times \{\mathrm{CN}(i)\}$ with the antipodal $S_{36,1} = \{\mathrm{CN}(i)\} \times \{i\}$.

3. *4-clique complex*: part of $\mathrm{B}_{\mathrm{edge}}\big(\mathcal{P}(3^3)\big)$ derived from a 4-clique.

Let the Figure 2.2 be a 4-clique of $\mathcal{P}(3^3)$

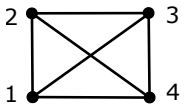

Figure 2.2: A 4-clique of $\mathcal{P}(3^3)$

The Figure 2.3 is the simplicial complex in $\mathrm{B}_{\mathrm{edge}}\big(\mathcal{P}(3^3)\big)$ produced by this 4-clique

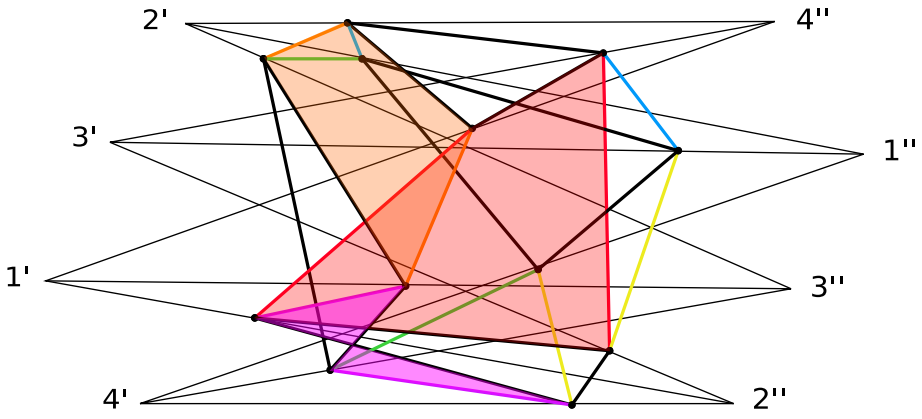

Figure 2.3: The simplicial complex of $\mathrm{B}_{\mathrm{edge}}\big(\mathcal{P}(3^3)\big)$ derived from a 4-clique

There are 8 triangles (like $\{1\} \times \{2, 3, 4\}$) and 6 tetrahedrons (like $\{1, 2\} \times \{3, 4\}$) in this simplicial complex. In order to decrease the number of edges in the figure instead of drawing all the edges of tetrahedrons we just drew four edges of each.

Also, instead of showing all the tetrahedrons, we only highlighted three of them by light purple, light orange, and light red. We can redraw it as the following:

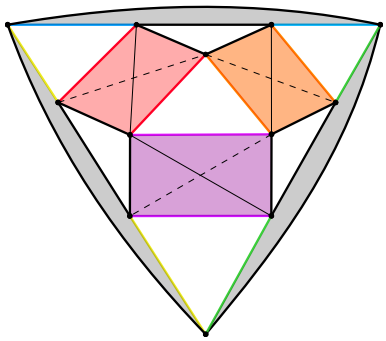

Figure 2.4: 4-clique complex

In the above figure the highlighted areas represent the tetrahedrons and the curvy triangle is a normal triangle but since its edges lie on the other edges we drew it curvy to be visible. The triangles are also filled, they are not highlighted here in order to be different from the tetrahedrons.

Each vertex of $\mathcal{P}(3^3)$ is included within twelve distinct 4-cliques. These 4-cliques consist of the primary vertex under consideration and all its neighbours. Now consider a vertex and two of its 4-cliques as below

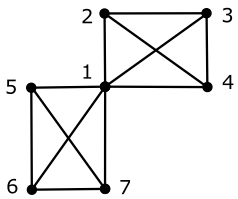

Figure 2.5: A vertex with two 4-cliques

The part of $\mathrm{B}_{\mathrm{edge}}\big(\mathcal{P}(3^3)\big)$ for this graph is too complicated to be drawn completely but we know it is formed by two 4-clique complexes and the simplices $\{1\} \times \{234567\}$ and $\{234567\} \times \{1\}$. The following figure shows these two simplices

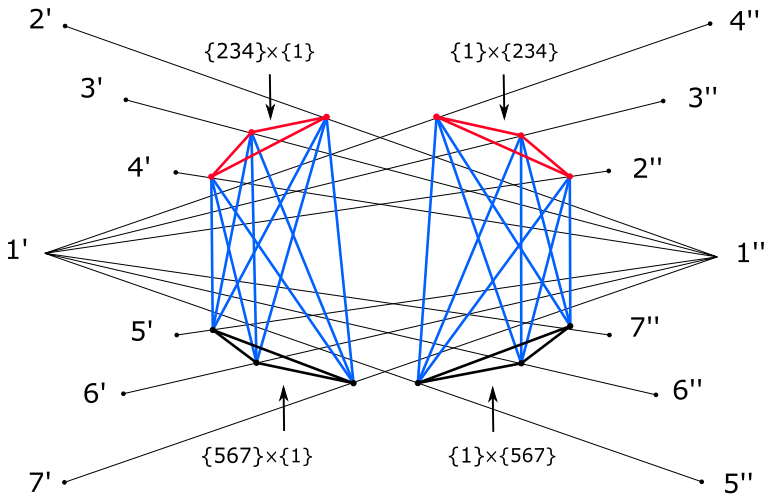

Figure 2.6: Simplex that attaches two 4-clique complexes

The red triangles are from the 4-clique with vertices $\{1, 2, 3, 4\}$ and the black triangles are from the 4-clique with vertices $\{1, 5, 6, 7\}$. The blue edges are part of a neighbourhood simplex that attaches two 4-clique complexes. In the real $\mathrm{B}_{\mathrm{edge}}\big(\mathcal{P}(3^3)\big)$ this simplex is much bigger than this figure because here we just considered 5 neighbours of the vertex 1 but this vertex has 36 neighbours by Proposition 2.1.6.

Figure 2.7 is another form of the 4-clique complex in Figure 2.2 In the recent

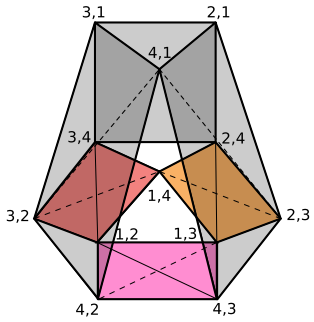

Figure 2.7: Another point of view of a 4-clique complex

Figure 2.7, we attempt to visualize a 4-clique complex in three dimensions. To facilitate this, we use the same colours as in Figure 2.2 to enable the reader to easily identify correspondences between the two representations.

An interesting property of a 4-clique complex is its symmetry: placing any of the triangles at the top results in the same three-dimensional structure. Furthermore, it can be deduced that the 4-clique complex is homotopy equivalent to an S^2. This is because it can be embedded in $\mathbb{R}^3$ centred around the origin and subsequently deformed into a sphere without changing its topological properties.

In the graph $\mathcal{P}(3^3)$, each vertex is adjacent to three others to form a 4-clique. Since each vertex is adjacent to 36 other vertices, it is part of 12 different 4-cliques. This creates 12 separate 4-clique groups in $\mathrm{B}_{\mathrm{edge}}\big(\mathcal{P}(3^3)\big)$.

These 12 4-clique complexes converge at a central, high-dimensional structure—a 35-dimensional neighbourhood simplex. This simplex serves as a hub, linking the 4-clique complexes via their constitutive triangles.

In other words, each triangle belonging to a 4-clique complex is shared with a neighbourhood simplex, while the tetrahedrons are uniquely contained within the 4-cliques themselves.

The Figure 2.8 serves as a visual aid, depicting a section of $\mathrm{B}_{\mathrm{edge}}\big(\mathcal{P}(3^3)\big)$ formed by vertex 1 and all the 4-cliques attached to it. The blue arrows indicate the neighbourhood simplex of vertex 1, offering a simplified representation of the blue simplex illustrated in Figure 2.6.

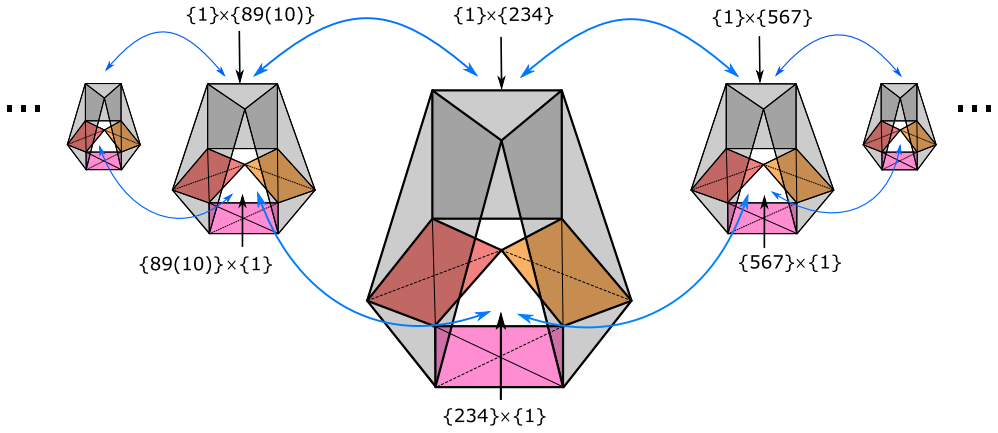

Figure 2.8: part of $\mathrm{B}_{\mathrm{edge}}\big(\mathcal{P}(3^3)\big)$ formed by the vertex 1 and all the attached 4-cliques

Consider once again a 4-clique consisting of vertices $1, 2, 3, 4$. Given that each 4-clique in $\mathcal{P}(3^3)$ encompasses four vertices, we have the flexibility to examine a 4-clique from four distinct viewpoints. Essentially, the analysis and visualizations performed for vertex 1 can be replicated for vertices 2, 3, and 4.

Translating this to $\mathrm{B}_{\mathrm{edge}}\big(\mathcal{P}(3^3)\big)$, it follows that each 4-clique complex is connected to four separate neighbourhood simplices through its triangles. To elaborate, each 4-clique complex has 8 triangles, with each triangle and its antipodal being a part of a neighbourhood simplex and its antipodal respectively.

Figure 2.9 visually represents a 4-clique complex centralized within four distinct chains of 4-cliques, each accompanied by their respective neighbourhood simplices for each vertex 1, 2, 3, and 4. Arrows of the same colour represent the same neighbourhood simplex and its antipodal.

This pattern is consistently reproduced for each 4-clique within $\mathcal{P}(3^3)$, leading to a corresponding structure within $\mathrm{B}_{\mathrm{edge}}\big(\mathcal{P}(3^3)\big)$.

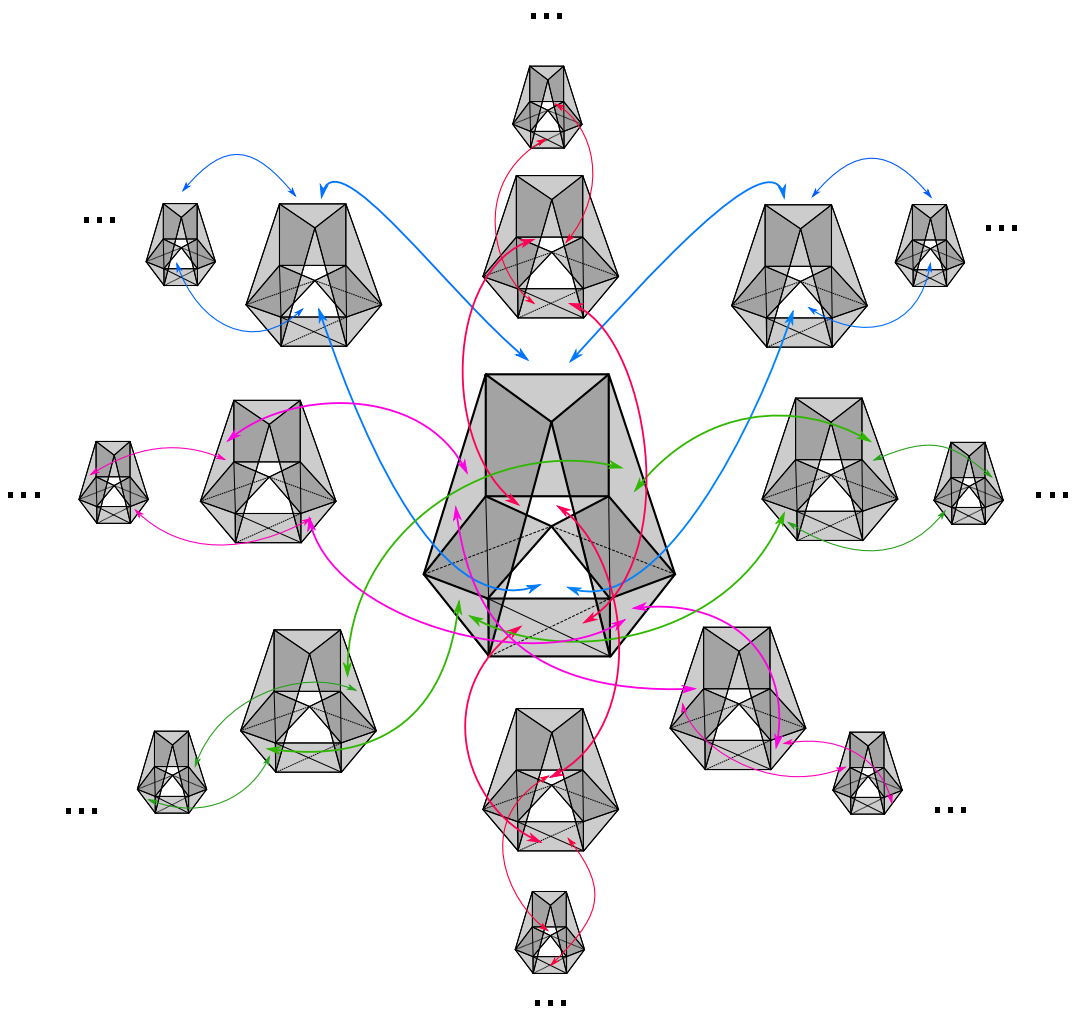

Figure 2.9: A segment of $\mathrm{B}_{\mathrm{edge}}\big(\mathcal{P}(3^3)\big)$ formed by a 4-clique complex and four related chains of 4-clique complexes linked by neighbourhood simplices

2.3 The Simplicies of $\mathrm{B}_{\mathrm{edge}}\big(\mathcal{P}(3^3)\big)$ Without an S^3

In the preceding section, we have uncovered a section of $\mathrm{B}_{\mathrm{edge}}\big(\mathcal{P}(3^3)\big)$. With this in mind, we can now assess whether a $\mathbb{Z}_2$-equivariant S^3 exists in this part. Recall that, the presence of a "hollow" $\mathbb{Z}_2$-equivariant S^4 within $\mathrm{B}_{\mathrm{edge}}\big(\mathcal{P}(3^3)\big)$ would indicate the non-existence of a $\mathbb{Z}_2$-map from $\mathrm{B}_{\mathrm{edge}}\big(\mathcal{P}(3^3)\big)$ to S^3. Consequently, we would have $\operatorname{ind}\mathrm{B}_{\mathrm{edge}}\big(\mathcal{P}(3^3)\big) \geq 4$ which implies $\chi(\mathcal{P}(3^3)) \geq 6$. However, our investigation

demonstrates that there is no S^3 present in this section of $\mathrm{B}_{\mathrm{edge}}\big(\mathcal{P}(3^3)\big)$. This absence, in turn, confirms that no S^4 exists in this segment.

It is important to note that by Proposition 2.1.3 the chromatic number $\chi(\mathcal{P}(3^3))$ must be less than or equal to 6. Thus, a $\mathbb{Z}_2$-map from the box complex $\mathrm{B}_{\mathrm{edge}}\big(\mathcal{P}(3^3)\big)$ to S^4 must indeed exist. If such a map were absent, then by hierarchy theorem 1.4.1 $5 \leq \mathrm{ind}(\mathrm{B}_{\mathrm{edge}}\big(\mathcal{P}(3^3)\big))$ would lead to the false conclusion that $7 \leq \chi(\mathcal{P}(3^3))$.

Before reaching the final objective of this chapter, we must establish a series of preliminary lemmas, to set a solid foundation for our conclusion.

Lemma 2.3.1. The 4-clique complexes are disjoint.

Proof: It is a direct result of Proposition 2.1.10. The vertices of $\mathrm{B}_{\mathrm{edge}}\big(\mathcal{P}(3^3)\big)$ are the directed edges of $\mathcal{P}(3^3)$, and each edge is included in one 4-clique. Therefore, there is no intersection between two or more 4-clique complexes. ∎

Lemma 2.3.2. The set of vertices of $\mathrm{B}_{\mathrm{edge}}\big(\mathcal{P}(3^3)\big)$ is the union of the vertices of all 4-clique complexes.

Proof: Each vertex of $\mathrm{B}_{\mathrm{edge}}\big(\mathcal{P}(3^3)\big)$ is a directed edge in $\mathcal{P}(3^3)$. In Proposition 2.1.10 we saw each edge is included in one 4-clique, so the two directions of each edge are included in that 4-clique. Also, in the previous lemma 2.3.1, we observed the 4-clique complexes are disjoint. Therefore, the union of all the vertices of the 4-cliques is equal to the set of vertices of $\mathrm{B}_{\mathrm{edge}}\big(\mathcal{P}(3^3)\big)$. ∎

The Lemma 2.3.1 and the fact that 4-clique complexes are homotopy equivalent to S^2 lead to the following theorem:

Theorem 2.3.3. The box complex $\mathrm{B}_{\mathrm{edge}}\big(\mathcal{P}(3^3)\big)$ derived from the 4-cliques of $\mathcal{P}(3^3)$ does not contain any sub-complex homotopy equivalent to a S^3.

Proof: The portion of $\mathrm{B}_{\mathrm{edge}}\big(\mathcal{P}(3^3)\big)$ formed by the 4-clique complexes consists of a disjoint union of complexes, each homotopy equivalent to S^2. It is important to note that no sub-complex of S^2 can be homotopy equivalent to S^3, as S^2 does not possess any higher-dimensional holes.

Moreover, the disjoint union of two or more S^2 complexes results in a disconnected space, while S^3 is known to be connected. Consequently, there can be no S^3 included in the part of $\mathrm{B}_{\mathrm{edge}}\big(\mathcal{P}(3^3)\big)$ formed by the 4-clique complexes. ∎

This theorem ensures that there is no sub-complex of all the 4-clique complexes homotopy equivalent to any S^n for $n \geq 3$ because each S^n includes S^m for $m < n$.

In Theorem 2.3.5, we extend our investigation by including another family of simplices from $\mathrm{B}_{\mathrm{edge}}\big(\mathcal{P}(3^3)\big)$, the neighbourhood simplices (introduced in Definition

2.2.1), to the 4-clique complexes and examine the existence of an S^3 in this complex. We do it by exploring the intersections between neighbourhood simplices and 4-clique complexes.

Before delving into the proof of the theorem, it is essential to grasp the concept of *triangulation*. In a broad sense, triangulation refers to the transformation of topological spaces into piecewise linear spaces via the selection of a homeomorphism to a suitable simplicial complex. Spaces that are homeomorphic to a simplicial complex are known as *triangulable*.

Definition 2.3.4. A triangulation of a topological space X is a homeomorphism $t : K \to X$ where K is a simplicial complex.

An illustrative example of this concept is the triangulation of a 3-dimensional ball B^3, which results in a filled tetrahedron.

Theorem 2.3.5. There is no S^3 in the portion of $\mathrm{B}_{\mathrm{edge}}\big(\mathcal{P}(3^3)\big)$ formed by the 4-clique complexes and neighbourhood simplicies.

Proof: To construct a triangulation of S^3, we seek a collection of tetrahedra glued together along their faces. However, upon examination of the 4-clique complexes and the neighbourhood simplices, we conclude that such a collection does not exist. This conclusion is reached by analyzing the intersections between 4-cliques and neighbourhood simplices. Let C be a 4-clique and C_s be the 4-clique complex of $\mathrm{B}_{\mathrm{edge}}\big(\mathcal{P}(3^3)\big)$ corresponding to the 4-clique C.

In the subsequent analysis, we will examine different cases of intersection between 4-clique complexes and neighbourhood simplices.

- Intersection of a 4-clique and a neighbourhood simplex:

  Recall that the simplices of $\mathrm{B}_{\mathrm{edge}}\big(\mathcal{P}(3^3)\big)$ are subsets of the ordered edges of the complete bipartite subgraphs of $\mathcal{P}(3^3)$. Let i be one of the vertices of C_s, and let $S_{1,36} = \{i\} \times \{\mathrm{CN}(i)\}$. Then, $C_s \cap S_{1,36} = \{i\} \times \{\mathrm{CN}(i)\} \cap C_s$, which contains all three ordered edges $\{i\} \times \{.\}$ of C where $\{.\}$ is other vertices of C. Thus, $|C_s \cap S_{1,36}| = 3$. If i is not one of the vertices of the 4-clique C, then $C_s \cap S_{1,36} = \emptyset$. The same analysis applies to a $S_{36,1}$. Since a 4-clique has 4 vertices, it shares 4 triangles with 4 neighbourhood simplices and 4 triangles with their antipodals.

- Intersection of two different neighbourhood simplices on a 4-clique:

  Let i, j be two vertices of the 4-clique C, and let $S_{1,36} = \{i\} \times \{\mathrm{CN}(i)\}$ and $S'_{1,36} = \{j\} \times \{\mathrm{CN}(j)\}$. Obviously, since $i \neq j$, these two simplices have no intersections on this 4-clique or anywhere else. However, each of them shares one vertex with the antipodal of the other one on this 4-clique and nowhere else. Namely, $S_{1,36} \cap S'_{36,1} = \{i\} \times \{j\}$ and $S_{36,1} \cap S'_{1,36} = \{j\} \times \{i\}$.

Additionally, if two different neighbourhood simplices connected to this 4-clique are not antipodal to each other, they are not part of another 4-clique. If both of them were part of another 4-clique, then both vertices i and j would be included in that 4-clique, and i and j would be adjacent in the corresponding 4-clique. We proved in Proposition 2.1.10 that each edge is included in only one 4-clique. Thus, these two neighbourhood simplices do not share anything with other 4-clique complexes.

It is clear that any two antipodal neighbourhood simplices do not share any elements. As previously demonstrated in Figure 2.8, these antipodal neighbourhood simplices are part of 12 distinct 4-cliques, sharing a triangle with each 4-clique complex.

Therefore, we can conclude that there is no path of tetrahedra glued together on their faces to form a triangulation of S^3 in this portion of $\mathrm{B}_{\mathrm{edge}}\big(\mathcal{P}(3^3)\big)$. ∎

Based on this theorem, it can be concluded that no S^n structures for $n \geq 3$ are present in the portion of $\mathrm{B}_{\mathrm{edge}}\big(\mathcal{P}(3^3)\big)$ composed of 4-clique complexes and neighbourhood simplices.

Chapter 3

Vertex Classification of $\mathcal{P}(3^3)$

"Are you ready?" Klause asked friendly.
"No", Sunny answered.
"Me neither", Violet said, "but if we wait until we're ready, we'll be waiting for the rest of our lives."

— Daniel Handler, A Series of Unfortunate Events

In this chapter, we delve deeper into the structure of the graph $\mathcal{P}(3^3)$, focusing specifically on the analysis of vertex pairs and triples. Initially, we establish a particular relationship between the vertex pairs, leading to their categorization into four equivalence classes. This classification is predicated on the existence of a permutation of $\mathrm{Sym}(3^3)$ within two vertex pairs of a class. Subsequently, we classify vertex triples into equivalence classes, a task more complex than the pairs. The results of these analyses provide the basis for the succeeding chapter, where we aim to identify and categorize all complete bipartite subgraphs of $\mathcal{P}(3^3)$.

Prior to our exploration of the vertex pairs within the specific graph $\mathcal{P}(3^3)$, we show that any general partition graph $\mathcal{P}(g^g)$ exhibits vertex-transitivity.

Let H be a group acting on some set X and $x \in X$. The stabilizer and orbit of x by group H are

$$\mathrm{stab}_H(x) = \{\gamma \in H : \gamma(x) = x\} \tag{3.0.1}$$
$$\mathrm{orb}_H(x) = \{\gamma(x) : \gamma \in H\} \tag{3.0.2}$$

The permutations of a symmetric group $\mathrm{Sym}(n)$ are bijective functions. Therefore, the group $\mathrm{Sym}(g^2)$ is an automorphism on $\mathcal{P}(g^g)$ because each permutation maps one vertex to another.

Proposition 3.0.1. The partition graph $\mathcal{P}(g^g)$ is vertex-transitive.

Proof: (**Proof by Examination of Structure**)
Consider each vertex of $\mathcal{P}(g^g)$ as a partition of $\{1, 2, \ldots, g^2\}$ into g cells, each of size g. Hence, these vertices exhibit a consistent structure. Let v and w be two vertices of $\mathcal{P}(g^g)$ as the following:

$$v = \{\{v_{1,1}, v_{1,2}, \ldots, v_{1,g}\}, \ldots, \{v_{g,1}, \ldots, v_{g,g}\}\}$$
$$w = \{\{w_{1,1}, w_{1,2}, \ldots, w_{1,g}\}, \ldots, \{w_{g,1}, \ldots, w_{g,g}\}\}.$$

To find permutations mapping vertex v to w, we first align the cells of v with those of w, map $v_{i,j}$ to $w_{i,j}$, and subsequently remove the brackets. As illustrated below:

$$\begin{pmatrix} \overbrace{v_{1,1}\ v_{1,2}\ \ldots v_{1,g}}^{\text{cell } v_1} \ldots \overbrace{v_{g,1} \ldots v_{g,g}}^{\text{cell } v_g} \\ \underbrace{w_{1,1}\ w_{1,2} \ldots w_{1,g}}_{\text{cell } w_1} \ldots \underbrace{w_{g,1} \ldots w_{g,g}}_{\text{cell } w_g} \end{pmatrix}$$

which is a permutation of the elements in $\{1, 2, \ldots, g^2\}$ that maps v to w. ∎

Proof: (**Proof by Application of the Orbit-Stabilizer Theorem**)
We define $H = \mathrm{Sym}(g^2)$, which acts on the vertices of $\mathcal{P}(g^g)$. Thus, $|H| = g^2!$. The orbit-stabilizer theorem then suggests the following relation for a vertex x of $\mathcal{P}(g^g)$:

$$|H| = |\mathrm{stab}_H(x)| \cdot |\mathrm{orb}_H(x)|.$$

Since the stabilizer of x, denoted $\mathrm{stab}_H(x)$, encompasses all permutations of g elements for each cell of x and all permutations of g cells of x, we find that $|\mathrm{stab_H}(x)| = (g!)^{g+1}$. Therefore, $|\mathrm{orb}_H(x)| = \frac{(g^2)!}{(g!)^{g+1}}$. Earlier in Proposition 2.1.5, we established that the number of vertices of $\mathcal{P}(g^g)$ equates to $\frac{\binom{g^2}{g}\binom{g^2-g}{g}\cdots\binom{g}{g}}{g!}$. It is readily apparent that $|\mathrm{orb}_H(x)|$ equals the number of vertices:

$$\begin{aligned} \frac{\binom{g^2}{g}\binom{g^2-g}{g}\cdots\binom{g}{g}}{g!} &= \frac{1}{g!}\Big(\frac{(g^2)!}{g!(g^2-g)!}\Big)\Big(\frac{(g^2-g)!}{g!(g^2-2g)!}\Big)\cdots\Big(\frac{(g^2-(g-2)g)!}{g!g!}\Big)\Big(\frac{(g^2-(g-1)g)!}{g!}\Big) \\ &= \frac{(g^2)!}{(g!)^{g+1}} = |\mathrm{orb}_H(x)|. \end{aligned}$$

Given that only a single orbit exists for each vertex of $\mathcal{P}(g^g)$, we conclude that this graph is indeed vertex-transitive. ∎

3.1 Vertex Pairs of $\mathcal{P}(3^3)$

In this section, we turn our attention to complete bipartite subgraphs in which one side is composed solely of two vertices within $\mathcal{P}(3^3)$. To accomplish this, we explore the different possibilities for all pairs of vertices in $\mathcal{P}(3^3)$.

Recall that each vertex in $\mathcal{P}(3^3)$ represents a partition of the set $1, 2, \ldots, 9$ into three cells, each containing three elements. Two vertices, u and v, are connected by an edge if and only if every cell of u intersects with every cell of v.

For clarity and convenience, we may depict a vertex $x = \{x_1, x_2, x_3\}$, where each x_i represents a cell $\{a, b, c\}$, $i \in 1, 2, 3$, and $a, b, c \in \{1, 2, \cdots, 9\}$. Sometimes we denote a vertex in an informal but practical table form as follows:

abc
def
ghi

This visual representation aids in understanding and communicating the structural arrangements of vertices in $\mathcal{P}(3^3)$.

3.1.1 Definition

Each vertex pair of type n can be succinctly represented using a 3×3 grid pattern. In this configuration, the union of the elements in each row corresponds to a cell of one vertex, while the union of elements in each column corresponds to a cell in the other vertex of the pair. Due to this arrangement, the shared elements between the cells of the two vertices occupy the same cell in this grid.

Let us consider vertices v and w with their respective cells given by $v = \{v_1, v_2, v_3\}$ and $w = \{w_1, w_2, w_3\}$. The grid pattern for the vertex pair v, w would then be as follows, where each row represents a cell from v and each column represents a cell from w:

$v_1 \cap w_1$	$v_1 \cap w_2$	$v_1 \cap w_3$
$v_2 \cap w_1$	$v_2 \cap w_2$	$v_2 \cap w_3$
$v_3 \cap w_1$	$v_3 \cap w_2$	$v_3 \cap w_3$

Table 3.1: The grid pattern of v and w

It is important to note that reordering the rows or columns of the grid does not alter the vertex pair. Additionally, transposing the grid (i.e., swapping rows with columns, akin to the transpose of a matrix) also leaves the pair unchanged. However, post-transposition, the cells of v become the columns and those of w become the rows.

As an example, consider a specific pair of vertices, v and w. In their grid pattern representation, the intersections of the cells of v and w are explicitly shown. Here, the rows correspond to the cells of v and the columns to the cells of w:

123	123
456	489
789	756
v	w

123		
	4	56
	89	7

The grid pattern of v and w

The following presents a categorization of vertex pairs within the graph $\mathcal{P}(3^3)$, as classified by their respective grid patterns. We initially focus on introducing vertex pairs' grid patterns of types 3, 5, 6, 7, and 9. Later, in Proposition 3.1.3, it will be demonstrated that these are the exclusive types of grid patterns that can be attributed to the vertex pairs.

Definition 3.1.1. Consider the elements $a_1, \ldots, a_9$, each belonging to the set $\{1, 2, \ldots, 9\}$ such that $a_i \neq a_j$ whenever $i \neq j$, and let v and w represent a pair of vertices within $\mathcal{P}(3^3)$. We define the vertex pair to be of a particular *type* - 3, 5, 6, 7, or 9 - if the grid pattern of the pair corresponds to the patterns shown in Table 3.3. For each vertex pair v, w, we use $\mathrm{T}(v, w) = n$ to denote that v, w are of type n. Given that each grid pattern's uniqueness extends to swapping rows, swapping columns, and transposition, we hereby establish these grids as the representatives of their respective types. We will refer to these as the *standard* grid pattern.

As the number of non-empty locations within each type's grid pattern is unique, we have chosen to denote the pattern type by the quantity of these non-empty spots on its grid. It is noteworthy that type 3, which refers to a pair of identical vertices within $\mathcal{P}(3^3)$, will not be of interest in our study, due to the fact that all the vertices of $\mathcal{P}(3^3)$ are distinct.

Lemma 3.1.2. If two vertices v and w within the graph are neither identical nor adjacent, it follows that there must exist at least one cell within v and another within w that share a pair of elements.

Proof: Let us consider v and w, two distinct vertices that are not adjacent. Recalling Definition 2.1.1, which outlines the conditions for adjacency, we note that there must be at least one cell within v and another within w that are disjoint. Given that there is no prescribed order to the cells within a vertex, we can, without loss of generality, posit that $v_1 \cap w_3 = \emptyset$.

The subsequent examination proceeds in two branches:

- Suppose cell v_1 is also disjoint from another cell in w, say w_2. In this case, v_1 must be equivalent to w_1. If we were to assume that v_2 is equivalent to

$a_1a_2a_3$		
	$a_4a_5a_6$	
		$a_7a_8a_9$

Type 3

$a_1a_2a_3$		
	a_4	a_5a_6
	a_7a_8	a_9

Type 5

a_1		a_2a_3
a_4a_5	a_6	
	a_7a_8	a_9

Type 6

a_1	a_2	a_3
a_4	a_5a_6	
a_7		a_8a_9

Type 7

a_1	a_2	a_3
a_4	a_5	a_6
a_7	a_8	a_9

Type 9

Table 3.3: The grid pattern of vertex pairs of different types

another cell of w, e.g., w_2, this would necessitate that v_3 is equivalent to w_3. Consequently, we would conclude that v equals w, a conclusion that contradicts our initial assumption. Therefore, v_2 cannot be equivalent to any cell of w, and it must share one element with either w_2 or w_3, and two elements with the remaining cell. The same argument can be applied to cell v_3.

- Should cell v_1 share elements with all other cells of w apart from w_3, it would thus share elements with both w_2 and w_1. Consequently, it would share one element with one of these cells, and two elements with the other.

Thus, regardless of the specific scenario, if vertices v and w are distinct and not adjacent, there must exist at least one cell of v and one cell of w sharing a pair of their elements. ∎

3.1.2 Equivalencies

In the previous section, we introduced the type of vertex pairs. In this section, we prove all the vertex pairs of $\mathcal{P}(3^3)$ are of type 3, 5, 6, 7, or 9, and all the pairs of the same type are equivalent.

Proposition 3.1.3. The vertex pairs of the graph $\mathcal{P}(3^3)$ are of type 3, 5, 6, 7, or 9.

Proof: Let v and w be a pair of vertices. The examination of their type follows three primary cases:

- When $v = w$, the respective cells are identical. As a result, the corresponding grid pattern of the pair v, w conforms to the type 3 pattern depicted in Table 3.3.

- In the instance where vertices v and w are adjacent, each cell of v shares a single element with every cell of w. Hence, the grid pattern of an adjacent pair aligns with the type-9 pattern.

- Owing to the graph's vertex-transitivity, we may select a single vertex and examine all possible vertex pairs containing this fixed vertex, the results of which can then be extended to the entirety of the vertices. For the purposes of this examination, let $v = \{\{1, 2, 3\}, \{4, 5, 6\}, \{7, 8, 9\}\}$, with w a vertex of $\mathcal{P}(3^3)$ such that $v \neq w$ and is not adjacent to v. We now assess the potential configurations of the cells of w.

  Based on Lemma 3.1.2, we understand that there exists a cell in v sharing a pair of elements with a cell of w. Without loss of generality, we may assume this pair to be $\{1, 2\}$. Given that $\{1, 2, 3\}$ is a cell of v, the position of element 3 within w becomes crucial for our analysis. Figure 3.1 visualises the following case analysis for vertices of $\mathcal{P}(3^3)$ where each dot within the vertices of this diagram symbolises an available space for an element from $\{1, 2, \ldots, 9\}$:

  – If 3 is placed within the same cell as $\{1, 2\}$ in w, then v and w share the cell $\{1, 2, 3\}$. If they were to share any other cell, they would effectively become the same vertex, a contradiction. The remaining elements to be allocated to the cells of w are $\{4, 5, 6, 7, 8, 9\}$. The sets $\{4, 5, 6\}$ and $\{7, 8, 9\}$, which form cells of v, cannot be repeated as cells within w. Hence, the elements from these sets are split across the remaining cells in w. This leads to a grid pattern of the v, w pair which corresponds to type 5.

123	123
456	457
789	896
v	w

123		
	45	6
	7	89

The grid pattern of v and w of type 5

Table 3.4: An example of a pair of type 5

  – If 3 is not placed alongside $\{1, 2\}$ in w, it is moved to another cell within w. Here, another element from $\{4, 5, 6, 7, 8, 9\}$, say 4, is placed next to $\{1, 2\}$. The elements 5 and 6, which share a cell with 4 in v, can either be

placed in a single cell of w or distributed across two different cells. This bifurcation of possibilities results in either a type-5 or type-6 grid pattern, or finally a type-7 grid pattern depending on the final placement of 7, 8, and 9. The details of this result are as follows:

* In the scenario where the pair $5, 6$ resides in the same cell as 3, it necessitates the placement of the remaining elements, 7, 8, and 9, into the last cell. As a consequence, the grid pattern that emerges for vertices v and w is:

123	124
456	356
789	789
v	w

12	3	
4	56	
		789

The grid pattern of v and w of type 5

Table 3.5: An example of a type-5 vertex pair

An alignment of the columns of this grid yields a grid that matches the standard type-5 grid, as found in Table 3.3.

* Conversely, should the pair $5, 6$ be allocated to a cell not including 3, then any possible arrangement of 7, 8, and 9 in the remaining cells leads to a grid pattern of type 6 as per Table 3.3:

123	124
456	389
789	567
v	w

12	3	
4		56
	89	7

The grid pattern of v and w of type 6

Table 3.6: An example of a type 6 vertex pair

* If either element 5 or 6 is positioned adjacent to 3, (assume it is 5 for our purposes), and the other member of the pair is situated in the third cell of w, then the final three elements, 7, 8, and 9, can occupy the remaining slots in any configuration. Consequently, the grid associated with the vertex pair v, w now aligns with the type 7 grid pattern illustrated in Table 3.3:

123	124
456	357
789	689
v	w

12	3	
4	5	6
	7	89

The grid pattern of v and w of type 7

Table 3.7: An example of a type-7 vertex pair

Summarising, the grid pattern of any two vertices aligns with one of the patterns specified in Table 3.3.

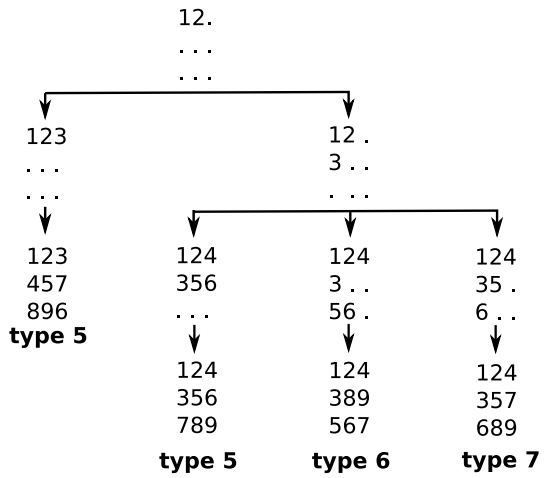

Figure 3.1: Possibilities of vertex w, and the types of the pair v, w

∎

Theorem 3.1.4. All vertex pairs of $\mathcal{P}(3^3)$ can be categorized into 4 equivalence classes where each class is the orbit of a pair of type 5, 6, 7, or 9 containing all vertex pairs of the same type.

Proof: First we prove that type of a pair is preserved under a permutation. Let the following grid pattern, represents the pair v, w:

A_1	A_2	A_3
A_4	A_5	A_6
A_7	A_8	A_9

Since the cells of a vertex are disjoint sets, the intersections in the grid pattern of a vertex pair are disjoint too, to recall the general form of a grid pattern look at Table 3.1. Let $\sigma \in \mathrm{Sym}(9)$. Therefore, the sets A_i with $i = 1, 2, \ldots, 9$ and thus their

images under permutation σ are disjoint (if $x \in \sigma(A_\alpha) \cap \sigma(A_\beta)$ for $\alpha, \beta \in \{1, 2, \ldots, 9\}$, then $\sigma^{-1}(x) \in A_\alpha \cap A_\beta$ which is a contradiction). Not only is the emptiness of A_i unchanged under σ, but also, the size of A_i and its image are the same because A_i are disjoint sets, and permutation is a bijection function. Hence, $|A_i| = |\sigma(A_i)|$ for $i \in \{1, 2, \ldots, 9\}$ and thus, the grid pattern of the pair $\sigma(v), \sigma(w)$ is of the same pattern as the grid pattern of v, w. Consequently, $\mathrm{T}(v, w) = \mathrm{T}(\sigma(v), \sigma(w))$.
Second, we show if v, w and p, q are of the same type, then there exists a $\sigma \in \mathrm{Sym}(9)$ such that $\sigma(v) = p$ and $\sigma(w) = q$. Let the following be the grid pattern of v, w and p, q, where v and p are the rows, and w and q are the columns of their grids:

A_1	A_2	A_3
A_4	A_5	A_6
A_7	A_8	A_9

the grid pattern of v, w

B_1	B_2	B_3
B_4	B_5	B_6
B_7	B_8	B_9

the grid pattern of p, q

Since v, w and p, q are of the same type, we can swap the rows and columns of their grids so they follow the standard pattern of that type in Table 3.3. Then $|A_i| = |B_i|$ for $i \in \{1, 2, \ldots, 9\}$. Hence, the permutation $\sigma(A_i) = B_i$ is the desired permutation mapping $v_i \cap w_j$ to $p_i \cap q_j$ for $i, j \in \{1, 2, 3\}$. Therefore each cell of v and w is mapped to a cell of p and q respectively. Thus, $\sigma(v) = p$ and $\sigma(w) = q$.
Since all pairs are of type 5, 6, 7, or 9 by Proposition 3.1.3, here we proved all pairs of vertices are included in one of the orbits of pairs of types 5, 6, 7, or 9. ∎

Let x, y and u, v be two vertex pairs. Since the vertices of a vertex pair are not ordered, the equivalence of these pairs implies the existence of permutations such that $\sigma(x) = u$ and $\sigma(y) = v$, as well as the existence of other permutations where $\gamma(x) = v$ and $\gamma(y) = u$.

In the context of pairs of type 9, which are endpoints of edges within the graph, the above result can be understood as the following corollary:

Corollary 3.1.5. The graph $\mathcal{P}(3^3)$ is both edge-transitive and arc-transitive.

3.1.3 Size of the Equivalence Classes

Recall the concepts of orbit and stabilizer from equation (3.0.1). For a group H acting on the set X and an element $x \in X$, the orbit-stabilizer theorem states:

$$|H| = |\mathrm{stab}_H(x)| \cdot |\mathrm{orb}_H(x)|$$

Consider, for example, $H = \mathrm{Sym}(9)$. Here, the permutations (12) and (14)(26)(35) belong to $\mathrm{stab}_H(v)$, while $\mathrm{orb}_H(v)$ includes all vertices, reflecting the fact that this

graph is vertex-transitive. Recall the proof of Proposition 3.0.1, in which we demonstrated that the size of an orbit of a vertex in a partition graph equals the number of its vertices. In the case of the partition graph $\mathcal{P}(3^3)$, the number of vertices is 280, as shown in equation (2.1.1).

Enumeration of type-9 pairs

Consider a pair of vertices v and w that exhibit the type-9 grid pattern, as referenced in Table 3.3. Assume H to be the stabilizer of v. Then, we can define $\text{stab}_H(w)$ as $\{\gamma \in \text{Sym}(9) : \gamma(w) = w, \gamma(v) = v\}$, which implies $\text{stab}_\text{H}(w) \subseteq H$.

Let $\sigma \in \text{Sym}(9)$. If σ swaps the columns or rows of the grid pattern, both vertices v and w remain unaffected. Consequently, $|\text{stab}_H(w)|$ can be calculated as $3! \cdot 3!$, or 6^2.

The orbit of w under H, denoted as $\text{orb}_H(w)$, includes the neighbours of v, as the elements of $\text{orb}_H(w)$ form new vertices while maintaining the adjacency relationship. By applying the orbit-stabilizer theorem, we find

$$\text{degree}(v) = |\text{orb}_H(w)| = \frac{|H|}{|\text{stab}_\text{H}(w)|} = \frac{6^4}{6^2} = 36.$$

This result aligns with Proposition 2.1.6. Applying the degree sum formula yields

$$|E| = \frac{280 \times 36}{2} = 140 \times 36.$$

Therefore, 140×36 represents the total count of type-9 pairs.

Enumeration of type-5 pairs

We can determine the number of vertices in a type-5 relationship with a given vertex by employing two distinct methods: the first approach involves calculating the size of the orbit and then determining the size of the stabilizer using the orbit-stabilizer theorem, while the second method involves directly enumerating the vertices in a type-5 relationship with a specific vertex. We shall initially explore the utilization of the orbit-stabilizer theorem.

Consider a pair of vertices, v and w, which exhibit a grid pattern characteristic of type 5, as illustrated below:

123	123
456	457
789	896
v	w

The grid pattern of v and w of type 5

123		
	45	6
	7	89

Table 3.9: An example of a pair of type 5

Here, a permutation conserves v and w only if it maps the cell $\{1,2,3\}$ to itself, and stabilizes $\{\{4,5\},\{8,9\}\}$ while maps 7 to 6. There are $3! = 6$ ways to permute the three elements within the set $\{1,2,3\}$.

There are $2! = 2$ ways to permute the elements within each of the sets $\{4,5\}$ and $\{8,9\}$. Since the permutations within these sets are independent, there are $2 \times 2 = 4$ permutations in total.

Lastly, the sets $\{4,5\}$ and $\{8,9\}$ can be swapped with each other or remain the same. Therefore, there are $2! = 2$ ways to permute these two sets. Therefore,

$$|\mathrm{stab}_H(w)| = 3! \times 2^3$$

and

$$|\mathrm{orb}_H(w)| = \frac{6^4}{3! \times 2^3} = 3^3. \tag{3.1.1}$$

This signifies that there exist 3^3 vertices maintaining a type-5 relationship with vertex v. Therefore, the total number of type-5 pairs in $\mathcal{P}(3^3)$ is $\frac{3^3 \times 280}{2} = 140 \times 3^3$.

To directly derive the number of vertices sharing a type-5 relationship with vertex v, we can enumerate the different possibilities for these vertices. The diagram in Figure 3.2 encapsulates this counting process. Since v and w are of type 5, we start the diagram with a cell that these two vertices share. Then fit the cells of v one by one at each step of the diagram into the cells of w. The newly added numbers at each step are coloured red. The details of the diagram are as the following:

Two vertices of type 5 share a cell. To build the vertex w there are three choices to fix a cell. Pick {1,2,3} as the shared cell. The next step, as shown in diagram 3.2, is to fit another cell of v to w in a way that they stay in a type-5 relationship. Take cell $\{4,5,6\}$ from v, we cannot place all of the elements of this cell in a cell of w because it makes the two vertices the same, so, put two of them in the second cell and the third one in the third cell (three choices), one option is to put $\{4,5\}$ together, and 6 in a different cell of w. Next, take the last cell of v, $\{7,8,9\}$. There are three ways to put one of 7, 8, or 9 in the second cell and two of them in the third cell of w which produces three more possibilities. All in all, there are 3^3 possible vertices to be in a type-5 relationship with vertex v.

Enumeration of type-6 pairs

The process of enumerating type-6 pairs can be approached in two distinct ways: using the orbit-stabilizer theorem, or employing direct counting. The following section employs both methods.

Consider two vertices v and w of type-6 grid pattern as illustrated in Table 3.10. Notably, the two vertices do not share a cell, yet they do share three distinct pairs of elements, each pair sourced from a unique cell. Any permutation that either maps the shared pairs together or leaves them as they are also has the effect of

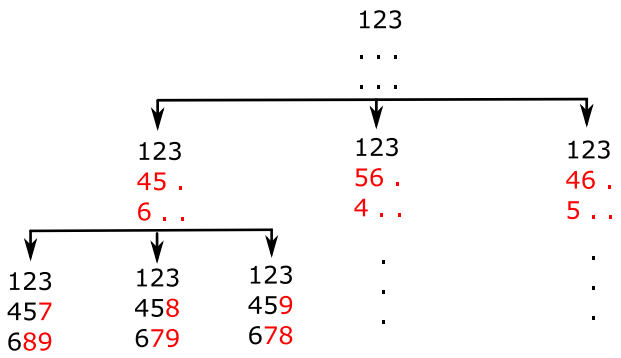

Figure 3.2: Possibilities of vertex w in a type-5 relationship with vertex v

123	124
456	389
789	567
v	w

12	3	
4		56
	89	7

The grid pattern of v and w of type 6

Table 3.10: An example of a type 6 vertex pair

stabilizing the vertices v and w. Given the existence of three shared pairs, there are 3! permutations for the three pairs. Additionally, within each set, there are $2! = 2$ possible permutations for the two elements. As there are three such sets, the total number of internal permutations becomes 2^3. Consequently, the size of the stabilizer is expressed as:

$$|\text{stab}_H(w)| = 3 \times 2^3.$$

From this, we can compute the size of the orbit as follows:

$$|\text{orb}_H(w)| = \frac{6^4}{3 \times 2^3} = 3^3 \times 2.$$

Consequently, there exist $3^3 \times 2$ distinct vertices in a type-6 relationship with v. As a result, the number of all type-6 pairs is $\frac{3^3 \times 2 \times 280}{2} = 280 \times 3^3$.

For direct counting of the vertices in a type-6 relationship with v, we apply a similar approach to the one employed for counting the type-5 pairs. This process is visualized in the diagram of Figure 3.3. The total number of possibilities obtained from the diagram is $9 \times 2 \times 3 \times 3$ (9 is the number of possible pairs that the diagram starts with). However, since three pairs are shared between v and w, this total number must be divided by 3. Overall, the number of feasible vertices in a type-6 relationship with v is $\frac{9 \times 2 \times 3 \times 3}{3} = 3^3 \times 2$.

The total amount derived from the diagram is $3^2 \times 2 \times 3 \times 3$ but since three pairs are shared between v and w, the total amount must be divided by 3. All together, there are $\frac{3^2 \times 2 \times 3 \times 3}{3} = 3^3 \times 2$ feasible vertices in type-6 relationship with v.

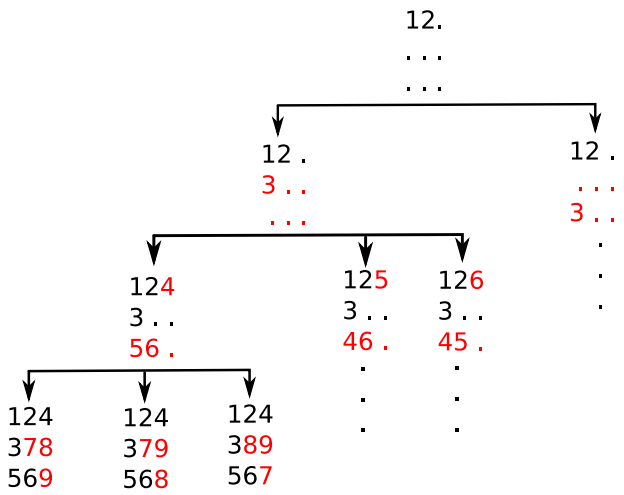

Figure 3.3: Possibilities of vertex w in a type-6 relationship with v

Enumeration of type-7 pairs

Take the two vertices v and w of type 7 from Table 3.11. It can be observed that

123	124
456	357
789	689
v	w

12	3	
4	5	6
	7	89

The grid pattern of v and w of type 7

Table 3.11: An example of a type-7 vertex pair

vertices of type 7 do not share a cell, although they share two pairs of numbers, each pair drawn from a distinct cell. The permutations that map the pair $1, 2$ to $8, 9$ and leave all other elements fixed form the $\text{stab}_H(w)$. Therefore, the size of the stabilizer is given by:

$$|\text{stab}_H(w)| = 2^3$$

and consequently, the size of the orbit can be computed as:

$$|\text{orb}_H(w)| = \frac{6^4}{2^3} = 3^4 \times 2.$$

From this, we ascertain that there are $\frac{3^4 \times 2 \times 280}{2} = 280 \times 3^4$ realizable type-7 pairs in $\mathcal{P}(3^3)$.

Direct counting of vertices in a type-7 relationship with v is illustrated in Figure 3.4. From the first step of the diagram, there are 9 possible choices for fixing a pair. With two shared pairs between v and w, the total number of feasible vertices w in a type-7 relationship with vertex v is $\frac{9 \times 2 \times 6 \times 3}{2} = 3^4 \times 2$.

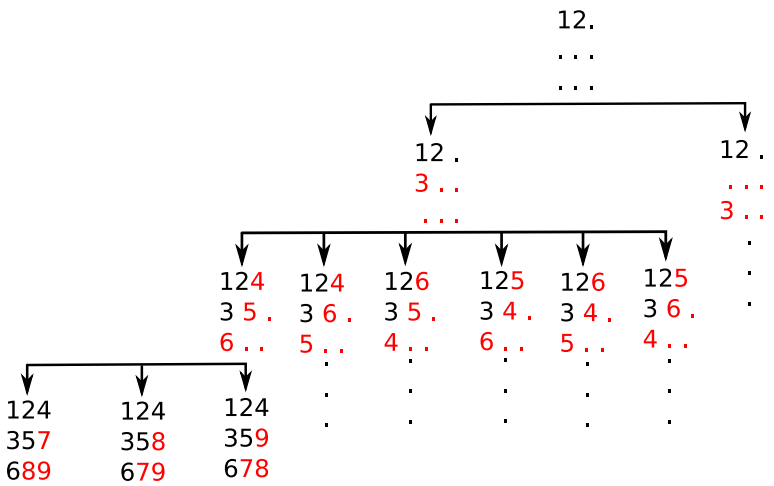

Figure 3.4: Possibilities of vertex w in a type-7 relationship with v.

Given the correspondence between edges and type-9 pairs, we can compute the quantity of non-edges in the graph. By subtracting the number of edges, or equivalently the number of type-9 pairs (equal to 140×36), from the total possible pairs $\binom{280}{2}$, we obtain 140×243 non-edges.

Notably, this figure is equivalent to the total count of pairs of types 5, 6, and 7. Consequently, no other categories of pairs exist within this graph.

This observation confirms the conclusion of Theorem 3.1.4, reinforcing the claim that the identified types of pairs provide a comprehensive classification within this graph. Therefore, the typology serves as a valuable tool in understanding and analyzing the graph's structure.

3.2 Vertex Triples of $\mathcal{P}(3^3)$

To fully comprehend the structure of the graph $\mathcal{P}(3^3)$, merely analyzing vertex pairs is insufficient. In this chapter, we will broaden our focus to include vertex triples, extending the analysis previously conducted on pairs.

This analysis is useful in Theorem 4.1.14 which identifies all the bipartite subgraphs of $\mathcal{P}(3^3)$.

3.2.1 Definition

We will now define a pattern for triples that generalizes the pattern established in Table 3.1 for vertex pairs.

Consider the tree vertices $v = \{v_1, v_2, v_3\}$, $w = \{w_1, w_2, w_3\}$, and $u = \{u_1, u_2, u_3\}$. This triple can be represented as a $3 \times 3 \times 3$ cube pattern. We express this cube using three 3×3 grid patterns as follows, with $k = 1, 2, 3$:

$v_1 \cap w_1 \cap u_k$	$v_1 \cap w_2 \cap u_k$	$v_1 \cap w_3 \cap u_k$
$v_2 \cap w_1 \cap u_k$	$v_2 \cap w_2 \cap u_k$	$v_2 \cap w_3 \cap u_k$
$v_3 \cap w_1 \cap u_k$	$v_3 \cap w_2 \cap u_k$	$v_3 \cap w_3 \cap u_k$

Table 3.12: The cube pattern of the triple v, w, u

A fitting analogy for this cube pattern is the familiar Rubik's cube. Each unit of the cube pattern can be viewed as a small cube within the Rubik's cube, and each grid corresponds to a layer of the Rubik's cube. However, the layer movements of a Rubik's cube do not apply to the cube pattern of a vertex triple.

The union of the units of the i-th row of all grids forms a cell of vertex v, the union of the units of the j-th column of all grids constitutes a cell of vertex w, and the union of all units of the k-th grid creates a cell of vertex u, for $i, j, k = 1, 2, 3$. Let each cell of the cube pattern of vertices v, w, u be $A_{i,j,k} = v_i \cap w_j \cap u_k$. Then, the cells of these vertices can be found as the union of 9 units of the cube pattern:

$$v_i = \bigcup_{j,k=1}^{3} (A_{i,j,k}), \quad w_j = \bigcup_{i,k=1}^{3} (A_{i,j,k}), \quad u_k = \bigcup_{i,j=1}^{3} (A_{i,j,k}). \tag{3.2.1}$$

Given the cube pattern of three vertices, we can now rigorously identify the cells of each vertex. Subsequently, we can derive the grid patterns of the vertex pairs included in the triple and determine their respective types. Recall the grid pattern of two vertices in Table 3.1. For example, consider the first unit of the first row of the grid pattern for vertices v and w. This unit corresponds to the intersection of the union of all units within the first rows of their cube pattern and the union of all units within the first columns of their cube pattern, denoted as $\bigcup_{j,k=1}^{3} A_{1,j,k} \cap \bigcup_{i,k=1}^{3} A_{i,1,k} = v_1 \cap w_1$.

A *vertex triple is classified as type* r, s, t if the pairs within the triple are of types r, s, and t, where $r, s, t \in \{5, 6, 7, 9\}$. In Proposition 3.1.3, we observed that all distinct vertex pairs of $\mathcal{P}(3^3)$ can be categorized into four equivalence classes. For vertex triples, the number of equivalence classes increases.

While vertex pairs of the same type are equivalent—indicating the existence of at least one automorphism (permutation) mapping one pair to another—this property does not hold true for all vertex triples of the same type. Nevertheless, these vertex triples can still be organized into equivalence classes.

To count the number of possible types of a triple, let r, s, t be a triple type with $r, s, t \in \{5, 6, 7, 9\}$. There are $\binom{4}{3}$ choices to make this triple type, where r, s, and t are distinct. There are 4 choices where $r = s = t$, and there are $4 \times 3 = 12$ ways to build the triple type where two of them are equal and the third one is distinct. Therefore, there are $4 + 4 + 12 = 20$ choices for the type of triple. Next lemma shows that two of the triple types are not possible.

Lemma 3.2.1. There are no triples of type 5,5,9 and 5,6,9 in $\mathcal{P}(3^3)$.

Proof: Let a, b, and c be three vertices such that $\mathrm{T}(a,b) = 9$ and $\mathrm{T}(a,c) = \mathrm{T}(b,c) = 5$. So, c has a common cell with b like b_1 and a common cell with a like a_1. Since $\mathrm{T}(a,b) = 9$, we know $a_1 \cap b_1 \neq \emptyset$. However, the cells of a vertex must be disjoint. Hence, there is no triple of type 5,5,9.
Consider the same vertices a and b with $\mathrm{T}(a,b) = 9$. Let c to be a vertex such that $\mathrm{T}(a,c) = 5$ and $\mathrm{T}(b,c) = 6$. Let a_1 be the common cell of a and c. On one hand, $\mathrm{T}(b,c) = 6$ and thus for two cells b_1 and b_2 of b we have $|a_1 \cap b_1| = 2$ and $|a_1 \cap b_2| = 1$. On the other hand, $\mathrm{T}(a,b) = 9$ and thus $|a_1 \cap b_1| = 1$ which is a contradiction. Therefore, there is no triple of type 5,6,9. ∎

This lemma can be confirmed by [1].

The following definition establishes a notation for the number of triples of a certain type.

Definition 3.2.2. [1] Given two vertices v and w of type k, the number of vertices u that are of type i with v and of type j with w is denoted as $\mathbf{p_{ij}^k}$.

Some of the values we have computed so far include $p_{99}^5 = 12$, $p_{99}^9 = 2$, $p_{99}^7 = 4$, and $p_{99}^6 = 4$ which are the number of the common neighbours of the vertex pairs of different types. If the reader is interested in further values of p_{ij}^k for $i, j, k = 3, 9, 7, 6, 5$, they can be found in reference [1]. However, please note that in the cited work, the types are labelled differently: types $3, 9, 7, 6, 5$ in our paper correspond to types $0, 1, 2, 3, 4$ in the cited work.

3.2.2 Equivalencies

Later in Section 4.1.2, we will require the equivalence classes of potential vertex triples that do not contain a pair of type 9 in order to examine their common neighbors. To this end, we will undertake a classification of vertex triples in this section. Table 3.13 provides a summary of this classification, illustrating the number of equivalence classes that exist for triples of a specific type.

The process of classifying triples of the same kind into respective equivalence classes varies depending on the specific type of the triple. Nevertheless, the methodology employed remains consistent across all types. In the following, we elaborate on this technique through an examination of a specific triple type. Detailed proofs for other triple types, while conceptually similar, are rather extensive and have therefore been relegated to Appendix A for the sake of brevity and clarity in the main body of the text.

Lemma 3.2.3. All the vertex triples of type 5,5,5 can be classified into two orbits.

Proof: Given the equivalence of all vertex pairs of type 5, we may arbitrarily select a pair of this type, denoted v, w, and explore various ways for constructing a

type of triples	number of equivalence classes
5,5,5	2
6,6,6	2
5,5,6	1
5,5,7	1
5,6,6	1
6,6,7	2
5,6,7	2
6,7,7	3
7,7,7	2
5,7,7	2

Table 3.13: Number of equivalence classes of the possible triples that do not include a pair of type 9.

third vertex, u, such that $\mathrm{T}(v,u) = 5$ and $\mathrm{T}(w,u) = 5$. Without loss of generality, consider v, w exhibiting the following grid pattern:

123	123
456	457
789	896
v	w

123		
	45	6
	7	89

The grid pattern of v and w of type 5

Table 3.14: An example of a pair of type 5

As asserted in the upcoming Lemma 4.1.9, if vertices of a triple exhibit pairwise type 5 relationships, they necessarily share a common cell. Thus, as v and w share cell $\{1,2,3\}$, any newly formed vertex must have the same cell. The next cell of the new vertex must include two elements from cell $\{4,5,6\}$. These two elements are either distributed across two different cells in w, namely $\{4,6\}$ or $\{5,6\}$ or are grouped together, i.e., $\{4,5\}$.

Denote u_1 as a new vertex that combines elements 4 and 6 into a single cell, and u_2 as a new vertex that unites elements 4 and 5 within the same cell. Observe that generating a third vertex grouping elements 5 and 6 within a cell follows the same process as constructing u_1, thereby obviating the need for separate consideration. Consequently, u_1 can be generated in two analogous cases. The resulting vertex configurations for u_1 and u_2 are as follows:

$$u_1 = \{\{1,2,3\},\{4,6,.\},\{5,.,.\}\}$$
$$u_2 = \{1,2,3\},\{4,5,.\},\{6,.,.\}\}.$$

As always, each dot denotes an empty slot in a cell.

The third cell of v, denoted as $\{7, 8, 9\}$, needs to be distributed among the remaining cells of u_1 and u_2. However, the assignment of these elements is subject to the constraint that $\mathrm{T}(u, w) = 5$.

Examining u_1, we find that the set $\{7, 8, 9\}$ can be distributed across the second and third cells in three distinct ways. Therefore, a vertex equivalent to u_1 can be constructed in $2 \times 3 = 6$ ways.

In the case of u_2, placing 7 in the same cell with 4 and 5 is prohibited because it would result in $u_2 = w$. Consequently, the set $\{7, 8, 9\}$ can be assigned to u_2 in only two unique ways.

In total, we have $6 + 2 = 8$ unique configurations to create the third vertex u. Using the notation in Definition 3.2.2, we deduce that $\mathrm{P}^5_{55} = 8$. Since this conclusion aligns with the reference [1], it confirms the absence of any other choice for the third vertex, thereby classifying all triples of type 5,5,5.

To illustrate, consider the following examples of u_1 and u_2:

$$u_1 = \{\{1, 2, 3\}, \{4, 6, 8\}, \{5, 7, 9\}\}$$
$$u_2 = \{\{1, 2, 3\}, \{4, 5, 9\}, \{6, 8, 7\}\}.$$

The corresponding cube patterns for the triples v, w, u_1 and v, w, u_2 are:

123		

	4	
6	5	

	8	9
	7	

Table 3.15: The cube pattern of the triple v, w, u_1 of the first kind of type 5,5,5.

123		

	45	
9		

		6
7	8	

Table 3.16: The cube pattern of the triple v, w, u_2 of the second kind of type 5,5,5.

A vertex triple a, b, c of type 5,5,5 is considered of the *first kind* if its cube pattern aligns with the v, w, u_1 cube pattern. Conversely, a triple of type 5,5,5 is of the *second kind* if its cube pattern conforms to the v, w, u_2 cube pattern. A permutation that maps the corresponding units of the cube pattern of two triples enables the mapping of the triples to each other.

The non-equivalence of these two classes is validated later by Lemma 4.1.8, which confirms that vertices of the first kind share six neighbours, whereas those of the second kind do not share any neighbours.

∎

It is important to note that equivalence is precluded when two triples belong to different types, given the lack of equivalence between the pairs. If two triples of identical type are equivalent, then a permutation exists that maps pairs of the same type to one another.

Chapter 4

Constructing $\mathrm{B}_{\mathrm{edge}}\big(\mathcal{P}(3^3)\big)$

"I have no special talent. I am only passionately curious."
— Albert Einstein

In this chapter, we will explore the construction of $\mathrm{B}_{\mathrm{edge}}\big(\mathcal{P}(3^3)\big)$. This involves two primary sections: the first focuses on 'Maximal Complete Bipartite Subgraphs of $\mathcal{P}(3^3)$', beginning with the construction from vertex pairs and progressing to the inclusion of triples and quadruples. We'll conclude this section by formulating and demonstrating the 'Main Theorem of Bipartite Subgraphs'. The second section will dive into the 'Maximal Simplices of $\mathrm{B}_{\mathrm{edge}}\big(\mathcal{P}(3^3)\big)$', specifically examining the 'Intersection of Maximal Simplices'. Through this chapter, we aim to provide a comprehensive understanding of the $\mathrm{B}_{\mathrm{edge}}\big(\mathcal{P}(3^3)\big)$ construction process, elucidating the methods and theories that underpin each step.

4.1 Maximal Complete Bipartite Subgraphs of $\mathcal{P}(3^3)$

In this section, we seek to comprehensively examine the maximal complete bipartite subgraphs of $\mathcal{P}(3^3)$. We start by scrutinizing the vertex pairs in our graph, focusing on uncovering the potential bipartite subgraphs. This involves systematically identifying common neighbors for vertex pairs and iterating the process by seeking common neighbors for those common neighbors, as elaborated in Remark 4.1.1. We leverage this method to construct complete bipartite graphs from the identified pairs of vertices.

Our preliminary categorization in previous chapter yielded four distinct equivalence classes for vertex pairs. In this chapter, we show this classification extends

to the bipartite graphs constructed from these pairs, resulting in four corresponding equivalence classes. In the ensuing discussions, we present a proof that these constructed bipartite subgraphs are the only maximal complete bipartite subgraphs of $\mathcal{P}(3^3)$. This serves as a cornerstone for our comprehension of $\mathcal{P}(3^3)$ and its bipartite subgraphs.

The importance of understanding these maximal complete bipartite subgraphs extends to the study of the edge box complex $\mathrm{B}_{edge}(G)$ in the next section.

4.1.1 Construction from Vertex Pairs

The reason we categorized the pairs in the previous chapter is to introduce a method to construct complete bipartite subgraphs of $\mathcal{P}(3^3)$. This method, formally explained in Remark 4.1.1, involves finding the common neighbours of a pair of vertices and finding the common neighbours of these common neighbours. We start by explaining how we intend to find the common neighbours of a pair.

In the process of identifying a common neighbor u for two vertices v and w, we adopt a sequential approach.

We commence by selecting a cell from either vertex v or w, without loss of generality, say from v. This chosen cell is then distributed across all cells of u, with each cell of u receiving exactly one element from the chosen cell of v. This process ensures that every cell of u has at least one element in common with the chosen cell of v.

Subsequently, we pick another cell from v and distribute its elements across the cells of u. This distribution is done such that no two elements from the selected cells of v and w co-occur in any cell of u.

We continue this distribution process for the third cell of v, ensuring at each stage that the intersection of any cell of u with each cell of both v and w is nonempty. This distribution approach maintains the condition that no two elements from the cells of v and w coexist within the same cell of u.

Ultimately, through this step-by-step procedure, we effectively generate a common neighbor u for the vertices v and w, with each cell of u intersecting nontrivially with each cell of v and w.

Remark 4.1.1. In this text, we primarily focus on complete bipartite subgraphs, as the definition of simplices in $\mathrm{B}_{\mathrm{edge}}\big(\mathcal{P}(3^3)\big)$ depends on these. To construct a complete bipartite subgraph, we start with a subset of vertices S in a graph G. We identify the common neighbours of the vertices of S, denoted by $\mathrm{CN}(S)$, and then determine the common neighbours of these common neighbours, $\mathrm{CN}\big(\mathrm{CN}(S)\big)$. This process yields a complete bipartite subgraph.

In specific, if we commence with a pair $\{a, b\}$ of vertices from $\mathcal{P}(3^3)$, the same procedure can be applied. The resulting complete bipartite subgraph is then denoted

as follows:

$$K_{i,j}(a,b) = \Big(\mathrm{CN}\big(\mathrm{CN}(a,b)\big), \mathrm{CN}(a,b)\Big)$$

where $|\,\mathrm{CN}\big(\mathrm{CN}(a,b)\big)| = i$ and $|\,\mathrm{CN}(a,b)| = j$.

In the following proposition, we prove the complete bipartite subgraphs we constructed in this remark, are maximal.

Proposition 4.1.2. The complete bipartite subgraphs built using the method of Remark 4.1.1 are maximal.

Proof: Suppose (A, B) is one of the subgraphs constructed by the method of the mentioned remark, and it is not maximal, with A being the left side and B the right side. This would imply there is a vertex v that could be added to one side, say A, such that v connects with all vertices in B, thereby maintaining the property of a complete bipartite subgraph. Thus, the common neighbours of the vertices of B would be $A \cup \{v\}$.

However, this would contradict the construction process of (A, B) which says the common neighbours of vertices of B are exactly the vertices in A, and vice versa. Therefore, no additional vertex can be added to (A, B) without disrupting this established relationship, meaning (A, B) must be a maximal complete bipartite subgraph. ∎

Proposition 4.1.3. Assume we have $a, b \in V(\mathcal{P}(3^3))$ such that $\mathrm{T}(a,b) = i$ where $i = 5, 6, 7, 9$, and let G be the maximal complete bipartite subgraph $\big(\mathrm{CN}(\mathrm{CN}(a,b)), \mathrm{CN}(a,b)\big)$ originating from the vertex pair a, b by applying the method of Remark 4.1.1 on this pair. Then for any pair of type i in $\mathrm{CN}(\mathrm{CN}(a,b))$, using this method yields the same bipartite subgraph G.

Proof: Consider a pair $\{s,t\} \subseteq \mathrm{CN}(\mathrm{CN}(a,b))$ with $\mathrm{T}(s,t) = i$. If we take common neighbours of both sides of the inclusion, this reverses the inclusion, yielding $\mathrm{CN}(a,b) \subseteq \mathrm{CN}(s,t)$. Since pairs a, b and s, t are of the same type, they have an equal number of common neighbours, resulting in $\mathrm{CN}(a,b) = \mathrm{CN}(s,t)$. Consequently, $\mathrm{CN}(\mathrm{CN}(a,b)) = \mathrm{CN}(\mathrm{CN}(s,t))$. Therefore, the maximal complete bipartite subgraph we get by applying the method from Remark 4.1.1 on the pair s, t is $\big(\mathrm{CN}(\mathrm{CN}(s,t)), \mathrm{CN}(s,t)\big)$, which matches G. ∎

Now we apply the method of Remark 4.1.1 to the vertex pairs of different equivalent classes to construct maximal complete bipartite subgraphs of $\mathcal{P}(3^3)$.

Constructing $K_{2,2}$

Consider the following vertices v and w of type 9. Next, we explore the common neighbours of these two vertices which is visualized in the diagram of Figure 4.1:

$$\begin{array}{cc} 123 & 147 \\ 456 & 258 \\ 789 & 369 \\ v & w \end{array} \tag{4.1.1}$$

First, we distribute the elements of the initial cell of v, namely $\{1, 2, 3\}$, into separate cells of u. The distribution of the subsequent cell, $\{4, 5, 6\}$, of v into cells of u depends on the relative positioning of these elements in w. The elements 4, 5, and 6 must be positioned in such a way that they do not co-occur with elements 1, 2, and 3, respectively, within the same cell of u. This constraint leaves us with only two viable arrangements, illustrated in the second row of diagram 4.1.

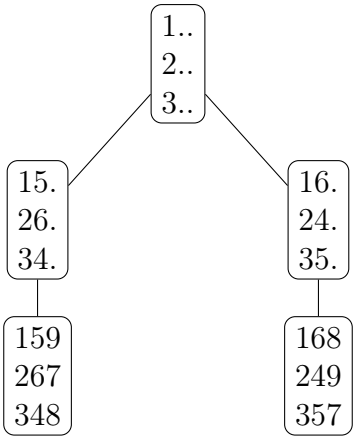

Figure 4.1: Constructing the common neighbours of a pair of vertices of type 9

Next, we place the elements of the cell $\{7, 8, 9\}$ into the cells of u. The arrangement of these elements within w dictates that they must not co-occur within the same cell of u with the pairs $\{1, 4\}$, $\{2, 5\}$, and $\{3, 6\}$, respectively. Once the distribution of the second cell of v, $\{4, 5, 6\}$, within cells of u is set, there exists a single valid way to place these elements in the cells of u, as depicted in the final row of the diagram.

Considering v and w as type-9 vertices, they are adjacent and share two common neighbors. This relationship forms a $K_{2,2}$ bipartite graph. In this context, $K_{2,2}$ represents the structure consisting of a pair of type-9 vertices, their shared neighbors, and the edges connecting the vertices with these common neighbors.

We further note that the shared neighbors of v and w are also adjacent. This observation culminates in the following two lemmas:

Lemma 4.1.4. Let A and B be two disjoint sets of vertices of size two, with every vertex in A adjacent to every vertex in B. If A contains a type-9 pair of vertices, then the induced subgraph of the bipartite graph $K_{2,2}$ is a complete graph K_4.

Lemma 4.1.5. Each bipartite graph $K_{2,2}$ is included in a 4-clique.

These lemmas shed light on the structural relationship between a $K_{2,2}$ bipartite graph and a 4-clique.

Constructing $K_{2,12}$

We now construct a bipartite graph $K_{2,12}$ starting from vertices v and w of type 5. Consider the two familiar vertices of type 5 with their grid pattern as below:

123	123
456	457
789	896
v	w

123		
	45	6
	7	89

The grid pattern of v and w of type 5

Table 4.1: An example of a pair of type 5

The process begins by distributing the common cell $\{1, 2, 3\}$ of v and w into separate cells of their common neighbour u, one element in each cell.

Due to the shared pairs $\{5, 6\}$ and $\{8, 9\}$ between v and w, the elements of each pair must be distributed into distinct cells. One possible distribution include **??**, which prevents elements 4 and 7 from co-occurring with elements from the shared pairs in the same cell of u.

Further, the elements of the shared pairs can be allocated to the cells of u in two ways: pairing 5 with 8, and 6 with 9, or pairing 5 with 9, and 6 with 8. With 3! ways to place the pairs $\{5, 8\}$, $\{6, 9\}$, and $\{4, 7\}$ adjacent to 1, 2, and 3, a total of $2 \times 3! = 12$ different configurations can generate a common neighbor of v and w of type 5.

Given the knowledge from section 2.2 that each vertex of the graph $\mathcal{P}(3^3)$ is included in 12 different 4-cliques and thus is adjacent to all vertices of 12 triangles as depicted in Figure 4.2, we can assert that the 12 common neighbors of v and w are a subset of vertices of 12 triangles adjacent to v.

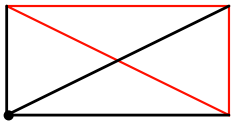

Figure 4.2: A vertex is adjacent to all the vertices of a triangle

Notably, when v and w are of type 5 and hence not adjacent, vertex w is adjacent to just one vertex from each triangle. If vertex w were adjacent to two vertices from the same triangle, according to Lemma 4.1.4, it would form a K_4 graph with v and the two triangle vertices, contradicting the non-adjacency of v and w. Therefore, two type 5 vertices generate a $K_{2,12}$ complete bipartite graph (look at Figure 4.3).

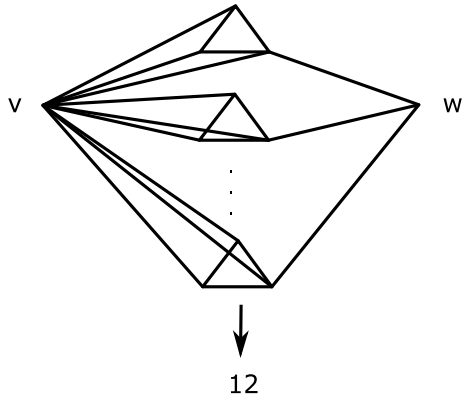

Figure 4.3: Common neighbours of v and w of type 5 leading to a $K_{2,12}$

We can determine three common neighbours of v and w utilizing the methodology described earlier in this chapter. Consider the following common neighbours of v and w:

$$a = \{\{1,4,8\},\{2,6,7\},\{3,5,9\}\}, \quad b = \{\{1,4,9\},\{2,5,8\},\{3,6,7\}\}$$
$$c = \{\{1,6,7\},\{2,4,8\},\{3,5,9\}\}$$

Upon investigating the common neighbours of vertices a, b, and c, we commence by distributing the first cell of a, i.e., $\{1,4,8\}$, among the three cells of a candidate common neighbour, denoted as u. To this end, we assign each of the elements 1, 4, and 8 to a separate cell in u, leading to an intermediate configuration of the form $u = \{\{1,.,.\},\{4,.,.\},\{8,.,.\}\}$.

Subsequently, we turn our attention to the second cell of a, $\{2,6,7\}$. Observing that the triplet $\{2,4,8\}$ forms a cell in vertex c, we deduce that element 2 cannot co-occur with elements 4 and 8 in the same cell of u. Hence, element 2 is allocated to the cell currently including element 1, leading to the updated form $u = \{\{1,2,.\},\{4,.,.\},\{8,.,.\}\}$.

For elements 6 and 7, our previous deduction implies that they can be assigned to the cells of elements 4 or 8 in u. This situation produces two viable configurations, namely:

$$u_1 = \{\{1,2,.\},\{4,6,.\},\{8,7,.\}\}, \quad u_2 = \{\{1,2,.\},\{4,7,.\},\{8,6,.\}\}.$$

Lastly, we wish to distribute the third cell of a, $\{3,5,9\}$, among the cells of both u_1 and u_2. Given that $\{3,6,7\}$ constitutes a cell in vertex b, element 3 cannot coexist with elements 6 and 7 within the same cell of u. Hence, the only suitable cell for element 3 is the one already containing 1 and 2. Furthermore, considering that both $\{2,5,8\}$ and $\{1,4,9\}$ are cells in vertex b, we can infer that element 5 cannot share a cell with element 8 and element 9 cannot share a cell with element 4. Consequently, the only feasible configurations for the common neighbours of a, b, c are:

$$u_1 = \{\{1,2,3\},\{4,6,5\},\{8,7,9\}\} u_2 = \{\{1,2,3\},\{4,7,5\},\{8,6,9\}\}$$

which are equal to the vertices v and w. Consequently, according to Lemma 1.2.3, we find that v and w are indeed the only common neighbours of all of their 12 common neighbours.

Constructing $K_{6,4}$

To find the common neighbours of vertices v and w, as depicted in Table 4.2, we apply a similar methodology to those used earlier. This method is summarized briefly in diagram 4.4, with detailed steps provided below. The process starts, as usual, with

123	124
456	389
789	567
v	w

12	3	
4		56
	89	7

The grid pattern of v and w of type 6

Table 4.2: An example of a type-6 vertex pair

distributing the elements of the first cell of v, i.e., $\{1,2,3\}$, into three different cells of a new candidate vertex u, leading to an intermediate configuration of u of the form $u = \{\{1,.,.\},\{2,.,.\},\{3,.,.\}\}$.

Next, we seek to distribute the elements of the second cell of v, namely $\{4,5,6\}$. In doing this, it is necessary to adhere to the condition that element 4 cannot be placed in the same cell as 1 and 2, since it is included in the same cell $\{1,2,4\}$ of w as these elements. Also, element 7 from the last cell of v cannot be placed with 5 and 6 due to its occurrence in the cell $\{5,6,7\}$ of vertex w. Hence, there is only one remaining spot for element 7. After distributing elements 4, 5, and 6 in compliance with these constraints, we arrive at the intermediate configurations depicted in step 2 of diagram 4.4.

In the final step, we distribute the elements 8 and 9 of the third cell of v into the remaining slots of the cells in u. Given the constraints already imposed, the placements of 8 and 9 in this step are not restricted, allowing for four viable configurations of u, which are all valid common neighbours of v and w.

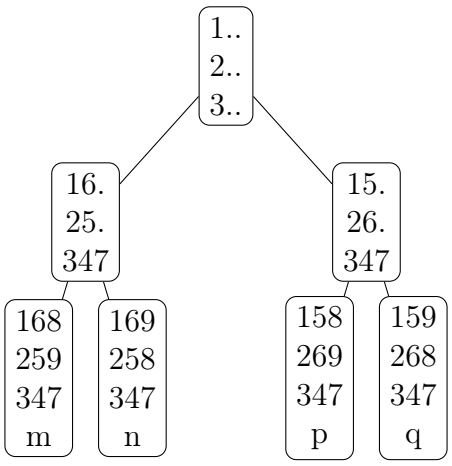

Figure 4.4: Common neighbours of a type-6 pair of vertices

To find the maximal complete bipartite subgraph derived from a type-6 pair v and w, we examine $\mathrm{CN}(\mathrm{CN}(v, w))$. We start by considering one of the common neighbours of v and w, m. We distribute the elements of the first cell of m, $\{1, 6, 8\}$, across the cells of a new vertex u.

Next, we aim to distribute the elements of the second cell of m, i.e., $\{2, 5, 9\}$. Given that $\{2, 6, 8\}$ is a cell of another common neighbour q of v and w, and $\{1, 5, 8\}$ is a cell of yet another common neighbour p of v and w, we face the constraints that element 2 cannot be in the same cell as elements 6 and 8, and element 5 cannot be in the same cell as elements 1 and 8. Then, there is only one spot that element 9 can be placed in, and thus, $u = \{\{1, 2, .\}, \{6, 5, .\}, \{8, 9, .\}\}$.

Finally, the elements of the third cell of m, i.e., $\{3, 4, 7\}$, can be placed in the remaining spots of u in any order due to the lack of any additional constraints. This implies that there are $3! = 6$ valid configurations for u, and hence $|\,\mathrm{CN}(\mathrm{CN}(v, w))| = 6$. Consequently, we have constructed a maximal complete bipartite subgraph $K_{6,4}$ derived from a pair of vertices of type 6 in $\mathcal{P}(3^3)$.

As we explore the common neighbours, it becomes critical to categorize the vertex pairs on each side of the $K_{6,4}$ subgraph. This classification is integral to subsequent chapters; for instance, it is employed in Section 4.2.1, where we analyze the intersections of simplices of $\mathrm{B}_{\mathrm{edge}}\big(\mathcal{P}(3^3)\big)$. These simplices, in essence, correspond to these bipartite subgraphs.

The vertex pairs comprising the 6 common neighbours of v and w display distinct grid patterns. Leveraging these patterns, we can seamlessly compute each pair's relationship type, as illustrated in Figure 4.5.The types of vertex pairs are indicated on the curves connecting them, which should not be mistaken for edges. Given that this is a complete bipartite subgraph, all vertices on the left side are adjacent to those on the right.

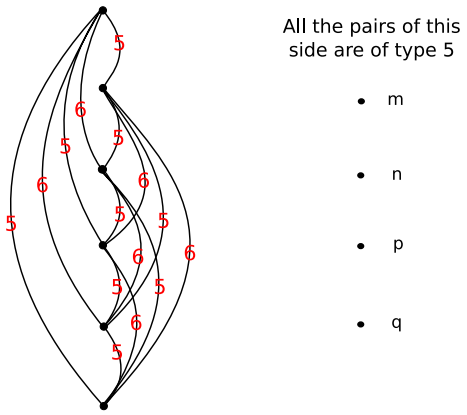

Figure 4.5: A $K_{6,4}$ with the types of its pair of vertices

All left-side pairs in a $K_{6,4}$ are either type 5 or 6, producing triples of type 5,5,6 or 6,6,6. On the right side, pairs and resulting triples are all of type 5. These findings can be cross-verified later with Table 4.4, where we list all non-equivalent vertex triples, classifying them by type, and identify the bipartite subgraphs they belong to.

Constructing $K_{4,4}$

Consider the vertices of type 7 in Table 4.3:

123	124
456	357
789	689
v	w

12	3	
4	5	6
	7	89

The grid pattern of v and w of type 7

Table 4.3: An example of a type-7 vertex pair

The methodology previously described allows us to identify the common neighbours of v and w, as depicted in diagram 4.4. Subsequently, diagram 4.7 showcases the common neighbours of b and c which are two mutual neighbours of v and w.

It is clear that two common neighbours of b and c are indeed v and w, but there are also two additional common neighbours e and f. A simple verification shows that these neighbours, e and f, are also adjacent to a and d. Consequently, $\mathrm{CN}(\mathrm{CN}(v, w))$ consists of the vertices e, f, v, and w. Hence, a pair of type 7 vertices generates the maximal complete bipartite subgraph $K_{4,4}$.

For a more in-depth understanding of the $K_{4,4}$ subgraph structure, we examine the vertex pair types on each side of the subgraph, as illustrated in Figure 4.8. This provides a clearer view of the internal arrangements within this bipartite configuration.

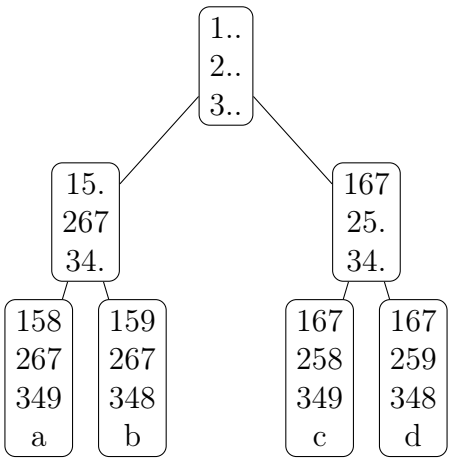

Figure 4.6: Common neighbours of a type-7 pair of vertices

In Figure 4.8, it is noticeable that all vertex pairs in a $K_{4,4}$ are of either type 5 or 7, and all triples conform to the type 5,5,7. Notably, the two sides of this subgraph are symmetric regarding the pairs' type. Any pair of type 7 within this subgraph can be used as a starting point to construct this exact subgraph. Further corroboration is provided later in Table 4.4, confirming that the only triple included in a $K_{4,4}$ is of the type 5,5,7.

Properties and Notations of Bipartite Subgraphs

In graph theory, the left-right designation of the sides of a bipartite graph is typically inconsequential. However, in the context of simplices in B_{edge}, which are subsets of edge sets of complete bipartite subgraphs in $\mathcal{P}(3^3)$ (recall definition 1.3.1), this order becomes crucial due to edge orientation. At times, we discuss the antipodal of a bipartite subgraph $K_{i,j}$. Essentially, it remains the same subgraph; however, the sides are interchanged, hence it is denoted as $K_{j,i}$.

Throughout this document, any references made to the subgraphs $K_{1,36}, K_{2,2}$, $K_{2,12}$, $K_{4,4}$, or $K_{6,4}$ pertain to the respective subgraphs we established earlier in this section. Proposition 4.1.2 confirms that these bipartite subgraphs, are indeed maximal. Furthermore, Theorem 4.1.14 certifies that these constitute the entire set of maximal complete bipartite subgraphs in $\mathrm{B}_{\mathrm{edge}}\big(\mathcal{P}(3^3)\big)$.

When the specific pair a, b that generates the bipartite subgraph $K_{i,j}(a, b)$ is of relevance, we use the notation $K_{i,j}(a, b)$. If the pair is insignificant, we simply write $K_{i,j}$.

The only maximal complete bipartite subgraph that does not originate from a pair of vertices is $K_{1,36}$, comprising of a single vertex w on one side, all its neighbours on the other, and the edges connecting the left side to the right. We denote this as $K_{1,36}(w) = (w, \mathrm{CN}(w))$.

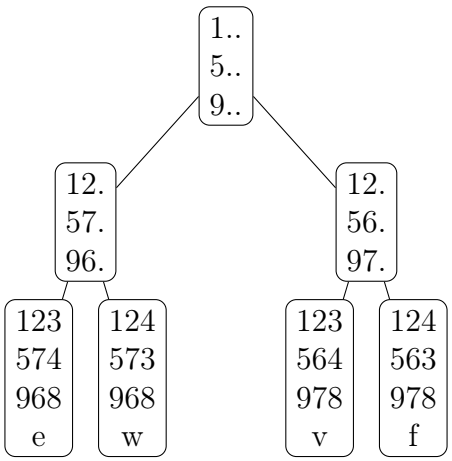

Figure 4.7: Common neighbours of b and c, two of the common neighbours of a vertex pair of type 7

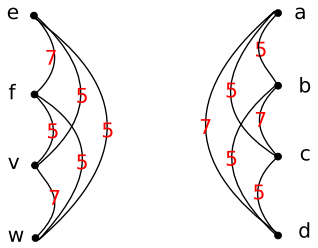

Figure 4.8: A $K_{4,4}$ with the types of its pair of vertices

On the right side of a $K_{1,36}$, pairs and triples of vertices of any type may appear, excluding triples of types 5,5,9 and 5,6,9 due to their non-existence as dictated later by Lemma 3.2.1. Types 5,6,6 and 6,6,7 are also excluded, as per Table 4.4, due to their lack of common neighbours.

Proposition 4.1.6. The set of bipartite subgraphs built from a vertex pair of type i, with $i \in \{5, 6, 7, 9\}$ by the process explained in Remark 4.1.1 are equivalent.

Proof: In constructing the bipartite subgraphs from a type i pair, we select all the common neighbours of the pair, then determine all their common neighbours in turn. This procedure's sole variable is the pair type. As per Theorem 3.1.4, pairs of the same type are equivalent. Hence, the set of all bipartite subgraphs constructed from one type of vertex pair are equivalent. ∎

A direct outcome of Lemma 4.1.4 and Lemma 4.1.2 is the following:

Proposition 4.1.7. The subgraphs $K_{2,12}, K_{4,4}$, and $K_{6,4}$ are induced subgraphs.

Proof: Assume, by way of contradiction, that $K_{i,j}$ is one of the above subgraphs and is not induced. This implies the existence of an edge e in the graph that does not belong to the subgraph $K_{i,j}$. Given that $K_{i,j}$ is a complete bipartite subgraph, the extraneous edge e must connect two vertices, say v and v', each of them on the same side of $K_{i,j}$. Since $K_{i,j}$ is a complete bipartite graph, both v and v' are adjacent to every vertex on the opposite side of the bipartite graph. By Lemma 4.1.4, this leads to the existence of a complete bipartite graph $K_{2,2}$ within $K_{i,j}$, which contains the vertices v, v', and two vertices from the opposite side. However, this is in contradiction with Lemma 4.1.4, which states that every $K_{2,2}$ is maximal. Thus, it follows that our initial assumption is false, and $K_{i,j}$ must indeed be an induced subgraph. ∎

4.1.2 Inclusion of Vertex Triples and Quadruples in Bipartite Subgraphs

In this section, we focus on vertex triples and quadruples belonging to different equivalence classes and aim to identify their common neighbours. Our objective is to demonstrate that the complete bipartite subgraphs, $\big(\mathrm{CN}(\mathrm{CN}(\text{triple})), \mathrm{CN}(\text{triple})\big)$, obtained through the same process used for vertex pairs in Remark 4.1.1, are encompassed within the known complete bipartite subgraphs.

Inclusion of Vertex Triples

In this section, we revisit Section 3.2.2, where we identified the equivalence classes into which vertex triples of specific types are divided. Utilizing these results, we will analyze each class to determine the common neighbours of the vertex triples.

Table 4.4 serves as a comprehensive version of Table 3.13 which classified all the vertex triples of different types. Table 4.4 includes not only the number of common neighbours for each triple class but also the maximal complete bipartite subgraph that is formed by applying the method of Remark 4.1.1 to the triple. The way these subgraphs are constructed guarantees their uniqueness.

After presenting this table, we will employ the familiar method detailed in Section 4.1.1 to determine the common neighbours of a triple of type 5,5,5. We also illustrate the maximal complete bipartite subgraph, in which this triple is included in.

Similar to the process for a triple of type 5,5,5 as described in Lemma 4.1.8, we can apply this approach to each class of vertex triples discussed in Appendix A. This methodology allows us to initially identify the common neighbours and the corresponding maximal complete bipartite subgraph.

While this analysis is relatively straightforward, it is also quite lengthy. As such, we believe it is not essential to include it in this text. Instead, we have provided

the results of this analysis in Table 4.4, which provides sufficient information for our subsequent discussions.

type of triples	equivalence classes	♯ of common neighbours	bipartite subgraph
5,5,5	one class	6	$K_{6,4}$
	one class	0	–
6,6,6	one class	4	$K_{6,4}$
	one class	1	$K_{1,36}$
5,5,6	one class	4	$K_{6,4}$
5,5,7	one class	4	$K_{4,4}$
5,6,6	one class	0	–
6,6,7	one class	0	–
	one class	0	–
5,6,7	one class	2	$K_{2,12}$
	one class	0	–
6,7,7	one class	2	$K_{2,12}$
	one class	1	$K_{1,36}$
	one class	0	–
7,7,7	three classes	1	$K_{1,36}$
	two classes	0	–
5,7,7	two classes	2	$K_{2,12}$
	three classes	0	–

Table 4.4: The possible triples that do not include a pair of type 9 lead to a bipartite subgraph $K_{1,36}$, $K_{2,12}$, $K_{6,4}$, or $K_{4,4}$.

Lemma 4.1.8. A triple of type 5,5,5 either shares six neighbours and the bipartite subgraph derived from it using the method of Remark 4.1.1 is consequently a $K_{4,6}$, or it does not share any neighbours.

Proof: Refer back to Lemma 3.2.3, where triples of type 5,5,5 are classified into two classes - first kind and second kind. Consider the first kind triple we computed in this lemma as follows:

$$\begin{array}{ccc} 123 & 123 & 123 \\ 456 & 489 & 468 \\ 789 & 756 & 579 \\ v & w & u_1 \end{array} \tag{4.1.2}$$

We use the same algorithm introduced in Section 4.1.1 to find the common neighbours of a group of vertices. The algorithm to find the common neighbours of the triple v, w, u_1 can be found in the diagram of Figure 4.9. The details of this analysis are

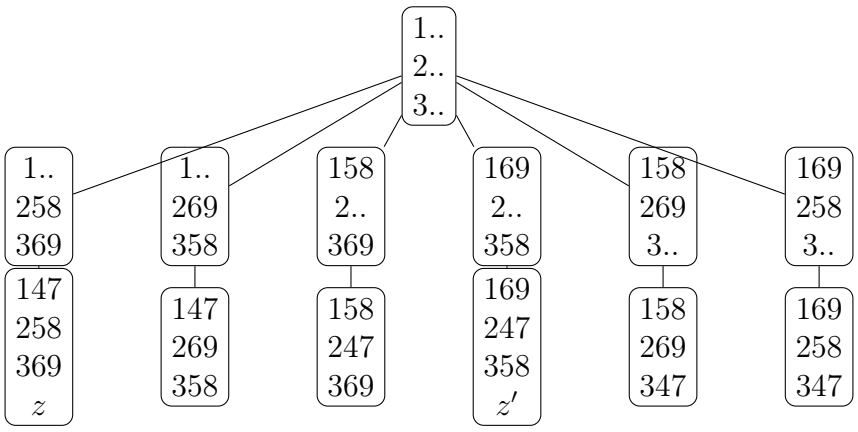

Figure 4.9: Common neighbours of a first kind triple of type 5,5,5

given subsequently. Let z be the common neighbour of the triple v, w, u_1. Initially, we distribute the shared cell of v, w, and u_1 across the three cells of z (the first step of the diagram).

The elements of each shared pair of v and w, $\{5, 6\}$ and $\{8, 9\}$, cannot be together in a cell of z. Since 5 and 9 are together in one cell of u_1 they cannot be in the same cell of their common neighbour; for the same reason, 8 and 6 cannot be in the same cell of z. Thus, there are six ways to place the pairs $\{5, 8\}$ and $\{6, 9\}$ in the cells of z (second step of the diagram).

In the diagram, after we arrange the vertex z in the second step, only two empty spots remain. These are the only available spaces for the remaining elements, 4 and 7. We can place them in these two spots without violating any rules. This is because neither of these elements co-exist with the elements 1, 2, or 3 in any of the cells belonging to the vertices of the triple v, w, u_1. This arrangement is validated by the third step of the diagram.

Therefore, vertices of the first kind of the 5,5,5 have 6 common neighbours, $|\operatorname{CN}(v, w, u_1)| = 6$.

Consider two of the common neighbours of v, w, u_1 which are denoted as z and z' in the diagram. Since z and z' are adjacent to all the vertices of the triple v, w, u_1, we have $\{v, w, u_1\} \subseteq \operatorname{CN}(z, z')$. By taking the common neighbours of both sides of the inclusion, we deduce that

$$\operatorname{CN}(\operatorname{CN}(z, z')) \subseteq \operatorname{CN}(v, w, u_1).$$

which holds by Lemma 1.2.3.

It is easy to verify that the type of z and z', denoted $\mathrm{T}(z, z')$, equals 6. Referencing Figure 4.5, we know $|\operatorname{CN}(z, z')| = 4$ and $|\operatorname{CN}(\operatorname{CN}(z, z'))| = 6$, and

$$\Big(\operatorname{CN}(z, z'), \operatorname{CN}\big(\operatorname{CN}(z, z')\big)\Big) = K_{4,6} \tag{4.1.3}$$

Taking into account our earlier result that $|\operatorname{CN}(v,w,u_1)| = 6$, we find that $|\operatorname{CN}(\operatorname{CN}(z,z'))| = |\operatorname{CN}(v,w,u_1)|$. This equality implies that

$$\begin{aligned}
&\operatorname{CN}(\operatorname{CN}(z,z')) = \operatorname{CN}(v,w,u_1) \\
\Rightarrow\quad &\operatorname{CN}\big(\operatorname{CN}(\operatorname{CN}(z,z'))\big) = \operatorname{CN}(\operatorname{CN}(v,w,u_1)) && \text{Taking CN of both sides} \\
\Rightarrow\quad &\operatorname{CN}(z,z') = \operatorname{CN}(\operatorname{CN}(v,w,u_1)). && \text{By Lemma 1.2.4}
\end{aligned}$$

which means the complete bipartite subgraph constructed by this triple by the method of Remark 4.1.1 forms a $K_{4,6}$ subgraph:

$$\big(\operatorname{CN}(\operatorname{CN}(v,w,u_1)), \operatorname{CN}(v,w,u_1)\big) = K_{4,6}.$$

Now, consider the triple v, w, u_2 of the second kind of type 5,5,5 we computed in Lemma 3.2.3 as the following:

123	123	123
456	489	467
789	756	589
v	w	u_2

The elements in a cell of each v, w, and u_2 are distributed across three distinct cells of their common neighbour. Therefore, element 7 cannot be placed in the same cell as 8, 9, 5, 6, or 4. Also, since $\{4,5,6\}$ forms a cell of v, each element of this cell is placed in a different cell of the shared neighbour, leaving no room for element 7. Thus, second-kind triples of type 5,5,5 do not share any neighbours.

∎

Inclusion of Vertex Quadruples

In this section, our objective is to establish that if we extract the common neighbours of a vertex quadruple and subsequently find the common neighbours of these initial common neighbours (the method of Remark 4.1.1), the resulting subgraph forms one of the known maximal complete bipartite subgraphs.

Before commencing the analysis for this section, we need the following lemma.

Lemma 4.1.9. If all the pairs of the vertices of the vertex set $V \subseteq V(\mathcal{P}(3^3))$ are of type 5, then they share a cell.

Proof: Suppose that $v = \{v_1, v_2, v_3\}$ and $w = \{w_1, w_2, w_3\}$ are two arbitrary vertices in V, with v_i and w_i denoting their respective cells for $i \in \{1,2,3\}$. Given

that $\mathrm{T}(v, w) = 5$, by reference to the grid pattern for type 5 pairs in 3.3, we deduce that v and w share a common cell.

Without loss of generality, assume that $v_1 = w_1$ is their common cell. Then for all $i, j \in \{2, 3\}$, $v_i \cap w_j \neq \emptyset$.

Consider another vertex $u \in V$. Since $\mathrm{T}(u, v) = \mathrm{T}(u, w) = 5$, vertex u shares a common cell with both v and a common cell with w. This common cell must be v_1 (which is equal to w_1) because:

1. Consider a situation where the common cell of u with v (or w) is different from v_1, and yet u shares a common cell with w (res. v) which is w_1. In this case, u would share two common cells with v (res. w). However, this would imply that $u = v$ (res. $u = w$), contradicting our initial assumption that all vertices in the set V are distinct.

2. If u shares a common cell with v and w that is different from v_1, then the common cell of u with v is v_i and the common cell of u with w is w_j for $i, j = 2$ or 3. This contradicts the property that the cells of a vertex are disjoint sets, as we have $v_i \cap w_j \neq \emptyset$.

Hence, the common cell of u with both w and v is indeed v_1 which is their common cell. ∎

Utilizing Table 4.4, we can infer if a vertex quadruple contains some special vertex triple, then the maximal complete bipartite subgraph derived from the quadruple by applying the method of Remark 4.1.1 to the quadruple, is one of the following forms:

- If there exists a triple of type 5,6,6 or 6,6,7 in the quadruple, then the quadruple does not share any common neighbours, and thus does not lead to a bipartite subgraph.

- If there exists a triple of type 7,7,7 in the quadruple, then the quadruple either does not share any common neighbours, or its corresponding maximal complete bipartite subgraph forms a $K_{1,36}$.

- If the triple type is 5,7,7; 6,7,7; or 5,6,7, then the quadruple corresponds to one of the following scenarios:

    1. It does not share any neighbours.
    2. It shares one neighbour and leads to a $K_{1,36}$ subgraph.
    3. It shares the same two common neighbours as the triple. We know the maximal complete bipartite subgraph corresponding to the triple is a $K_{2,12}$. Let $K_{2,12} = (A, B)$, where $|A| = 2$ and $|B| = 12$. Then the quadruple is

a subset of $\mathrm{CN}(A)$ and we know that $\mathrm{CN}(A) = B$. Hence, the quadruple forms a subset of B. Consequently, in this case, the maximal complete bipartite subgraph derived from the quadruple forms a $K_{2,12}$.

Given these observations, we only need to analyze quadruples that do not contain any triples of the aforementioned types. The remaining types to consider are 5,5,5; 5,5,6; 5,5,7; and 6,6,6. In Table 4.5, we will demonstrate that quadruples formed by these triples are contained within either a $K_{6,4}$ or $K_{4,4}$ subgraph.

Consider a vertex quadruple v, w, u, p in $\mathcal{P}(3^3)$. In Table 4.5, the first column represents the case number, while the other columns, excluding the final one, detail the possible types of vertex pairs within the quadruple v, w, u, p. The table is organized into four sections, each section holding constant the types $\mathrm{T}(u, w)$, $\mathrm{T}(v, w)$, and $\mathrm{T}(u, v)$.

The last column, labelled "bipartite subgraph", contains the outcomes for each case, which are subsequently proven. In this column, the symbol "$\times$" denotes the absence of a quadruple with the specified types. Conversely, "$K_{i,j}$" implies that applying the method of Remark 4.1.1 to the given quadruple results in a $K_{i,j}$ subgraph.

case ♯	$\mathrm{T}(p, w)$	$\mathrm{T}(p, u)$	$\mathrm{T}(p, v)$	$\mathrm{T}(u, w)$	$\mathrm{T}(v, u)$	$\mathrm{T}(w, v)$	bipartite subgraph
1	5	7	5	5	5	6	$\times$
2	5	6	5	5	5	6	$K_{6,4}$
3	5	5	5	5	5	6	$\times$
4	6	5	6	5	5	6	$K_{6,4}$
5	5	5	5	5	5	5	$K_{6,4}$
6	5	5	7	5	5	5	$\times$
7	5	5	5	6	6	6	$K_{6,4}$
8	6	6	6	6	6	6	$\times$
9	5	7	5	5	5	7	$K_{4,4}$

Table 4.5: Inclusion of quadruples with the triples of types 5,5,5 or 5,5,6 or 5,5,7 or 6,6,6 in the known bipartite subgraphs

Having already classified vertex triples into various types, our current approach involves selecting a triple from a specific equivalence class and then scrutinizing all potential candidates for the fourth vertex. As an illustration, we will prove the first case in Table 4.5, which asserts that no maximal complete bipartite subgraph can originate from a quadruple with the pair types stated in this case. The succeeding cases listed in this table are substantiated in a similar manner and are detailed in Appendix B.

Lemma 4.1.10. Given a vertex triple u, v, w of type 5,5,6, the application of the method specified in Remark 4.1.1 to any vertex quadruple incorporating this triple will either yield no bipartite subgraph or will generate a $K_{6,4}$ bipartite subgraph.

Proof: By Table 4.4, all triples of type 5,5,6 are equivalent. Consider the triple v, w, u of this type as the following:

$$\begin{array}{ccc} 123 & 124 & 123 \\ 456 & 389 & 567 \\ 789 & 567 & 489 \\ v & w & u \end{array} \tag{4.1.4}$$

The common neighbours of the triple v, w, u are the same as the common neighbours of v and w presented in the diagram of Figure 4.4. So, $|\operatorname{CN}(v, w, u)| = 4$. From Table 4.4, we see the complete bipartite subgraph derived from a triple of type 5,5,6 is a $K_{6,4}$:

$$\big(\operatorname{CN}(\operatorname{CN}(v, w, u)), \operatorname{CN}(v, w, u)\big) = K_{6,4}. \tag{4.1.5}$$

Here, we study cases number 1, 2, 3, and 4 of Table 4.5:

1. Since $\mathrm{T}(p, v) = 5$, we need to choose a common cell between these two vertices. The common cell cannot be $\{1, 2, 3\}$ because it would make a common cell with u which contradicts $\mathrm{T}(p, u) = 7$. If the common cell is $\{4, 5, 6\}$ or $\{7, 8, 9\}$, then the common cell with w has to be $\{3, 8, 9\}$ or $\{1, 2, 4\}$ respectively, due to the fact that they are the only cells of w disjoint from the corresponding cells in v. Then no cell of v would share one element with each cell of u which contradicts $\mathrm{T}(p, u) = 7$. Therefore, there is no quadruple of the types of the first case.

2. Since $\mathrm{T}(p, v) = 5$, we need to choose a cell shared between p and v. This cell cannot be $\{1, 2, 3\}$ because it contradicts $\mathrm{T}(p, u) = 6$. If the cell is $\{4, 5, 6\}$ or $\{7, 8, 9\}$, then the common cell of p and w would be $\{3, 8, 9\}$ or $\{1, 2, 4\}$, respectively. Then the last cell of p is formed with the remaining elements. Therefore, the fourth vertex p can take on two potential configurations, denoted as p_1 and p_2:

$$p_1 = \{\{4, 5, 6\}, \{3, 8, 9\}, \{1, 2, 7\}\}$$
$$p_2 = \{\{7, 8, 9\}, \{1, 2, 4\}, \{3, 5, 6\}\}.$$

   Upon further examination, we see p_1 and p_2 are adjacent to all the common neighbours of the triple v, w, u presented in the diagram of Figure 4.4. This implies that $\{v, w, u, p\} \subseteq \operatorname{CN}(\operatorname{CN}(v, w, u))$. After taking the common neighbours of both sides, the direction of the inclusion is reversed, then by Lemma 1.2.4, the inclusion $\operatorname{CN}(v, w, u) \subseteq \operatorname{CN}(v, w, u, p)$ holds. Moreover,

since we have the set inclusion $\{v, w, u\} \subseteq \{v, w, u, p\}$, taking the common neighbours of both sides gives $\mathrm{CN}(\{v, w, u, p\}) \subseteq \mathrm{CN}(v, w, u)$. This results in $\mathrm{CN}(v, w, u, p) = \mathrm{CN}(v, w, u)$; and taking common neighbours of both sides confirms that $\mathrm{CN}(\mathrm{CN}(v, w, u, p)) = \mathrm{CN}(\mathrm{CN}(v, w, u))$. Therefore, by equation (4.1.5) the complete bipartite subgraph derived by applying the method of Remark 4.1.1 to the quadruple v, w, u, p forms a $K_{6,4}$:

$$\big(\,\mathrm{CN}(\mathrm{CN}(v, w, u, p)), \mathrm{CN}(v, w, u, p)\big) = K_{6,4}.$$

3. Since the triple v, u, p is of type 5,5,5, they share a common cell. By Lemma 4.1.9, the common cell is $\{1, 2, 3\}$ because it is the common cell of v and u. Similarly, the triple w, u, p is of type 5,5,5, so the vertices must share a cell. The cell is $\{5, 6, 7\}$ as it is the common cell of w and u. Then the last cell of p is formed with the remaining elements $\{4, 8, 9\}$. However, this choice of cells makes two vertices p and w equal. Consequently, there is no distinct vertex that satisfies the conditions of case number 3.

4. Since $\mathrm{T}(p, u) = 5$, they share a cell. This cell cannot be $\{1, 2, 3\}$ or $\{5, 6, 7\}$ as it contradicts $\mathrm{T}(p, v) = 6$ and $\mathrm{T}(p, w) = 6$, respectively. Consequently, one cell of p is $\{4, 8, 9\}$. To follow $\mathrm{T}(p, w) = 6$, the choices for the next cell of p are $\{3, 6, 7\}$, $\{3, 5, 7\}$, and $\{3, 5, 6\}$. However, the two first ones are not valid because they contradict $\mathrm{T}(p, v) = 6$. Therefore, the only option for p is:

$$p = \{\{4, 8, 9\}, \{3, 5, 6\}, \{1, 2, 7\}\}.$$

It can be easily verified that p is adjacent to all the common neighbours of the triple v, w, u presented in the diagram of Figure 4.5. Thus, $\{v, w, u, p\} \subseteq \mathrm{CN}(\mathrm{CN}(v, w, u))$. Then similar to case number 2, we see the complete bipartite subgraph derived from the quadruple v, w, u, p is a $K_{6,4}$.

∎

4.1.3 Main Theorem of Bipartite Subgraphs

In this subsection, we present Theorem 4.1.14, which stands as a pivotal result of this work. This theorem serves to classify all maximal complete bipartite subgraphs of $\mathcal{P}(3^3)$, thereby facilitating the construction of simplices in $\mathrm{B}_{\mathrm{edge}}\big(\mathcal{P}(3^3)\big)$. The foundation of this theorem relies on our accumulated understanding of the maximal complete bipartite subgraphs of $\mathcal{P}(3^3)$, as well as the equivalencies related to vertex pairs, triples, and quadruples, and their respective inclusion in bipartite subgraphs. To fully develop this theorem, we will introduce some supporting lemmas in the following.

Lemma 4.1.11. Let $V = \{v_1, v_2, \ldots, v_t \mid t \geq 2\}$ be a set of distinct vertices of $\mathcal{P}(3^3)$ such that each pair of vertices in V has 5 or more common neighbours. Then every pair of vertices in V is of type 5.

Proof: Assume by contradiction that there exist vertices $v, v' \in V$ such that $\mathrm{T}(v, v') \neq 5$, but rather $\mathrm{T}(v, v') \in \{6, 7, 9\}$. In this case, the number of common neighbours of v and v', and consequently of all vertices in V, would be less than or equal to 4, contradicting the assumption that each pair of vertices in V has 5 or more common neighbours. ∎

The following corollary directly results from the Lemmas 4.1.11 and 4.1.9:

Corollary 4.1.12. Let $V = \{v_1, v_2, \ldots, v_k\}$ be a set of distinct vertices of $\mathcal{P}(3^3)$ with $k \geq 2$, such that each pair of vertices in V has 5 or more common neighbours. Then, all vertices in V share a common cell.

Lemma 4.1.13. The largest set $S \subseteq V(\mathcal{P}(3^3))$ such that every triple of vertices in S belongs to the first kind of type 5,5,5 consists of 4 vertices.

Proof: As indicated by Lemma 4.1.9, all vertices of set S share a common cell. Looking at the grid pattern for a pair of type 5 (as demonstrated in 3.3), it is clear that creating a pair of vertices of type 5 requires a common cell and two distinct pairs of elements, each from a non-shared cell. Furthermore, the cube pattern of a triple of the first kind of type 5,5,5 (shown in Table 3.15) does not share any pair of elements across the three vertices. This leads us to focus on pairs of vertices of type 5 which share unique pairs of elements.

Now, consider a vertex v with cell structure denoted as $\{v_1, v_2, v_3\}$. Suppose v_1 is the common cell between v and a new vertex w. Our goal is to determine the number of potential vertices w such that the pair v, w is of type 5. The cell v_2 must share two elements with one of w's cells. However, we are specifically interested in vertices w that share unique pairs of elements with v's cells.

Given that $|v_2| = 3$, it comprises three distinct pairs of elements. Consequently, we can generate at most three different vertices w each of type 5 with v. Therefore, we end up with a total of 4 vertices: v and the three vertices w. Since all these vertices share a cell, all pairs among them are of type 5. Furthermore, by uniquely choosing the shared pairs, all triples among these vertices belong to the first kind of type 5,5,5.

∎

In the following theorem, we show all the complete bipartite subgraphs of $\mathcal{P}(3^3)$ are of one of the forms $K_{1,36}$, $K_{2,12}$, $K_{2,2}$, $K_{4,4}$, or $K_{6,4}$.

Theorem 4.1.14. Let $(M, N) = K_{m,n}$ be a complete bipartite subgraph of $\mathcal{P}(3^3)$, where $M, N \neq \emptyset$. The subgraph (M, N) is included in or equal to a $K_{1,36}$, $K_{2,12}$, $K_{2,2}$, $K_{4,4}$, or $K_{6,4}$.

Proof: The proof is done by a case study on the side N of the subgraph (M, N), which equivalently can be done on M too.

Case 1: $37 \leq n$. As each vertex has a degree of 36, this case is not possible.

Case 2: $13 \leq n \leq 36$. Earlier in Section 4.1.1 we proved the largest number of the common neighbours of a vertex pair is 12. Then, in this case, M contains just one vertex, and thus, (M, N) is a subgraph of a $K_{1,36}$.

Case 3: $5 \leq n \leq 12$. By Lemma 4.1.11 all the vertex pairs of M are of type 5. Since $n \geq 5$, triples of M are of the first kind of type 5,5,5. Now we study the cases of the side M:

- $m = 1$: (M, N) is included in a $K_{1,36}$.
- $m = 2$: From subsection 4.1.1, we know that the maximal complete bipartite graph derived from a pair of type 5 is a $K_{2,12}$. So, (M, N) is a subgraph of $K_{2,12}$.
- $m = 3$: Since the triple in M is of the first kind of type 5,5,5, then based on the Table 4.4, (M, N) is a subgraph of a $K_{6,4}$.
- $m = 4$: We know from Table 4.5 that a set of four vertices, where all pairs are of type 5, is a subgraph of $K_{6,4}$.
- $m \geq 5$: By Lemma 4.1.13, no set of vertices of size 5 or more exists where all the triples are of the first kind of type 5,5,5.

Case 4: $2 \leq n \leq 4$. Again we break it down to the following cases of M:

- $m = 2$: By our earlier categorization of pairs, (M, N) is a subgraph of (or equal to) one of: $K_{2,2}, K_{2,12}, K_{4,6}$, or $K_{4,4}$.
- $m = 3$: If one of the pair types of M was 9, then (M, N) is a subgraph of $K_{2,2}$. However, $K_{2,2}$ is maximal, so there is no pair of type 9 in M. Then all the pair types in M are 5, 6, or 7. The pairs of M cannot be all of type 5 because they share no common neighbours or 6 common neighbours, and here $0 \neq n \leq 4$. The rows 2 to 10 of Table 4.4 show the subgraph (M, N) either does not form a bipartite subgraph or is a subgraph of a $K_{4,4}$, $K_{6,4}$, $K_{2,12}$, or $K_{1,36}$.
- $m = 4$: The common neighbours of all four vertices of M are a subset of the common neighbours of each triple of M. Similar to the previous case where $m = 3$, we exclude type 9. With the help of Table 4.4 we can make the following analysis:
  - If one of the triples is of the type 7,6,6 or 5,6,6, then the vertices of M do not share any neighbours.

- If one of the triples is 6,7,7, or 5,6,7, or 5,7,7, or 7,7,7 we know this triple is a subgraph of a $K_{12,2}$ or $K_{36,1}$, or the vertices do not share any neighbours (refer to the explanations before Table 4.5).
- In the Table 4.5 we observe if one of the triples of M is 5,5,5 or 5,5,6 or 5,5,7 or 6,6,6, then (M, N) either does not exist, or it is a subgraph of a $K_{6,4}$ or a $K_{4,4}$.

- $m \geq 5$: Since vertices of N share a common cell, this case is the same as the case where $n \geq 5$.

Case 5: $n = 1$. In this case $m \leq 36$ and (M, N) is a subgraph of a $K_{36,1}$. ∎

4.2 Maximal Simplices of $\mathrm{B}_{\mathbf{edge}}\big(\mathcal{P}(3^3)\big)$

In this section, we explore the maximal simplices of $\mathrm{B}_{\mathrm{edge}}\big(\mathcal{P}(3^3)\big)$, building upon our understanding of the maximal complete bipartite subgraphs of $\mathcal{P}(3^3)$. In the context of the edge box complex $\mathrm{B}_{\mathrm{edge}}(G)$ as defined in 1.3.1, each complete bipartite subgraph is associated with a unique simplex, which is in turn constructed uniquely from said subgraph.

Building on the results from the previous section, we use the identified maximal complete bipartite subgraphs of $\mathcal{P}(3^3)$ as a foundation to construct and introduce the maximal simplices of $\mathrm{B}_{\mathrm{edge}}\big(\mathcal{P}(3^3)\big)$. Our exploration does not stop here; we then venture into the analysis of the intersections of these simplices. The intention is to understand their structure and interconnections more profoundly, which is paramount to comprehending the intricate details of the edge box complex $\mathrm{B}_{\mathrm{edge}}\big(\mathcal{P}(3^3)\big)$.

Prior to embarking on our exploration, we need to establish some notations. Remember Remark 4.1.1 detailing the construction process of the maximal complete bipartite subgraphs of $\mathcal{P}(3^3)$. Also, recall the notations defined in Section 4.1.1 pertaining to these subgraphs. We will adopt similar notations for the simplicies of $\mathrm{B}_{\mathrm{edge}}\big(\mathcal{P}(3^3)\big)$.

Remark 4.2.1. The simplex of $\mathrm{B}_{\mathrm{edge}}\big(\mathcal{P}(3^3)\big)$ that stems from the bipartite subgraph

$$K_{i,j}(a,b) = \Big(\mathrm{CN}\big(\mathrm{CN}(a,b)\big), \mathrm{CN}(a,b)\Big)$$

where $|\,\mathrm{CN}\big(\mathrm{CN}(a,b)\big)| = i$ and $|\,\mathrm{CN}(a,b)| = j$, is represented as

$$S_{i,j}(a,b) = \{\mathrm{CN}\big(\mathrm{CN}(a,b)\big)\} \times \{\mathrm{CN}(a,b)\} = \{(v,w) | v \in \mathrm{CN}\big(\mathrm{CN}(a,b)\big), w \in \mathrm{CN}(a,b)\}.$$

where each (v, w) is a vertex of the simplex $S_{i,j}(a, b)$. We use $S_{i,j}$ to denote the simplex $S_{i,j}(a, b)$ when the pair is not crucial. The act of swapping the sides of the

simplex $S_{i,j}$ gives rise to a new simplex $S_{j,i}$, termed the antipodal of $S_{i,j}$. Sometimes, a simplex and its antipodal are generally denoted as S and $\widetilde{S}$, respectively. Similar to the maximal complete bipartite subgraphs, the simplices $S_{2,2}, S_{4,4}, S_{6,4}, S_{2,12}, S_{1,36}$ and their antipodals are the only maximal simplices in $\mathrm{B}_{\mathrm{edge}}\big(\mathcal{P}(3^3)\big)$, as articulated in Corollary 4.2.3.

The following lemma establishes a natural connection between maximal simplices and maximal complete bipartite subgraphs. This connection serves as a bridge between these two fundamental components.

Lemma 4.2.2. A simplex in $\mathrm{B}_{\mathrm{edge}}\big(\mathcal{P}(3^3)\big)$ is maximal if and only if its corresponding complete bipartite subgraph of $\mathcal{P}(3^3)$ is maximal in the set of all complete bipartite subgraphs of $\mathcal{P}(3^3)$.

Building on Theorem 4.1.14 and Lemma 4.2.2, we can identify the maximal simplices in $\mathrm{B}_{\mathrm{edge}}\big(\mathcal{P}(3^3)\big)$:

Corollary 4.2.3. The simplices $S_{2,2}, S_{4,4}, S_{6,4}, S_{2,12}, S_{1,36}$, and their antipodals, are the only maximal simplices of $\mathrm{B}_{\mathrm{edge}}\big(\mathcal{P}(3^3)\big)$.

4.2.1 Intersection of Maximal Simplicies

Now that we know all the maximal simplicies of $\mathrm{B}_{\mathrm{edge}}\big(\mathcal{P}(3^3)\big)$, we are able to study their intersections. The result of this section will be needed in Section 6.2.4 to reduce the dimension of $\mathrm{B}_{\mathrm{edge}}\big(\mathcal{P}(3^3)\big)$ using elementary collapses and discrete Morse functions. The following lemma states that a simplex cannot intersect with both another simplex and its opposite at the same time.

Lemma 4.2.4. Let A and B be any maximal simplicies of $\mathrm{B}_{\mathrm{edge}}\big(\mathcal{P}(3^3)\big)$ except the $S_{2,2}$ and $S_1, 36$, with antipodals $\widetilde{A}$ and $\widetilde{B}$. If $A \cap B \neq \emptyset$, then $A \cap \widetilde{B} = \emptyset$ and $\widetilde{A} \cap B = \emptyset$.

Proof: Revisiting the notations in Remark 4.2.1, let $A = A_1 \times A_2$ and $B = B_1 \times B_2$. Then $\widetilde{B} = B_2 \times B_1$. Since $A \cap B \neq \emptyset$, there exist elements $x_1 \in A_1 \cap B_1$ and $x_2 \in A_2 \cap B_2$. Assume there exists a vertex $(y_1, y_2) \in A \cap \widetilde{B}$. It follows that $y_1 \in A_1 \cap B_2$ and $y_2 \in A_2 \cap B_1$. This implies that $\{x_1, y_2\} \subseteq B_1$ and $\{x_2, y_1\} \subseteq B_2$. As elements of A_1 and A_2 are adjacent in $\mathcal{P}(3^3)$, x_1 and y_1 are adjacent to x_2 and y_2. However, according to Proposition 4.1.7, the bipartite subgraph corresponding to the simplex B is induced, leading to a contradiction with the edges x_1y_2 and y_1x_2. Therefore, it must be that $A \cap \widetilde{B} = \emptyset$ and, by a similar argument, $\widetilde{A} \cap B = \emptyset$. ∎

The previous Lemma 4.2.4 does not apply to the simplices A and B being $S_{2,2}$, because this subgraph is not induced. As a result, it is possible for B to intersect both A and $\widetilde{A}$.

Next, we turn our attention to the intersections of maximal simplices within the box complex $\mathrm{B}_{\mathrm{edge}}\big(\mathcal{P}(3^3)\big)$. The table in reference 4.6 outlines the maximum size of intersections between each pair of these simplices. Below, we provide a thorough explanation of the reasoning behind this table, along with further insights into the structure of these intersections. In certain instances, the intersection of specific simplices is not explicitly mentioned. This is due to the fact that these intersections are empty.

Intersection of the 4-clique complex with maximal simplicies:

Although a 4-clique complex (recall Figure 2.7 and Definition 2.2.1) is not a maximal simplex of $\mathrm{B}_{\mathrm{edge}}\big(\mathcal{P}(3^3)\big)$, it originates from the maximal clique of the graph $\mathcal{P}(3^3)$. Therefore, it is important to examine the intersection of this structure with maximal simplices.

Consider the following 4-clique, C, and let C_s be the 4-clique complex of $\mathrm{B}_{\mathrm{edge}}\big(\mathcal{P}(3^3)\big)$ corresponding to this 4-clique:

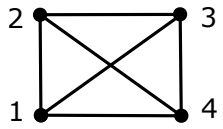

Figure 4.10: A 4-clique

Let i be one of the vertices of C_s, and let $S_{1,36} = \{i\}\times\{\mathrm{CN}(i)\}$. Then, $C_s \cap S_{1,36} = \{i\} \times \{\mathrm{CN}(i) \cap C\}$, which contains all three ordered edges of C connected to vertex i. Thus, $|C_s \cap S_{1,36}| = 3$. If i is not one of the vertices of the 4-clique C, then $C_s \cap S_{1,36} = \emptyset$. The same analysis applies to a $S_{36,1}$.

Let $S_{2,2} = \{i, j\} \times \{k, l\}$, where i, j, k, l are the vertices of the 4-clique C. Since this $S_{2,2}$ is a subset of C_s, then $S_{2,2} \cap C_s = S_{2,2}$ and $|S_{2,2} \cap C_s| = 4$, which includes the ordered edges from i, j to k, l.

Based on Lemma 2.3.1, we know the 4-clique complexes are disjoint. Moreover, by Lemma 4.1.5, we know each $K_{2,2}$ is a subgraph of a 4-clique. Therefore, the only $S_{2,2}$ having a non-empty intersection with C_s are the ones included in C_s. There are three $S_{2,2}$ that are included in a 4-clique complex along their antipodals.

Since all the vertices of the 4-clique are adjacent, and the simplices $K_{2,12}, S_{4,4}$, and $K_{6,4}$ are induced subgraphs (recall Proposition 4.1.7), the largest intersection size of C_s and each of these simplices is one, i.e. their corresponding bipartite subgraphs intersect at most on an edge.

Intersection of $S_{1,36}$ with other maximal simplicies:

Let z be a vertex in $\mathcal{P}(3^3)$ and

$$S_{1,36} = \{z\} \times \{\mathrm{CN}(z)\}$$

be a maximal simplex of $\mathrm{B}_{\mathrm{edge}}\big(\mathcal{P}(3^3)\big)$. If $A\times B$ is any maximal simplex of $\mathrm{B}_{\mathrm{edge}}\big(\mathcal{P}(3^3)\big)$, and $z \notin A \cup B$, then $S_{1,36} \cap A \times B = \emptyset$. Remember that the vertices of the simplicies of $\mathrm{B}_{\mathrm{edge}}\big(\mathcal{P}(3^3)\big)$ are ordered pairs. So, if $S'_{1,36} = \{x\} \times \{\mathrm{CN}(x)\}$ for a vertex $x \in \mathcal{P}(3^3)$ and $x \neq z$, then $S_{1,36} \cap S'_{1,36} = \emptyset$; however, if $z \in \mathrm{CN}(x)$, for the antipodal simplex $S_{36,1} = \{\mathrm{CN}(x)\} \times \{x\}$, we have $S_{1,36} \cap S_{36,1} = \{z\} \times \{x\}$, and if $z \notin \mathrm{CN}(x)$, then $S_{1,36} \cap S_{36,1} = \emptyset$.

Let $\{a_i, b_i\} \subseteq V(\mathcal{P}(3^3))$ for $i = 1, 2, 3, 4$, and

$$\mathrm{T}(a_1, b_1) = 5, \quad \mathrm{T}(a_2, b_2) = 6, \quad \mathrm{T}(a_3, b_3) = 7, \quad \mathrm{T}(a_4, b_4) = 9.$$

Let the following be the $\mathrm{B}_{\mathrm{edge}}\big(\mathcal{P}(3^3)\big)$ simplicies constructed from these pairs, created by the method of Remark 4.2.1:

$$S_{2,12} = \mathrm{CN}(\mathrm{CN}(a_1, b_1)) \times \mathrm{CN}(a_1, b_1), \quad S_{6,4} = \mathrm{CN}\big(\mathrm{CN}(a_2, b_2)\big) \times \mathrm{CN}(a_2, b_2),$$
$$S_{4,4} = \mathrm{CN}\big(\mathrm{CN}(a_3, b_3)\big) \times \mathrm{CN}(a_3, b_3), \quad S_{2,2} = \mathrm{CN}(\mathrm{CN}(a_4, b_4)) \times \mathrm{CN}(a_4, b_4).$$

and the antipodals:

$$S_{12,2} = \mathrm{CN}(a_1, b_1) \times \mathrm{CN}(\mathrm{CN}(a_1, b_1)), \quad S_{4,6} = \mathrm{CN}(a_2, b_2) \times \mathrm{CN}\big(\mathrm{CN}(a_2, b_2)\big).$$

It should be noted that $\mathrm{CN}\big(\mathrm{CN}(a_i, b_i)\big) = \{a_i, b_i\}$ is applicable when $i = 1, 4$ (refer to Section 4.1 for more detail).

As observed in Section 4.1, the antipodal sets of $S_{2,2}$ and $S_{4,4}$ correspond to another $S_{2,2}$ and $S_{4,4}$, respectively. Therefore, we are not required to investigate the intersection of simplicial complexes with their antipodal simplex, as it follows the same structural pattern as the intersection with $S_{2,2}$ and $S_{4,4}$.

Let S be any of the above simplicies created by the pair $\{a_i, b_i\}, i = 1, 2, 3, 4$. If $z \in \mathrm{CN}\big(\mathrm{CN}(a_i, b_i)\big)$, then

$$S_{1,36} \cap S = \{z\} \times \mathrm{CN}(a_i, b_i)$$

and if $z \in \mathrm{CN}(a_i, b_i)$, then

$$S_{36,1} \cap S = \{z\} \times \mathrm{CN}\big(\mathrm{CN}(a_i, b_i)\big).$$

The sizes of these intersections are different which depends on the type of the pair a_i, b_i:

$$|S_{1,36} \cap S_{2,12}| = 12, \quad |S_{1,36} \cap S_{6,4}| = 4, \quad |S_{1,36} \cap S_{4,4}| = 4, \quad |S_{1,36} \cap S_{2,2}| = 2$$

and for the antipodals:

$$|S_{1,36} \cap S_{12,2}| = 2, \quad |S_{1,36} \cap S_{4,6}| = 6.$$

Intersection of $S_{2,2}$ with other maximal simplicies:

Given that the bipartite subgraphs corresponding to the simplices $S_{2,12}$, $S_{6,4}$, $S_{4,4}$ and their antipodals are induced subgraphs, it follows that $S_{2,2}$ does not have more than one vertex in common with them.

Given that each bipartite subgraph $K_{2,2}$ is included in exactly one 4-clique (as shown in Lemma 4.1.5), and given that 4-cliques are edge-distinct (by Proposition 2.1.10), it follows that if two $K_{2,2}$ are part of two distinct 4-cliques, their corresponding simplicies $S_{2,2}$ do not intersect.

Consider the 4-clique $C = \{1, 2, 3, 4\}$ in Figure 4.10. Then, the following three $S_{2,2}$ simplicies exist within the 4-clique complex of C:

$$\{1, 2\} \times \{3, 4\}, \quad \{1, 3\} \times \{2, 4\}, \quad \{1, 4\} \times \{2, 3\}.$$

The intersection of each pair of these $S_{2,2}$ has cardinality one.

Intersection of $S_{2,12}$ with other maximal simplicies:

The intersection with $S_{1,36}$ and $S_{2,2}$ has already been studied in previous cases. Let $S_{2,12} = \{v, w\} \times \mathrm{CN}(v, w)$ and consider another simplex $S'_{2,12} = \{s, t\} \times \mathrm{CN}(s, t)$ where $v, w, s, t \in V\big(\mathcal{P}(3^3)\big)$ and $\mathrm{T}(v, w) = \mathrm{T}(s, t) = 5$.

- Intersections of $S_{2,12}$ with $S'_{2,12}$, and $S_{2,12}$ with the antipodal of $S'_{2,12}$ are as follows:

  If $\{v, w\}$ and $\{s, t\}$ are two disjoint sets, then $S_{2,12} \cap S'_{2,12} = \emptyset$. Additionally, if $\{v, w\} \subseteq \mathrm{CN}(s, t)$, then $S_{2,12} \cap S'_{12,2} = \{v, w\} \times \{s, t\}$.

  Now assume $v = s$. The intersection $S_{2,12} \cap S'_{2,12}$ depends on $\mathrm{T}(w, t)$:

  - If $\mathrm{T}(w, t) = 7$, then this pair leads to the simplex $S_{4,4} = \mathrm{CN}\big(\mathrm{CN}(w, t)\big) \times \mathrm{CN}(w, t)$. Hence, $S_{2,12} \cap S'_{2,12} = \{v\} \times \mathrm{CN}(v, w, t)$. From Figure 4.6 we know $|\,\mathrm{CN}(w, t)| = 4$. Since $\mathrm{CN}(v, w, t) \subseteq \mathrm{CN}(w, t)$, we conclude that $|S_{2,12} \cap S'_{2,12}| \leq 4$.
  - If $\mathrm{T}(w, t) = 6$, then this pair leads to the simplex $S_{6,4} = \mathrm{CN}\big(\mathrm{CN}(w, t)\big) \times \mathrm{CN}(w, t)$. Then $S_{2,12} \cap S'_{2,12} = \{v\} \times \mathrm{CN}(v, w, t)$. From Figure 4.4 we know $|\,\mathrm{CN}(w, t)| = 6$. Since $\mathrm{CN}(v, w, t) \subseteq \mathrm{CN}(w, t)$, we know $|S_{2,12} \cap S'_{2,12}| \leq 6$.
  - If $T(w, t) = 5$ and the triple v, w, t is of the first kind of type 5, then by Lemma 4.1.8 they have 6 common neighbours. So, $S_{2,12} \cap S'_{2,12} = \{v\} \times \mathrm{CN}(v, w, t)$ and $|S_{2,12} \cap S'_{2,12}| \leq 6$.
  - If the triple v, w, t is of the second kind of type 5, then they do not have any common neighbours, so $S_{2,12} \cap S'_{2,12} = \emptyset$.

– The vertices w, t cannot be of type 9 because there does not exist any triple of type $5, 5, 9$ which is followed by Lemma 3.2.1.

- Intersection of $S_{2,12}$ with a $S_{4,4}$:

  Let $\{a, b\} \subset V(\mathcal{P}(3^3))$ where $\mathrm{T}(a, b) = 7$ and $S_{4,4} = \mathrm{CN}\big(\mathrm{CN}(a, b)\big) \times \mathrm{CN}(a, b)$. The intersection of $S_{2,12}$ with $S_{4,4}$ is the following:

  – If $v, w \notin \mathrm{CN}\big(\mathrm{CN}(a, b)\big)$, then $S_{2,12} \cap S_{4,4} = \emptyset$.

  – If $\{v, w\} \subset \mathrm{CN}\big(\mathrm{CN}(a, b)\big)$, then $\mathrm{CN}(a, b) \subseteq \mathrm{CN}(v, w)$, and thus $S_{2,12} \cap S_{4,4} = \{v, w\} \times \mathrm{CN}(a, b)$. Since $|\,\mathrm{CN}(a, b)| = 4$, we have $|S_{2,12} \cap S_{4,4}| = 8$.

  – If $v \in \mathrm{CN}\big(\mathrm{CN}(a, b)\big)$ and $w \notin \mathrm{CN}\big(\mathrm{CN}(a, b)\big)$, then $S_{2,12} \cap S_{4,4} = \{v\} \times A$ where $A \subset \mathrm{CN}(a, b)$. The size of $S_{2,12} \cap S_{4,4}$ cannot be 4 because $w \notin \mathrm{CN}\big(\mathrm{CN}(a, b)\big)$. So, $|S_{2,12} \cap S_{4,4}| \leq 3$.

  – The case that $v \in \mathrm{CN}(a, b)$ and $w \in \mathrm{CN}\big(\mathrm{CN}(a, b)\big)$ and vice versa is impossible because $\mathrm{T}(v, w) = 5$ and they cannot be adjacent.

- Intersections of $S_{2,12}$ with a $S_{6,4}$, and $S_{2,12}$ with the antipodal of $S_{6,4}$ are as follows:

  Let $\{c, d\} \subset V(\mathcal{P}(3^3))$ where $\mathrm{T}(c, d) = 6$ and $S_{6,4} = \mathrm{CN}\big(\mathrm{CN}(c, d)\big) \times \mathrm{CN}(c, d)$. The intersection of $S_{2,12}$ with $S_{6,4}$ and its antipodal $S_{4,6}$ is the following:

  – If $\{v, w\} \subseteq \mathrm{CN}\big(\mathrm{CN}(c, d)\big)$, then $S_{2,12} \cap S_{6,4} = \{v, w\} \times \mathrm{CN}(c, d)$. From Figure 4.4 we know $|\,\mathrm{CN}(c, d)| = 4$, and thus, $|S_{2,12} \cap S_{6,4}| = 8$. If $\{v, w\} \subset \mathrm{CN}(c, d)$, then $S_{2,12} \cap S_{4,6} = \{v, w\} \times \mathrm{CN}\big(\mathrm{CN}(c, d)\big)$ and $|S_{2,12} \cap S_{4,6}| = 12$ because $|\,\mathrm{CN}(\mathrm{CN}(c, d))| = 6$.

  – If $v \in \mathrm{CN}\big(\mathrm{CN}(c, d)\big)$ and $w \notin \mathrm{CN}\big(\mathrm{CN}(c, d)\big)$, then $S_{2,12} \cap S_{6,4} = \{v\} \times A$ where $A \subset \mathrm{CN}(c, d)$, and $|S_{2,12} \cap S_{6,4}| \leq 3$. The size of this intersection cannot be equal to 4 because of $w \notin \mathrm{CN}\big(\mathrm{CN}(c, d)\big)$. If $v \in \mathrm{CN}(c, d)$ and $w \notin \mathrm{CN}(c, d)$, then $S_{2,12} \cap S_{4,6} = \{v\} \times B$ where $B \subset \mathrm{CN}\big(\mathrm{CN}(c, d)\big)$, and $|S_{2,12} \cap S_{4,6}| \leq 5$. This size of intersection cannot be equal to 6 because of $w \notin \mathrm{CN}(c, d)$.

  – The case that $v \in \mathrm{CN}(c, d)$ and $w \in \mathrm{CN}\big(\mathrm{CN}(c, d)\big)$ and vice versa is impossible because $\mathrm{T}(v, w) = 5$ and they cannot be adjacent.

Intersection of a $\mathbf{S_{6,4}}$ with other maximal simplicies:

The intersection of an $S_{6,4}$ with the simplicies $S_{1,36}$ and $S_{2,12}$ have been studied in the previous cases. Following the notation of the previous case, let $S_{6,4}$ be $\mathrm{CN}\big(\mathrm{CN}(c, d)\big) \times \mathrm{CN}(c, d)$.

- Intersections of $S_{6,4}$ with $S'_{6,4}$, and $S_{6,4}$ with the antipodal of $S'_{6,4}$ are as follows:

  Consider $p, q \in V(\mathcal{P}(3^3))$ such that $\mathrm{T}(p,q) = 6$. We define $S'_{6,4}$ as $\mathrm{CN}\big(\mathrm{CN}(p,q)\big) \times \mathrm{CN}(p,q)$. Referring to Figure 4.5, we can observe that all vertex triples on the left side of $S_{6,4}$ and $S'_{6,4}$ are of type 5,5,6 while all the triples on the right side are of type 5,5,5. Consequently, the left side of these simplices cannot have more than a type-5 pair in common with the right side of the other simplex.

  Consider the case where the left sides, $\mathrm{CN}\big(\mathrm{CN}(p,q)\big)$ and $\mathrm{CN}\big(\mathrm{CN}(c,d)\big)$, share more than a pair of type 5. Then, they must share a pair s, t of type 6, leading to the equivalence of the simplices $S_{6,4}$ and $S'_{6,4}$. This equivalence arises from the fact that the maximal complete bipartite subgraph derived from any pair of type 6 in $\mathrm{CN}(\mathrm{CN}(p,q))$ leads to a unique subgraph by Proposition 4.1.3. Hence, the left sides cannot share more than a type-5 pair.

  Consider now the case where the right sides, $\mathrm{CN}(c,d)$ and $\mathrm{CN}(p,q)$, share more than a pair of type 5. This implies the existence of a triple of type 5,5,5. Referring to Table 4.4, we observe that the maximal complete bipartite subgraph built from a triple of type 5,5,5 is a unique $K_{6,4}$. Again, this implies equivalence of the simplices and thus, the right sides cannot share more than a pair of type 5.

  Suppose $\mathrm{T}(x,y) = \mathrm{T}(v,w) = 5$ and $x, y \subseteq \mathrm{CN}\big(\mathrm{CN}(c,d)\big) \cap \mathrm{CN}\big(\mathrm{CN}(p,q)\big)$ and $v, w \subseteq \mathrm{CN}(c,d) \cap \mathrm{CN}(p,q)$. Hence, the maximum intersection of $S_{6,4}$ and $S'_{6,4}$ is given by:

  $$S_{6,4} \cap S'_{6,4} = \{x, y\} \times \{v, w\}.$$

  If $\{x, y\} \subseteq \mathrm{CN}\big(\mathrm{CN}(c,d)\big) \cap \mathrm{CN}(p,q)$ and $\{v, w\} \subseteq \mathrm{CN}(c,d) \cap \mathrm{CN}\big(\mathrm{CN}(p,q)\big)$, then the maximum intersection of $S_{6,4}$ and $S'_{4,6}$ is:

  $$S_{6,4} \cap S'_{4,6} = \{x, y\} \times \{v, w\}.$$

  Therefore, the maximum intersection size is 4:

  $$|S_{6,4} \cap S'_{6,4}| = |S_{6,4} \cap S'_{4,6}| = 4.$$

- Intersection of $S_{6,4}$ with a $S_{4,4}$:

  As before consider $S_{4,4} = \mathrm{CN}\big(\mathrm{CN}(a,b)\big) \times \mathrm{CN}(a,b)$ where $\mathrm{T}(a,b) = 7$. As shown in Figure 4.8, all the vertex triples in $\mathrm{CN}(a,b)$ and $\mathrm{CN}\big(\mathrm{CN}(a,b)\big)$ are of type 5,5,7. So, the only vertices that $S_{4,4}$ and $S_{6,4}$ can share is a pair of type 5 at each side.

  Similar to the previous case, the maximum intersection size is 4:

  $$|S_{4,4} \cap S_{6,4}| = |S_{4,4} \cap S_{4,6}| = 4$$

Intersection of a $\mathbf{S_{4,4}}$ with another $\mathbf{S'_{4,4}}$:

This particular case can be validated in a manner similar to the intersection of two simplices of the form $S_{6,4}$. By referencing Figure 4.8, where all types of the vertex pairs on each side of a $K_{4,4}$ are specified, we deduce that the maximum size of the intersection between $S_{4,4}$ and $S'_{4,4}$ is 4.

The following Table 4.6 summarises the largest intersection sizes of the pairwise maximal simplicies of $\mathrm{B}_{\mathrm{edge}}\big(\mathcal{P}(3^3)\big)$.

Simplicies	$S_{2,2}$	$S_{1,36}$	$S_{36,1}$	$S_{2,12}$	$S_{12,2}$	$S_{6,4}$	$S_{4,6}$	$S_{4,4}$
4-clique complex	4	3	3	1	1	1	1	1
$S_{2,2}$	1	2	2	1	1	1	1	1
$S_{1,36}$	2	$\emptyset$	1	12	2	4	6	4
$S_{2,12}$	1	12	2	6	4	8	12	8
$S_{6,4}$	1	4	6	8	12	4	4	4
$S_{4,4}$	1	4	4	8	8	4	4	4

Table 4.6: Maximum size of the intersection of all pairs of simplicies of the $\mathrm{B}_{\mathrm{edge}}\big(\mathcal{P}(3^3)\big)$

The following equality holds for two simplicial complexes S and S' in $\mathrm{B}_{\mathrm{edge}}\big(\mathcal{P}(3^3)\big)$:

$$S \cap S' = \widetilde{S} \cap \widetilde{S'}. \tag{4.2.1}$$

It is easy to check its validity because the elements of $\widetilde{S}$ are the elements of S when the order is changed. It is also obvious that $\widetilde{\widetilde{S}} = S$.

Chapter 5

Computational Approaches to Compute $\mathrm{B}_{\mathbf{edge}}\big(\mathcal{P}(3^3)\big)$

"The best way to predict the future is to create it."
— George Orwell, 1984

In this chapter, we explore two computational approaches for computing the edge box complex of a graph, $\mathrm{B}_{\mathrm{edge}}(G)$. The first approach is a brute-force method that works on a general graph. This method explores all possible vertex partitions to find the maximal complete bipartite subgraphs of the graph. The second approach is an efficient method that leverages the Theorem 4.1.14 to classify the complete bipartite subgraphs of the graph $\mathcal{P}(3^3)$, reducing the time complexity significantly. We present the algorithms for each approach, analyze their time complexity, and discuss their advantages and limitations.

5.1 Brute Force Approach

This section presents the algorithm implementing the brute force approach and analyzes its time complexity to understand its performance and efficiency. Although this method can provide accurate results for small graphs, its practicality for larger graphs is limited due to its high time complexity. As an illustration, we applied this algorithm to the Petersen graph and received the correct result on a regular system.

5.1.1 Algorithm

The following brute force algorithm receives the vertices and edges of a graph G, finds the maximal complete bipartite subgraphs of G, and then builds the simplicies of the edge box complex of G, $\mathrm{B}_{\mathrm{edge}}(G)$.

Algorithm 1 Find All Simplicies of the Edge Box Complex of the Graph G

Require: *Vertices, Edges*
Ensure: Simplicies of the box complex of G

```
for each integer i in [1, n] do
    Combinations ← All combinations of vertices of length i
    for each combination in Combinations do
        for each integer j in the range [1, [i/2]] do
            subCombs ← All sub-combinations of combination of length j
            for each subComb in subCombs do
                left ← subComb
                right ← combination\ left
                c ← 0
                for each vertex pair [l, r] where l is in left and r is in right do
                    if [l, r] or [r, l] exists in Edges then
                        Increment the counter
                if c = size(left).size(right) then
                    Append [left, right] to Bipartites
Remove duplicates from Bipartites
Remove non-maximal bipartite subgraphs from Bipartites
for each bipartite in Bipartites do
    for each vertex1 in left side of bipartite do
        for each vertex2 in right side of bipartite do
            simplex1 ← [vertex1, vertex2]
            simplex2 ← [vertex2, vertex1]
    Append simplex1 and simplex2 to simplicies
```

5.1.2 Complexity

The brute force approach is indeed capable of constructing all the simplices of $\mathrm{B}_{\mathrm{edge}}\big(\mathcal{P}(3^3)\big)$; however, its effectiveness is heavily reliant on time complexity, as well as the size of the graph.

As the quantity of vertices and edges in the graph escalates, the number of potential simplices increases exponentially, posing a significant challenge in processing and storing this information.

We executed this pseudocode using a SageMath program, which successfully generated accurate results for small graphs such as the Petersen graph. Nonetheless, it failed to yield results for the partition graph $\mathcal{P}(3^3)$ even when utilizing large computer clusters with substantial memory and processing time. We tried it with two clusters Narval and Graham from Compute Canada. The largest memory given to the task was 3022G with 24 hours of operation. In all attempts the job failed due to running out of memory. Even using `Parallelism().set()` led to an error.

To analyze the time complexity of this pseudocode, we need to consider the various nested loops and the sizes of the structures created. Let the number of the vertices be n.

- The outer loop iterates through all vertices, which is $O(n)$.
- The next loop generates combinations of vertices. In the worst case, the number of combinations is 2^n (each vertex can either be in or out of a combination), so the complexity is $O(2^n)$.
- The next loop iterates through half the size of the current combination. In the worst case, the combination size is n, so the complexity is $O(n/2) = O(n)$.
- The next loop iterates through the sub-combinations generated from the current combination. In the worst case, the number of sub-combinations is also $2^{n/2}$ (each vertex in the combination can either be in or out of a sub-combination), so the complexity is $O(2^n)$.
- The next loop iterates through all pairs of vertices in *left* and *right*, which in the worst case is $O(n^2)$.
- All the loops of the second nested loop on bipartite subgraphs are $O(n)$. Then the nested loop is $O(n^3)$.

To determine the overall time complexity of the algorithm, we must consider the time complexities of the nested loops. The first nested loop has a time complexity of $O(n \cdot 2^n \cdot n \cdot 2^n \cdot n^2) = O(n^4 \cdot 4^n)$. Since this is greater than the time complexity of the second nested loop, the overall time complexity of the algorithm is dominated by the first nested loop, resulting in a time complexity of $O(n^4 \cdot 4^n)$.

5.2 An Efficient Approach

The algorithm presented in this section is founded on Theorem 4.1.14, which classifies all complete bipartite subgraphs of $\mathcal{P}(3^3)$ into five distinct classes. Remark 4.1.1 provides insight into constructing these subgraphs. The efficiency of this approach stems from its ability to avoid the exhaustive examination of all possible vertex divisions

that generate complete bipartite subgraphs. Successfully implemented in a SageMath program, this method has been executed on a standard computer, yielding precise results.

5.2.1 Algorithm

The algorithm 2 constructs the simplicies of the box complex of the graph $\mathcal{P}(3^3)$, given vertex pairs of the graph. This algorithm is self-contained, as it constructs the vertices of the graph $\mathcal{P}(3^3)$ based on its definition and then computes the type of the vertex pairs.

The function *Type* calculates the type of a given pair of vertices. Utilizing this function, we categorize pairs into their respective types and store them in the lists *type5*, *type6*, *type7*, and *type9*. Furthermore, we compile the neighbours of all vertices in the list *Neighbours*.

The function *Int_Nb* computes the intersection of neighbours for a given list of vertices, which is essential for the *Creat_Simplicies* function. This function takes a list of vertex pairs of a specific type and constructs the corresponding simplicies of the edge box complex of $\mathcal{P}(3^3)$, denoted as $\mathrm{B}_{\mathrm{edge}}(\mathcal{P}(3^3)$.

5.2.2 Complexity

In this section, we will discuss the improvements in time complexity achieved by the efficient approach compared to the brute force method. By employing the insights from Theorem 4.1.14 and Remark 4.1.1, our algorithm has managed to significantly reduce the time complexity required for constructing the $\mathrm{B}_{\mathrm{edge}}\big(\mathcal{P}(3^3)\big)$. The following is a detailed analysis, demonstrating the efficiency of this method and its benefits over the brute force approach.

- Creating vertices: $O(1)$, as it is a fixed size set.
- *Type* function: $O(1)$, as it iterates over a fixed size set (3 elements).
- Finding pairs of different types: $O(n^2)$, where n is the number of vertices.
- Finding neighbors: $O(n^2)$.
- *Int_Nb* function: $O(n)$, as it iterates over a list of vertices.
- *Creat_simplicies* function: $O(n^3)$, as it iterates over pairs and it calls the Int_Nb function with $O(n)$ complexity.
- Building simplicies for $S_{1,36}$: $O(n^2)$, as it iterates over vertices and their neighbours.

Overall, the algorithm's time complexity is $O(n^3)$, as this is the most dominant factor in the algorithm.

Comparing the complexities of the brute force method and our approach, we observe a significant improvement in time complexity. The time complexity has been reduced from $O(n^4 \cdot 4^n)$ to $O(n^3)$.

Algorithm 2 Create All Simplices of the Box Complex $\mathrm{B}_{\mathrm{edge}}(\mathcal{P}(3^3))$

Require: –
Ensure: Simplicies of the box complex of $\mathcal{P}(3^3)$

1: *Vertices* ← The orbit of the permutation group S_9 acting on the set $\{\{1,2,3\},\{4,5,6\},\{7,8,9\}\}$.
▷ Find the type of a pair of vertices:
2: **function** TYPE($vertex1, vertex2$)
3: **for** each *cell* in $vertex1$ **do**
4: Append the number of the cells of $vertex2$ that have a non-empty intersection with *cell* to the list *int*
5: c ← Summation of the elements of the list *int*
6: **return** c
▷ Find all the pairs of different types
7: **for** each pair of indices i, j in $Vertices$ **do**
8: **if** $Type(i,j) = 5$ **then**
9: *type5* ← $[i,j]$
10: **if** $Type(i,j) = 6$ **then**
11: *type6* ← $[i,j]$
12: **if** $Type(i,j) = 7$ **then**
13: *type7* ← $[i,j]$
14: **if** $Type(i,j) = 9$ **then**
15: *type9* ← $[i,j]$
16: Delete the repetitive pairs in *type5, type6, type7,* and *type9*
▷ Find the neighbours of all the vertices.
17: **for** each *vertex* in *Vertices* **do**
18: *Neighbour* ← Vertices of type 9 relationship with *vertex*
19: Append *Neighbour* to the list *Neighbours*
▷ Find the common neighbours of a set of vertices.
20: **function** INT_NB(*ListOfVertices*)
Common Nb ← Intersection of the neighbours of the vertices of *ListOfVertices*
21: **return** *CommonNb*

Algorithm 2 Create All Simplices of the Box Complex $\mathrm{B}_{\mathrm{edge}}\big(\mathcal{P}(3^3)\big)$(Continued)

▷ Continuing from the previous page...
▷ Create the simplicies of the box complex $\mathrm{B}_{\mathrm{edge}}\big(\mathcal{P}(3^3)\big)$
function CREAT_SIMPLICIES($Pairs$)
▷ $Pairs$ is the list of all vertex pairs of a particular type
  for each *pair* in *Pairs* **do**
    right ← Int_Nb(first vertex of *Pair*, second vertex of *Pair*)
    left ← Int_Nb(*right*)
    if Type(*pair*) = 7 or 9 **then**
      for each x in *left* and each y in *right* **do**
        Append $[x, y]$ to $Simplex1$
      Append $Simplex1$ to *Simplicies*
  ▷ Owing to the symmetric properties of the simplices generated from pairs of type 7 and 9, their antipodal counterparts are naturally created in the process of building these simplicies. In contrast, constructing the antipodal simplices for those arising from pairs of type 5 and 6 requires an explicit building process.
    if Type(*pair*) = 5 or 6 **then**
      for each x in *left* and each y in *right* **do**
        Append $[x, y]$ to $Simplex1$
        Append $[y, x]$ to $Simplex2$
      Append $Simplex1$ to *Simplicies*
      Append $Simplex2$ to *Anti_Simplicies*
  Delete the repeated simplicies from *Simplicies* and *Anti_Simplicies*
  return *Simplicies* and *Anti_Simplicies*
▷ Since $S_{1,36}$ simplicies are not made of pairs of vertices, we build them and their antipodals without the help of the Create_Simplicies function
for *vertex* in $Vertices$ **do**
  for each *nb* in $Neighbour(vertex)$ **do**
    Append $[vertex, nb]$ to $simplex1$ and $[nb, vertex]$ to $simplex2$
  Append $simplex1$ to *Simplicies_ {1,36}* and $simplex2$ to *Simplicies_ {36,1}*
Delete the repeated simplicies of *Simplicies_ {1,36}* and *Simplicies_ {36,1}*
▷ Call the function Create_Simplicies to build the rest of the simplicies
Simplicies_ {2,2} ← Creat_Simplicies(*Type9*)
Simplicies_ {2,12} and *Simplicies_ {12,2}* ← Creat_Simplicies(*Type5*)
Simplicies_ {6,4} and *Simplicies_ {4,6}* ← Creat_Simplicies(*Type6*)
Simplicies_ {4,4} ← Creat_Simplicies(*Type7*)

Chapter 6

Morse Theory

"I win or I learn, but I never lose."
— Marie Forleo, Everything Is Figureoutable

Morse theory is a powerful tool for studying the topology of spaces by analyzing the critical points of real-valued functions defined on these spaces. It has been influential in the development of many areas of mathematics, including algebraic topology, differential geometry, and mathematical physics. Furthermore, it has inspired the development of discrete Morse theory, which extends the ideas of Morse theory to discrete settings, such as cell complexes.

Continuous Morse theory, first developed by Marston Morse in the 1920s and 1930s, establishes a relationship between the critical points of a smooth function (also called a Morse function) on a manifold and the underlying topology of the manifold.

The relationship between continuous and discrete Morse theory can be understood as follows: In the discrete version, instead of utilizing a suitable class of continuous functions on the spaces as Morse functions, a single numerical value is assigned to each cell of the complex, rendering all associated processes discrete in nature. This approach demonstrates that, even in the absence of continuity, it is possible to develop a comprehensive theory within the realm of combinatorial spaces that captures many of the complexities of the smooth theory. Moreover, this theory can be employed as an effective tool for addressing a wide range of combinatorial and topological problems.

In this chapter, we aim to provide a brief overview of continuous Morse theory, followed by a more in-depth exploration of discrete Morse theory. We will draw analogies between the continuous and discrete versions, highlighting the similarities and differences between the two. Discrete Morse theory equips us with the required tools to simplify and analyze simplicial complexes, making it particularly valuable

for our research on the $\mathrm{B}_{\mathrm{edge}}\big(\mathcal{P}(3^3)\big)$ simplicial complex. For readers not interested in the foundations of the Morse theory, the continuous Morse Theory section may be skipped. However, it introduces CW complexes and attaching maps, which are relevant to the discrete version. If familiar with these concepts, readers can focus on discrete Morse theory, which is sufficient for understanding the research presented in this work.

6.1 Continuous Morse Theory

In this section, we now describe the background of classical Morse theory that we hope will provide a good foundation on which to begin studying the discrete analog. A Morse function is a smooth real-valued function on a manifold such that all its critical points (where the gradient is zero) are non-degenerate, meaning the Hessian matrix (the matrix of second derivatives) is non-singular at these points. Morse theory is based on the observation that the topology of a manifold can be described by the behaviour of the Morse function in the vicinity of its critical points. Each critical point is associated with an index, which is the number of negative eigenvalues of the Hessian matrix at that point.

In this section, we present theorems that enable us to construct a smooth manifold using cell complexes. To fully comprehend this section, we first need to introduce some definitions. For a more in-depth understanding, we recommend Milnor's book [6].

A *Morse function* on a manifold is a smooth, real-valued function. A *critical* point of a Morse function is a point in the domain of the function where the gradient (the first derivative) vanishes. The function value at a critical point is called a *critical value*. *Non-degenerate* critical points are critical points where the Hessian matrix (the second derivative matrix) is non-singular (has a non-zero determinant) and *degenerate* critical points are critical points where the Hessian matrix is singular (has a zero determinant). The *index* of a critical point is the number of negative eigenvalues of the Hessian matrix evaluated at the critical point.

Throughout this section, f is a smooth real-valued function on a manifold M, and let M^a be the set of all points $x \in M$ such that $f(x) \leq a$ unless stated otherwise.

We start by introducing an essential lemma in Morse theory called the Lemma of Morse.

Lemma 6.1.1. [6] (Lemma of Morse.) Let p be a non-degenerate critical point for f. Then, there is a local coordinate system $(y_1, ..., y_n)$ in a neighbourhood U of p with $y_i(p) = 0$ for all i and such that the identity

$$f = f(p) - (y_1)^2 - ... - (y_\lambda)^2 + (y_{\lambda+1})^2 + ... + (y_n)^2$$

holds throughout the neighbourhood U where λ is the index of p.

This lemma states that in a suitable local coordinate system, a Morse function can be expressed as a quadratic form near a non-degenerate critical point.

Now, we present a theorem that shows the relationship between two sublevel sets when there are no critical values between their respective function values. Recall the deformation retraction concept from Chapter 1 in Definitions 1.2.8 and 1.2.7.

Theorem 6.1.2. [6] Let $a, b \in M$ and $a < b$ and suppose that the set $f^{-1}[a, b]$ consisting of all $p \in M$ with $a \leq f(p) \leq b$, is compact, and contains no critical points of f. Then, M^a is a deformation retract of M^b, so that the inclusion map $M^a \to M^b$ is a homotopy equivalence.

This theorem implies that if there are no critical values between a and b, the sublevel sets M^a and M^b have the same homotopy type.

For the next theorems of this section, we need to familiarize ourselves with some definitions.

Let B^d denote the closed unit ball in d-dimensional Euclidean space, defined as $B^d = \{x \in E^d : |x| \leq 1\}$. The boundary of B^d is the unit $(d-1)$-sphere $S^{(d-1)} = \{x \in E^d : |x| = 1\}$.

Definition 6.1.3. A *d-cell* is a topological space homeomorphic to B^d. For a d-cell σ, we use $\partial\sigma$ to represent the boundary of σ, the subset of σ corresponding to $S^{(d-1)} \subset B^d$ under any homeomorphism between B^d and σ.

The disjoint union of X and σ quotiented out by the equivalence relation where each point $s \in \partial\sigma$ is identified with $f(s) \in X$ is denoted as $X \cup_f \sigma$. Then $X \cup_f \sigma$ is the result of attaching the cell σ to X, with f being the *attaching map*. Note that the attaching map must be defined on the entire $\partial\sigma$.

A *finite CW complex* is a topological space X for which there exists a finite nested sequence $X_0 \subset X_1 \subset \cdots \subset X$, where, for each $i = 0, 1, 2, \ldots, n$, X_i is obtained by attaching a cell to $X_{(i-1)}$. Additionally, X_0 is a 0-cell.

In this text, we only work with finite CW complexes. It is a well-established yet noteworthy fact that every simplicial complex can be regarded as a CW complex. For more details on CW-complexes look at [5, Chapter 0].

Next, we consider the case when there is a non-degenerate critical point with a value between the function values of two sublevel sets.

Theorem 6.1.4. [6] Let p be a non-degenerate critical point with index λ. Setting $f(p) = c$, suppose that $f^{-1}[c-\epsilon, c+\epsilon]$ is compact, and contains no critical point of f other than p, for some $\epsilon > 0$. Then, for all sufficiently small ϵ, the set $M^{c+\epsilon}$ has the homotopy type of $M^{c-\epsilon}$ with a $\lambda-$cell attached.

This theorem reveals that when a non-degenerate critical point is present, it contributes a λ-dimensional cell to the homotopy type of the manifold.

More generally suppose that there are k non-degenerate critical points $p_i, ..., p_k$ with indices $\lambda_1, ..., \lambda_k$ in $f^{-1}[c-\epsilon, c+\epsilon]$. Then $M^{c+\epsilon}$ has the homotopy type of $M^{c-\epsilon}$ with λ_1-cell, $\cdots$, λ_k-cell attached.

The next theorem demonstrates how the homotopy type of a manifold can be represented as a CW-complex when f does not have any non-degenerate critical points.

Theorem 6.1.5. [6] If f is a differentiable function on a manifold M with no degenerate critical points, and if each M^a is compact, then M has the homotopy type of a CW-complex, with one cell of dimension λ for each critical point of index λ.

Example. If M is a compact manifold and f is a differentiable function on M with only two critical points, both of which are non-degenerate, then M is homomorphic to a sphere.

In this example, we see the application of the theorem to a specific case. This illustrates the power of Morse theory in determining the topological structure of a manifold based on the properties of the differentiable function defined on it.

6.2 Discrete Morse Theory

Discrete Morse theory, introduced by Robin Forman, is a combinatorial analog of classical Morse theory. Discrete Morse theory has been successfully applied in various fields of applied mathematics and computer science, including topological data analysis [12, 13], geometry [10], denoising [16], mesh compression [15] image processing and computer graphics [14, 11], among others. It provides an efficient and elegant way to study the topology of cell complexes, and it often leads to significant computational advantages over traditional methods.

In discrete Morse theory, a discrete Morse function is defined on the cells of a cell complex. This function assigns a real number to each cell in the complex in such a way that it satisfies certain conditions related to the boundaries of the cells. These conditions ensure that the function behaves similarly to a classical Morse function on a smooth manifold.

The main idea behind discrete Morse theory is to pair cells using pairings of cells that satisfy certain conditions with respect to the discrete Morse function. The unpaired cells, or critical cells, provide a simplified description of the cell complex's topological structure, much like critical points in classical Morse theory provide a simplified description of the topology of smooth manifolds.

If we wish to know whether a given property holds for a certain topological space, our question can often be reduced to the question of whether the space is equivalent to another space for which the property holds.

6.2.1 Definitions

The main theorems of both discrete and continuous Morse theory are most effectively conveyed through the framework of CW complexes, as previously defined in 6.1.3. Utilizing discrete Morse theory, we can simplify a simplicial complex into a smaller simplicial complex or a CW complex with fewer cells.

In this section, we will consider X as an abstract simplicial complex, with α, β, and γ representing simplices of X. Recall the concept of simplicial complexes from Chapter 1 in subsection 1.1.

Definition 6.2.1. A simplex α is a *face* of simplex β, and β is a *coface* of α, if $\alpha \subseteq \beta$.

Definition 6.2.2. For a simplex α with n vertices, we have $\dim(\alpha) = n - 1$ and $\text{rank}(\alpha) = n$.

A simplex X with n vertices is denoted as an n-simplex. A face of α with i vertices and a coface of α with j vertices are denoted as i-face and j-coface of α, respectively. When α is a face of β we denote it by $\alpha \in \beta$, and if $\dim(\alpha) = \dim(\beta) - 1$, it is denoted by $\alpha \in \partial\beta$.

Definition 6.2.3. [8] A *DMF (discrete Morse function)* f on a simplicial complex X is a real-valued function on the set of simplices of X such that for each n-simplex β both conditions 1 and 2 hold:

1. At most one $(n-1)$-face α of β has a value greater than or equal to that of β.
2. At most one $(n+1)$-coface γ of β has a value less than or equal to that of β.

It is worth noting that under the conditions stipulated by Definition 6.2.3, it is a logical impossibility for both conditions 1 and 2 to be satisfied simultaneously. The proof substantiating this assertion can be found in [9, Lemma 2.5.].

Definition 6.2.4. [8] A *critical* n-simplex α of a discrete Morse function f on X is a simplex for which:

1. No $(n-1)$-face α of β has a value greater than or equal to that of β.
2. No $(n+1)$-coface γ of β has a value less than or equal to that of β.

If α is a critical simplex, then $f(\alpha)$ is called a *critical value* of f.

Definition 6.2.5. For $a \in \mathbb{R}$ define the level subcomplex X^a as

$$X^a = \bigcup_{\beta \in X, f(\beta) \leq a} \; \bigcup_{\alpha \leq \beta} \alpha.$$

That is, X^a denotes all simplicies β such that $f(\beta) \leq a$, as well as all of their faces. In particular, X^a is a subcomplex of X.

The next theorem is the analog of the Theorem 6.1.2 of the continuous Morse theory.

Theorem 6.2.6. [8, Lemma 2.6.] If $a < b$ are real numbers such that $(a, b]$ contains no critical values of f, then X^b is homotopy equivalent to X^a.

The following theorem is the analog of the Theorem 6.1.4 of the continuous Morse theory.

Theorem 6.2.7. [8, Lemma 2.7.] Suppose α is a critical simplex of dimension p with $f(\alpha) \in (a, b]$ and $f^{-1}((a, b])$ does not contain any other critical simplicies. Then there is a map $F : S^{(p-1)} \to X^a$ such that X^b is homotopy equivalent to $X^a \cup_F B^p$.

Let $X_p(f)$ (or simply X_p if it will not cause confusion) denote the number of critical points of f of dimension p. The following is the result of the two last theorems. This is the analog of the Theorem 6.1.5 in continuous Morse theory.

Corollary 6.2.8. [8, Theorem 2.5.] The simplicial complex X is homotopy equivalent to a simplicial complex with exactly $X_p(f)$ simplicies of dimension p.

In the context of discrete Morse theory, a pairing refers to a matching of cells (in particular, simplices) of a complex such that each cell is either matched with one of its faces or one of its cofaces. The pairing forms the basis for identifying critical cells in the complex, which correspond to the unmatched cells in the pairing.

Definition 6.2.9. [8] Let f be a DMF on the simplicial complex X. The *pairing* P is the set of all paired simplicies $\{\alpha, \beta\}$; such that, $\alpha, \beta \in X$, $\alpha \in \partial\beta$, and $f(\alpha) \geq f(\beta)$.

The critical simplices as we have defined them above are exactly those that do not appear in the pairing P.

6.2.2 Elementary Collapses

In the context of Discrete Morse Theory, the concept of 'elementary collapses' plays a vital role in revealing the topological equivalences between different simplicial complexes. Essentially, an elementary collapse is a simple operation that allows for the reduction of a complex while preserving its homotopy type. This makes it a powerful tool for topological simplification and computation, such as the calculation of homology groups.

In this section, we delve into the notion of elementary collapses, formally defining the operation and exploring its implications. Central to our discussion is a lemma which will be stated and proven. This lemma illuminates the process of dimension reduction in a simplicial complex, utilizing the mechanism of elementary collapses.

Definition 6.2.10. [8] Let α, β be faces of X, with $\alpha \in \partial\beta$. If α is not a face of any other simplex $\beta' \in X$, then α is a *free face* of β.

Definition 6.2.11. [8] Let α be a free face of β. The deformation retract $\| X \| \backslash\{\text{int}(\alpha), \text{int}(\beta)\}$ is called an *elementary collapse*, where $\| X \|$ is the geometric realization of the abstract simplicial complex X.

When we perform an elementary collapse by removing the interiors of α and β, all of their respective faces persist in the resulting space. This process can be perceived as the removal of faces α and β from the abstract simplex X because what we are actually eliminating are the sets of vertices that constitute the simplices α and β, not their faces.

For the sake of simplicity in our text, we will henceforth use the notation X to represent the geometric realization of the simplicial complex X, when it is clear from the context that we are referring to a topological space. Furthermore, $X\backslash\alpha, \beta$ will denote the result of an elementary collapse. In order to avoid the confusion between removing an element of a set and collapsing, when we want to remove the element x from X, we denote it by $X - \{x\}$.

Since a deformation retraction is a special case of a homotopy equivalence, we have the following:

Corollary 6.2.12. [8] If α is a free face of β, then X is homotopy equivalent to $X\backslash\{\alpha, \beta\}$ which is denoted by $X \simeq X\backslash\{\alpha, \beta\}$.

The following lemma provides a way to simplify the study of homotopy properties of simplicial complexes by replacing maximal simplices with simpler ones.

Lemma 6.2.13. Let $\mathcal{C}$ be an abstract simplicial complex and let X be one of its maximal simplices of rank m. Suppose Y is an $(m-1)$-face of X, and let y be the vertex of X not included in Y. For $1 \leq i \leq m$, define

$$X_i = \{j\text{-faces of } X : 1 \leq j \leq i\} - \{i\text{-faces of } Y\}. \tag{6.2.1}$$

If the largest intersection of X with another maximal simplex X' of $\mathcal{C}$ is the n-face Z, where $n < m$, then $X \simeq X_{n+1}$, and consequently

$$\mathcal{C} \simeq \mathcal{C} - \{\text{faces } \gamma \in X : n+1 < \text{rank}(\gamma) \leq m\}. \tag{6.2.2}$$

If X does not intersect any other maximal simplex of $\mathcal{C}$, then it it homotopy equivalent to a single point.

Proof: Define $Y' = \{\gamma \subseteq X : y \in \gamma\}$ as the set of all faces of X containing the vertex y. It follows that $X = Y \cup Y'$. From the definition of X_i we know when $i = m$, $X_m = X$ and when $i = n+1$, $X_{n+1} = \{j\text{-faces of } X : 1 \leq j \leq n+1\} - \{(n+1)\text{-faces of } Y\}$.

For $2 \leq i \leq m$, let α be an $(i-1)$-face of Y and $\beta = \alpha \cup \{y\}$ be the unique coface of α in X that contains y. Suppose the largest intersection of X with another maximal simplex X' of $\mathcal{C}$ is the n-face Z.

To demonstrate the homotopy equivalence $X \simeq X_{n+1}$, we adopt a backwards induction strategy, starting from m and proceeding downwards to $n+1$. As part of our inductive hypothesis, we propose that for all $n+1 \leq i \leq m$, α serves as a free face of β. Given this hypothesis, we assert that the elementary collapse $X_i \backslash \{\alpha, \beta\}$ is valid. Our inductive step involves demonstrating the equality $X_i \backslash \{\alpha, \beta\} = X_{i+1}$, which consequently implies the homotopy equivalence $X_i \simeq X_{i+1}$. By following the inductive process through to its conclusion, we confirm the desired homotopy equivalence $X \simeq X_{n+1}$.

The base case of the induction is when $i = m$. In this case, $\alpha = Y$ and $\beta = X$. Since $n < m-1$, Y cannot be a face of any other maximal simplex of $\mathcal{C}$, and thus, the only coface of Y is X. This implies that Y is a free face of X. Hence, the first collapse, i.e., $X_m \backslash \{\alpha, \beta\} = X_m \backslash \{Y, X\}$, is valid. Also, since Y is the only $(m-1)$-face of Y, X is the only m-face of X, and $X_{m-1} = \{j\text{-faces of } X : 1 \leq j \leq m-1\} - \{(m-1)\text{-faces of } Y\}$, we have $X_m \backslash \{Y, X\} = X_{m-1}$.

As α is an $(i-1)$-face of Y for $n+1 < i \leq m$, one of the cofaces of α, $\beta = \alpha \cup \{y\}$, is not included in Y but is included in X_i. Other cofaces of α belong to Y as they do not include y. They are i-faces of Y and consequently do not belong to X_i by the definition of X_i. Then β is the unique coface of α in X_i. Therefore, α is free in X_i.

On the other hand, if $i = n+1$, then α may have another coface in X', so it may not be a free face in X_{n+1}. Therefore, we can only guarantee that α is a free face in X_i for $n+1 < i \leq m$, and hence we can perform an elementary collapse on the pair (α, β) in each such dimension. This implies that $X_i \simeq X_i \setminus \{\alpha, \beta\}$ for all $n+1 < i \leq m$.

To show that $X_i \simeq X_{i-1}$ for an $n+1 < i \leq m$, we will collapse all $(i-1)$-faces α of Y and their corresponding cofaces $\beta = \alpha \cup \{y\}$ in X_i, and show that the resulting simplicial complex is precisely X_{i-1} as the following equality:

$$X_{i-1} = X_i \setminus \big\{\{\alpha, \beta\} : \alpha \text{ is an } (i-1)\text{-face of } Y,\ \beta = \alpha \cup \{y\}\big\}. \tag{6.2.3}$$

The following are the steps to prove the recent claim. The reasoning behind each equation is given afterwards in detail.

$$\begin{aligned}
X_{i-1} &= \{j\text{-faces of } X : 0 \leq j \leq i-1\} - \{(i-1)\text{-faces of } Y\} \\
&= X_i - \{i\text{-faces of } X \text{ and } (i-1)\text{-faces of } Y\} \\
&= X_i - \{i\text{-faces of } Y' \text{ and } (i-1)\text{-faces of } Y\} \\
&= X_i - \big\{\{\alpha, \beta\} : \alpha \text{ is an } (i-1)\text{-face of } Y, \beta = \alpha \cup \{y\} \text{ is an } i\text{-face of } Y'\big\} \\
&= X_i \setminus \big\{\{\alpha, \beta\} : \alpha \text{ is an } (i-1)\text{-face of } Y,\ \beta = \alpha \cup \{y\}\big\}.
\end{aligned}$$

We can explain the reasoning behind each equality as follows:

- The first equality follows directly from Definition 6.2.1.
- The second equality follows from the fact that X_i contains all j-faces of X for $0 \leq j \leq i$, except for the i-faces of Y. Thus, when we remove the i-faces of X and $(i-1)$-faces of Y, we have X_{i-1}.
- The third equality follows from the fact that $X = Y \cup Y'$, so the set of i-faces of X is the union of the set of i-faces of Y' and the set of i-faces of Y. Since the i-faces of Y were excluded from X_i, instead of removing i-faces of X in the second equality, we can be more precise and write i-faces of Y'.
- The fourth equality follows from the fact that the set of $(i-1)$-faces of Y coincides with the set of i-faces of Y'. For any such face $\alpha \in Y$, there exists $\beta = \alpha \cup \{y\}$, which is an i-face of Y'; and for any i-face β of Y', there is an $(i-1)$-face $\alpha = \beta - \{y\}$ in Y.
- The fifth equality follows from the fact that removing a free face and its coface from an abstract simplicial complex is equivalent to collapsing them.

Therefore, we have shown that for $n+1 < i \leq m$, the elementary collapses $X_i \setminus \{\alpha, \beta\}$ is valid, and hence, $X_i \simeq X_{i-1}$. Consequently, we obtain that $X \simeq X_{n+1}$ by induction on i from m to $n+1$. This shows that the homotopy of the simplicial complex $\mathcal{C}$ remains unchanged when we collapse its maximal simplex X to X_{n+1}.
If X does not intersect any other simplex, then $X \cap X' = \emptyset$ which is a 0-face, so $n = 0$ and $X \simeq X_1$. When $i = 1$, X_1 is all the 1-faces (vertices) of X except the 1-faces of Y. The only 1-face of X that is not included in Y is vertex y. Thus, X is homotopy equivalent to a single point. ∎

6.2.3 Homotopy Equivalence of n-Simplex to a Point

The theorem presented in this section, originally proved by Forman [8], will be revisited. While Forman used Hasse diagrams in his proof, we will explore alternative proof methods that align more closely with the focus of this work. Specifically, we will offer two distinct proofs: one leveraging Lemma 6.2.13, and another utilizing the properties of a discrete Morse function. These alternative viewpoints can provide additional insight into the theorem and its applicability to our discussions.

Theorem 6.2.14. A n-simplex is homotopy equivalent to a point.

In order to establish the validity of this theorem, we will employ two distinct methods of proof:

1. Using Lemma 6.2.13 to perform elementary collapses on the n-simplex until it collapses to a point.

2. Applying a DMF on the n-simplex and proving that it is a valid DMF with only one critical simplex which is a vertex.

Both approaches lead to the same conclusion, that an n-simplex is homotopy equivalent to a single point.

Proof: (**Using elementary collapses**)
Let X be an abstract n-simplex. Then it is a simplicial complex consisting of just one maximal simplex X. There is no intersection of maximal simplicies, therefore, by Lemma 6.2.13, X is homotopy equivalent to a single point. ∎

Proof: (**Using a DMF**)
We introduce a discrete Morse function (DMF) on an n-simplex, and demonstrate that the only critical simplex in this setting is a vertex.

Adhering to the notations established in Lemma 6.2.13, we let Y denote an $(n-1)$-face of X, and let y represent the vertex of X not present in Y. For a face $\beta \in X$, we construct the function f accordingly:

$$f(\beta) = \begin{cases} \text{rank}(\beta) & y \in \beta \\ \text{rank}(\beta) + 1 & y \notin \beta \end{cases}$$

Now we check the validity of this DMF. Let $\alpha \subset \beta$, then $\text{rank}(\alpha) < \text{rank}(\beta)$. Suppose $f(\beta) \leq f(\alpha)$. If $y \in \beta \cap \alpha$, or $y \notin \beta \cup \alpha$, then they do not satisfy $f(\beta) \leq f(\alpha)$. The only possibility is $y \in \beta$ and $y \notin \alpha$, then, $f(\beta) = \text{rank}(\beta)$ and $f(\alpha) = \text{rank}(\alpha) + 1$, and the following is true:

$$\text{rank}(\beta) \leq \text{rank}(\alpha) + 1 < \text{rank}(\beta) + 1.$$

Thus, $\text{rank}(\alpha) = \text{rank}(\beta) - 1$ and $\alpha = \beta - \{y\}$. Since $y \in \beta$, all the cofaces of β contain y and have greater f-value than that of β. Since $\alpha = \beta - \{y\}$ is unique, f is valid on X by definition of a DMF, in 6.2.3.

In the case where $y \in \beta$, there will always exist a face $\alpha = \beta - \{y\}$ (given that β possesses any faces) such that $f(\alpha) \geq f(\beta)$. Conversely, when $y \notin \beta$, there will exist a coface $\gamma = \beta \cup \{y\}$ such that $f(\beta) \geq f(\gamma)$.

In light of this, none of the faces of X can be critical, with the exception of the vertex y. The uniqueness of y lies in its dual identity: it is a face of X that includes y and does not possess any other faces. By the Definition of a pairing in 6.2.9, we see $\{\beta - \{y\}, \beta\}$ are the simplex pairs of f except when $\beta = \{y\}$. Therefore, by applying Corollary 6.2.8, we conclude that X is homotopy equivalent to y. ∎

6.2.4 Dimension Reduction of $\mathbf{B_{edge}}\big(\mathcal{P}(3^3)\big)$

The next proposition provides a concrete example of how discrete Morse theory can be applied to $\mathrm{B}_{\text{edge}}\big(\mathcal{P}(3^3)\big)$. We introduce a function f on faces of $\mathrm{B}_{\text{edge}}\big(\mathcal{P}(3^3)\big)$ and show how it satisfies the conditions of a discrete Morse function.

Proposition 6.2.15. Let y be a vertex of the simplicial complex $\mathrm{B}_{\text{edge}}\big(\mathcal{P}(3^3)\big)$ and let β be any face of $\mathrm{B}_{\text{edge}}\big(\mathcal{P}(3^3)\big)$. Then, the function $f : \mathrm{B}_{\text{edge}}\big(\mathcal{P}(3^3)\big) \to \mathbb{R}$ defined as follows is a valid discrete Morse function on $\mathrm{B}_{\text{edge}}\big(\mathcal{P}(3^3)\big)$, where Z and Z' refer to any two distinct maximal simplices of $\mathrm{B}_{\text{edge}}\big(\mathcal{P}(3^3)\big)$:

$$f(\beta) = \begin{cases} \operatorname{rank}(\beta) & \text{if } y \in \beta \text{ or there exist } Z \text{ and } Z' \text{ s.t. } \beta \subseteq Z \cap Z' \\ \operatorname{rank}(\beta) + 1 & \text{otherwise.} \end{cases}$$

Proof: If $\alpha \subset \beta$, then $\operatorname{rank}(\alpha) < \operatorname{rank}(\beta)$. The only β and α that satisfy $f(\beta) \leq f(\alpha)$ are those where $\beta \nsubseteq Z \cap Z', y \in \beta, y \notin \alpha$, and $\alpha \nsubseteq Z \cap Z'$ for any Z, Z'. Hence, we have $f(\alpha) = \operatorname{rank}(\alpha) + 1$ and $f(\beta) = \operatorname{rank}(\beta)$. Then, we get

$$\operatorname{rank}(\beta) \leq \operatorname{rank}(\alpha) + 1 < \operatorname{rank}(\beta) + 1$$

and thus $\operatorname{rank}(\alpha) = \operatorname{rank}(\beta) - 1$. This implies that α is obtained from β by removing the vertex y, i.e., $\alpha = \beta - \{y\}$. Furthermore, since $y \in \beta$, any coface γ of β has a strictly greater f-value than that of β.
Since $\alpha = \beta - \{y\}$ is unique, f is valid on X by definition of a DMF, in 6.2.3. Therefore, the only pairs of this DMF are $\{\beta - \{y\}, \beta\}$ where $\beta \nsubseteq Z \cap Z', y \in \beta, \beta - \{y\} \nsubseteq Z \cap Z'$ for any Z and Z'.
We know critical simplices γ of a given DMF as the simplices that do not appear in a pair. We can further classify these critical simplices into three categories:

1. $\big\{\gamma : \exists (Z, Z'), \gamma \subseteq Z \cap Z'\big\}$. This is because all the faces of γ are included in the intersection $Z \cap Z'$ and therefore have a smaller rank than γ.

2. $\big\{\gamma : \big(\forall (Z, Z'), \gamma \nsubseteq Z \cap Z'\big) \wedge (\exists y \in \gamma) \wedge \big(\exists (Z, Z') : \gamma - \{y\} \subseteq Z \cap Z'\big)\big\}$. This is because $f(\gamma) = \operatorname{rank}(\gamma)$ and $f(\gamma - \{y\}) = \operatorname{rank}(\gamma) - 1$, which means they cannot form a pair. Other faces of γ that include y also cannot form a pair with γ because their rank is smaller than γ.

3. $\big\{\gamma : (y \notin \gamma) \wedge \big(\forall (Z, Z'), \gamma \nsubseteq Z \cap Z'\big) \wedge (\gamma \cup \{y\} \text{ is not a simplex})\big\}$. This is because $f(\gamma) = \operatorname{rank}(\gamma) + 1$, and therefore the rank of all its faces are smaller than γ. Also, the only coface of γ that can form a pair with γ is $\gamma \cup \{y\}$ because $f(\gamma \cup \{y\}) = \operatorname{rank}(\gamma) + 1$. However, $\gamma \cup \{y\}$ is not a simplex, so γ is a critical simplex.

∎

In the subsequent theorem, we present a key result which utilizes both elementary collapses (as established in Lemma 6.2.13) and the discrete Morse function introduced in Proposition 6.2.15. The theorem identifies a subcomplex of $\mathrm{B}_{\text{edge}}\big(\mathcal{P}(3^3)\big)$ of dimension 12 which is homotopy equivalent to $\mathrm{B}_{\text{edge}}\big(\mathcal{P}(3^3)\big)$.

Theorem 6.2.16. The box complex $\mathrm{B}_{\text{edge}}\big(\mathcal{P}(3^3)\big)$ is homotopy equivalent to a dimension 12 sub-complex of itself.

Proof: (**Using elementary collapses**)
Recall that the dimension of $\mathrm{B}_{\text{edge}}\big(\mathcal{P}(3^3)\big)$ is 35. In Section 4.2, we provided a comprehensive classification of all maximal simplices of the simplicial complex $\mathrm{B}_{\text{edge}}\big(\mathcal{P}(3^3)\big)$. Moreover, in Table 4.6, we calculated the maximal intersection sizes of these simplices. According to this table, the largest intersection size among all maximal simplices of $\mathrm{B}_{\text{edge}}\big(\mathcal{P}(3^3)\big)$ is 12.

Let X be a maximal simplex of $\mathrm{B}_{\text{edge}}\big(\mathcal{P}(3^3)\big)$. Since its rank is at most 36, applying Lemma 6.2.13, we deduce that $\mathrm{B}_{\text{edge}}\big(\mathcal{P}(3^3)\big) \simeq \mathrm{B}_{\text{edge}}\big(\mathcal{P}(3^3)\big) - \{\gamma \in X : 13 < \mathrm{rank}(\gamma) \leq 36\}$. By successively applying the same lemma to all maximal simplices X of $\mathrm{B}_{\text{edge}}\big(\mathcal{P}(3^3)\big)$, we obtain:

$$\mathrm{B}_{\text{edge}}\big(\mathcal{P}(3^3)\big) \simeq \mathrm{B}_{\text{edge}}\big(\mathcal{P}(3^3)\big) - \bigcup_{X \in \mathrm{B}_{\text{edge}}(\mathcal{P}(3^3))} \{\gamma \in X : 13 < \mathrm{rank}(\gamma) \leq 36\}.$$

This can be interpreted as:

$$\mathrm{B}_{\text{edge}}\big(\mathcal{P}(3^3)\big) \simeq \bigcup_{X \in \mathrm{B}_{\text{edge}}(\mathcal{P}(3^3))} \{\gamma \in X : \mathrm{rank}(\gamma) \leq 13\}.$$

Hence, $\mathrm{B}_{\text{edge}}\big(\mathcal{P}(3^3)\big)$ is homotopy equivalent to a sub-complex of itself with dimension 12. ∎

Proof: (**Using a DMF**)
Consider an arbitrary vertex y of $\mathrm{B}_{\text{edge}}\big(\mathcal{P}(3^3)\big)$ and let X be a maximal simplex of $\mathrm{B}_{\text{edge}}\big(\mathcal{P}(3^3)\big)$ that contains y. Remember the Morse function and its critical simplices as we defined in Proposition 6.2.15. First, we determine which simplices of X are critical.

Let γ be a simplex of X.

1. If $\mathrm{rank}(\gamma) = 13$, then γ cannot be a critical simplex of the first type, because the rank of the largest intersecting simplices in $\mathrm{B}_{\text{edge}}\big(\mathcal{P}(3^3)\big)$ is 12, hence γ is not included in any intersection.

If $y \in \gamma$, γ is not a critical simplex of the third type. The simplex $\gamma - \{y\}$ has rank 12, so if it is included in an intersection (which is possible), γ is a critical simplex of the second type. If not, γ is not a critical simplex of the second type.

If $y \notin \gamma$, γ cannot be a critical simplex of the second type. Furthermore, as $\gamma \cup \{y\}$ is a simplex (since γ is not a maximal simplex), γ is not a critical simplex of the third type.

Hence, there exist critical simplices of rank 13 in X.

2. If $14 \leq \text{rank}(\gamma) < 36$, γ cannot be a critical simplex of the first type, since it is not included in any intersection. If $y \in \gamma$, it is not a critical simplex of the second type, because $\gamma - \{y\}$ has a rank of at least 13 and is not included in any intersection. As $y \in \gamma$, γ is not a critical simplex of the third type.

   If $y \notin \gamma$, γ is not a critical simplex of the second type. Since $\gamma \cup \{y\}$ is a simplex (because γ is a sub-simplex of X), γ is not a critical simplex of the third type.

3. If $\text{rank}(\gamma) = 36$ (i.e., $\gamma = X$), it can be readily confirmed that γ cannot be a critical simplex of any type.

According to Definition 6.2.5, the subcomplex X^{13} consists of all simplices $\beta \subseteq X$ such that $f(\beta) = \text{rank}(\beta) \leq 13$. Since there are no critical simplices of rank greater than 13 in X, Theorem 6.1.2 implies that X is homotopy equivalent to X^{13}.

Next, consider a maximal simplex Z of $\mathrm{B}_{\text{edge}}\big(\mathcal{P}(3^3)\big)$ that does not contain y and is distinct from X. Since Z is not included in any intersection of other maximal simplices, and because $Z \cup \{y\}$ is not a simplex (given Z is maximal), Z is a critical simplex of the third type. Hence, this Morse function reduces the simplices containing y to a 12-dimensional sub-complex of themselves while not affecting the maximal simplices that do not contain y.

In the final step, we select another vertex y' from a different maximal simplex that has not been reduced yet, and apply the same process to reduce its dimension to 12. Upon reducing the dimensions of all maximal simplices of $\mathrm{B}_{\text{edge}}\big(\mathcal{P}(3^3)\big)$, we conclude that $\mathrm{B}_{\text{edge}}\big(\mathcal{P}(3^3)\big)$ is homotopy equivalent to $\mathrm{B}_{\text{edge}}\big(\mathcal{P}(3^3)\big)^{13}$, which is a 12-dimensional subcomplex of $\mathrm{B}_{\text{edge}}\big(\mathcal{P}(3^3)\big)$. ∎

Chapter 7

Conclusion and Future Work

"Everything worthwhile is hard. Excruciatingly hard."
— Marie Forleo, Everything Is Figureoutable

In this thesis, we embarked on a comprehensive journey through the interplay of graph theory and topology, all woven around the study of the chromatic number of the partition graph $\mathcal{P}(3^3)$. Starting with Lovász's work in 1978 [2], where topological methods were deployed to deduce the chromatic number of the Kneser graph. This led to the exploration of various topological lower bounds of the chromatic number and their hierarchical arrangement, known as the Hierarchy theorem. Through this study, we discovered both the strength and limitations of these lower bounds, thereby highlighting their utility in certain scenarios and their divergence from the actual chromatic number in others.

One of our major achievements was the construction of the box complex $\mathrm{B}_{\mathrm{edge}}(\mathcal{P}(3^3))$ of the partition graph $\mathcal{P}(3^3)$. Our understanding of the properties of this graph, and our classification of its vertex pairs, triples, and quadruples, proved crucial in this task. Moreover, our categorization of the maximal complete bipartite subgraphs was pivotal in identifying all the maximal simplices of $\mathrm{B}_{\mathrm{edge}}(\mathcal{P}(3^3))$ and their antipodes, leading to discovering the structure of the pairwise intersections of the simplices and the size of the maximal intersections.

In parallel with the theoretical developments, we also proposed an algorithm to construct the box complex of $\mathcal{P}(3^3)$, which boasted a time complexity of $O(n^3)$, a significant improvement over the $O(n^4 \cdot 4^n)$ time complexity of a brute-force approach. This result represented not just a theoretical advance, but a practical tool for handling large graphs.

Finally, to tame the complexity of the box complex of $\mathcal{P}(3^3)$, we used the framework of discrete Morse theory. By allocating numerical values to each cell within the complex, we fashioned a discrete Morse function. We were able to develop a homotopy equivalent simplicial complex with reduced dimensionality in two ways: via the application of the developed discrete Morse function, and through a series of elementary collapses on the box complex. This reduction, from 35 to 12, significantly simplified the future calculation of the $\mathbb{Z}_2$-index and thus the Lovász bound. It also provided a more manageable object for future analyses.

Looking forward, the research outlined in this thesis paves the way for several intriguing opportunities for future investigation. Our work in constructing the box complex of the partition graph $\mathcal{P}(3^3)$ and significantly reducing its dimensionality represents a substantial advancement in this area of study. Nonetheless, the complex's topological and combinatorial properties remain a fertile ground for further exploration. One promising avenue for future research lies in the attempt to decrease the dimension of the complex even further. By developing innovative strategies and refining the techniques employed in this study, it may be possible to create a lower-dimensionality representation of the box complex.

While our findings confirm that certain regions of the box complex $\mathrm{B}_{\mathrm{edge}}(\mathcal{P}(3^3))$ lack a $\mathbb{Z}_2$-invariant S^4 with non-trivial homology, future research may yet uncover such an S^4 within this box complex. Application of the Borsuk-Ulam theorem to such a discovery would establish that $\chi(\mathcal{P}(3^3)) = 6$ - a result previously affirmed through exhaustive search, but which stands to be further substantiated through our proposed approach.

Furthermore, our study on the chromatic number of the partition graph $\mathcal{P}(3^3)$ could be expanded to consider different types of partition graphs. The analysis of their chromatic numbers and the application of topological methods could yield new insights into the interplay between graph theory and topology.

Lastly, our algorithm to construct the box complex of $\mathcal{P}(3^3)$ could be generalized to handle a wider class of graphs. Its performance in terms of time complexity could be further optimized, and its implementation could be extended and refined.

In summary, this thesis constitutes a step forward in our understanding of the structure of the box complexes of the partition graph $\mathcal{P}(3^3)$, the lower bounds of the chromatic number of this graph, and the role of topological methods in graph theory. The journey is far from over, however, and we look forward to the advancements that future research will bring.

Appendix A

Equivalencies of Vertex Triples

In Table 3.13, the classification of vertex triples into distinct equivalence classes based on their types was summarised. Detailed proofs concerning the equivalence classes of triples of type 5,5,5 were subsequently presented. The focus of this appendix will be the detailed proof for the equivalence classes of the remaining triples types, which might be of interest to some readers.

Lemma A.0.1. All triples of type 5,6,6 are equivalent.

Proof:

In the light of Theorem 3.1.4, which shows that all vertex pairs of type 5 are equivalent, consider a pair of vertices v and w of type 5.

123	123
456	489
789	567
v	w

123		
	4	56
	89	7

Table A.1: The vertices v and w and their grid pattern of type 5

The task is to identify all the possible third vertices u that are in a type-6 relationship with v and w, leading to non-equivalent v, w, u triples. The grid pattern for the third vertex u must comply with the type-6 grid pattern in relation to v and w:

a_1a_2	a_3	
a_4		a_5a_6
	a_7a_8	a_9

Table A.2: The grid pattern of u with v and u with w.

where $a_1, \ldots, a_9 \in \{1, 2, \ldots, 9\}$.

From the grid pattern of v and w in A.1, we observe that they share the cell $\{1, 2, 3\}$, and the pairs $\{5, 6\}$ and $\{8, 9\}$. From the grid pattern of u with v and u with w in Table A.2, it is apparent that each cell of vertex u must share a pair with a cell of v and a cell of w. These shared pairs can either be a common pair of v and w or a non-shared pair of v and w.

Assume a cell in u contains a common pair of v and w and an element from a different common pair. For example, the cell $\{8, 9, 5\}$, where $\{8, 9\}$ is a common pair and 5 is from another common pair.

This arrangement requires 6 and 7 to be in a different cell of u because of the cell $\{5, 6, 7\}$ in w. This could lead to a cell $\{6, 7, 4\}$ in u, contradicting $\mathrm{T}(v, u) = 6$ as $\{1, 2, 3\}$ would become a common cell of v and u.

Adding an element from $\{1, 2, 3\}$ to $\{6, 7\}$ in u results in a cell sharing no pairs with any cell in v. Thus, u cannot feasibly contain a common pair and another element from a different common pair.

Next, we will explore potential arrangements of u by investigating possible placements of the common pairs of v and w within u.

Assume that u contains two common pairs of v and w, denoted as $5, 6$ and $8, 9$. By this assumption, elements 7 and 4 cannot coexist within the same cell as these pairs, as this would generate a common cell among u, v, and w. Therefore, they must be collocated with an element from the set $\{1, 2, 3\}$ in a cell like $\{1, 4, 7\}$. However, this cell does not comply with the requirements, as it does not share two elements with any cell from v and w. Consequently, u cannot feasibly contain both common pairs of v and w, contradicting our initial assumption.

- Suppose u does not share any common pairs of v and w with these vertices. Then the pairs can be placed in the cells of u in two ways.
  - Consider a situation where u shares two pairs, $\{5, 6\}$ and $\{8, 9\}$, with vertices v and w. These pairs could potentially be arranged within u such that no two elements from the same pair coexist within a single cell:

    $$u = \{\{\ldots\}, \{8, 6, .\}, \{5, 9, .\}\}.$$

    If no elements from the cell $1, 2, 3$ are placed in conjunction with the pair elements, u is defined as:

    $$u = \{\{1, 2, 3\}, \{8, 6, 4\}, \{5, 9, 7\}\}$$

    This configuration is problematic as the cell $\{1, 2, 3\}$ becomes common among u, v, and w, invalidating u. Alternatively, if an element from $\{1, 2, 3\}$ is placed alongside one of the pairs, for example:

    $$u = \{\{4, 2, 3\}, \{8, 6, 1\}, \{5, 9, 7\}\}$$

the resulting cell $\{8, 6, 1\}$ does not share any pair with any cell of v or w, invalidating u once more.

– We can also consider a situation where u does not share any common pairs of v and w and the common pairs of v and w are distributed across three distinct cells of u:

$$\{\{8, ., .\}, \{9, 5, .\}, \{6, ., .\}\}.$$

If an element from $\{1, 2, 3\}$, for instance 1, is placed next to 9 and 5, then the resulting cell $\{9, 5, 1\}$ does not share a pair with v or w. Alternatively, if one of either 4 or 7, say 7, is placed next to $\{9, 5\}$, and two elements from $\{1, 2, 3\}$, for example 1 and 2, are placed next to 8, then u is:

$$u = \{\{1, 2, 8\}, \{9, 5, 7\}, \{6, 3, 4\}\}.$$

In this case, the cell $6, 3, 4$ does not share a pair with w, invalidating u.

- Now suppose u shares a single common pair with v and w, and each element of the other pair is placed in a different cell, not cohabiting with the shared pair, such as:

$$u = \{\{8, ., .\}, \{5, 6, .\}, \{9, ., .\}\}.$$

The element to be placed alongside 5 and 6 cannot be either 4 or 7, as this would create a common cell with either v or w. It must, therefore, be an element from $1, 2, 3$, say 3. If the elements 4 and 7 are placed in different cells alongside 8 and 9, and two elements from $1, 2, 3$, for instance 1 and 2, are in two different cells, then:

$$u = \{\{8, 4, 1\}, \{5, 6, 3\}, \{9, 7, 2\}.\}$$

In this scenario, the cells $8, 4, 1$ and $9, 7, 2$ do not share a pair with v and w respectively, invalidating u. Consequently, the only feasible configuration for u is when 1 and 2 are in the same cell, and 4 and 7 are in the same cell:

$$u = \{\{8, 1, 2\}, \{5, 6, 3\}, \{9, 4, 7\}\}.$$

The cube pattern of this triple of type 5,6,6 is

12		
	8	

3		
		56

	4	
	9	7

Table A.3: The cube pattern of the triple v, w, u of type 5,6,6

where the union of the i-th rows is a cell of v, the union of the i-th columns is a cell of w, and the union of all the units of the i-th grid is a cell of u with $i = 1, 2, 3$.

The permutation that maps the corresponding units of two sets of triples of type 5,6,6 maps the vertices of the triple to each other. Hence, all the triples of type 5,6,6 are equivalent. ∎

Lemma A.0.2. All the triples of type 5,5,6 are equivalent.

Proof:

Consider the vertices of type 6 with their cube pattern as follows:

123	124
456	389
789	567
v	w

12	3	
4		56
	89	7

The grid pattern of v and w of type 6

Table A.4: An example of a type 6 vertex pair

In constructing the third vertex u such that $\mathrm{T}(v,u) = 5$ and $\mathrm{T}(w,u) = 5$, it is necessary to determine a common cell between v and u as well as a common cell between w and u. In the case of v, every cell has an empty intersection with precisely one cell of w. The common cell between v and u can be selected from any cell of v. After determining this cell, denoted v_α, the common cell between v and w will be the one that does not intersect with v_α. Subsequently, the remaining cell of u comprises the elements of $\{1, 2, \ldots, 9\}$ that have not been included in the first two cells of u. One possible configuration of u is when $v_\alpha = \{1, 2, 3\}$:

$$u = \{\{1, 2, 3\}, \{5, 6, 7\}, \{4, 8, 9\}\}.$$

The selection of a different cell from v does not alter the results of our analysis. This is due to the consistent nature of the relationship between all cells of v and w. Irrespective of which cell is selected from v, the interactions with the cells of w follow the same patterns and principles, thus leading to consistent outcomes in the formation of vertex u.

The resulting cube of this triple follows a specific pattern. For each cell of v, the cell consists of a union of elements from all units in the i-th row of all grids. For each cell of w, it is a union of all elements from the units in the i-th column of the following grids. Each cell of u is the union of all the elements of the units in each respective grid:

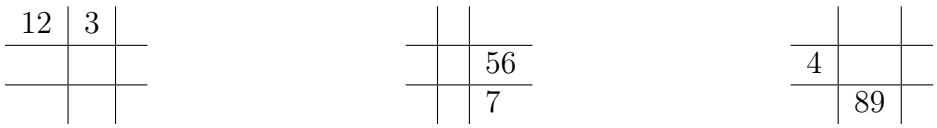

Table A.5: The cube pattern of the triple v, w, u of type 5,5,6

Permutations that map corresponding units of the cube pattern between two triples of type 5,5,6 also facilitate mapping one triple to another. ∎

Lemma A.0.3. All triples of type 6,6,6 are classified into two equivalence classes.

Proof:

Consider the same pair v and w of type 6 as in Table A.4 in the previous proposition.

Given vertices v and w sharing triple pairs $\{1,2\}$, $\{5,6\}$, and $\{8,9\}$, we investigate possible configurations of a third vertex that upholds type-6 relationships with both v and w. Each cell of the new vertex interacts with cells of v and w, sharing two elements with one cell and one element with another. These interactions can occur in two primary ways:

- The intersection in question could comprise one of the common pairs of vertices v and w. Assume, without loss of generality, that $\{1,2\}$ forms the intersection between a cell of the new vertex u_1, $\{1,2,3\}$ of v, and $\{1,2,4\}$ of w. As such, elements 3 and 4 cannot be in a cell with the pair $\{1,2\}$ in u_1, resulting in two feasible scenarios:
  - The elements 3 and 4 are together in a cell of u_1:

    $$u_1 = \{\{1,2,.\},\{3,4,.\},\{.,.,.\}\}.$$

    Given that the cell $\{3,4,.\}$ in u_1 must share two elements with a cell of v, and elements 1 and 2 from cell $\{1,2,3\}$ of v have already been allocated to another cell in u_1, these elements cannot be employed to complete this cell. The only other option is to use the cell $\{4,5,6\}$ of v. We can complete the cell $\{3,4,.\}$ as either $\{3,4,5\}$ or $\{3,4,6\}$. However, neither of them shares a common pair with any cell of w, which contravenes the condition that $\mathrm{T}(w,u_1) = 6$. Therefore, elements 3 and 4 cannot share a cell in u_1.
  - The second scenario materializes when elements 3 and 4 are incorporated into distinct cells of u_1:

    $$u_1 = \{\{1,2,.\},\{3,.,.\},\{4,.,.\}\}.$$

Since $\{1,2,3\}$ constitutes a cell of v and elements 1 and 2 are included in other cells of u_1, they cannot complete the cell $\{3,.,.\}$ of u_1. Therefore, this cell mandates the inclusion of two elements from a cell of v. The pair $\{8,9\}$ is not viable, as this would yield $\{3,8,9\}$, a cell of w, creating a common cell between w and u_1. This conflicts with the type 6 constraint. Equally, neither the pair $\{7,8\}$ nor $\{7,9\}$ are permissible, as if $\{3,7,8\}$ or $\{3,7,9\}$ were to be a cell of u_1, then $\{4,5,6\}$, an existing cell of v, would emerge as the remaining cell of u_1, resulting in a common cell between v and u_1. This would contradict the type 6 constraint for vertices v and u_1. The only valid option is to form $\{3,5,6\}$:

$$u_1 = \{\{1,2,.\},\{3,5,6\},\{4,.,.\}\}.$$

At this stage, the pairs $\{7,8\}$, $\{7,9\}$, and $\{8,9\}$ are the candidates from v to be co-located with 4. However, only the pair $\{8,9\}$ resides within the same cell of w, and the objective is for cell $\{4,.,.\}$ to share a common pair with cells from both v and w. Consequently:

$$u_1 = \{\{1,2,7\},\{3,5,6\},\{4,8,9\}\}.$$

In observing the cube pattern for the triple v, w, u_1, it becomes apparent that all the common pairs of v and w exist across all vertices of this triple. In the ensuing cube pattern, the union of the i-th rows composes a cell of v, the union of the i-th columns constitutes a cell of w, and the union of all the units of the i-th grid forms a cell of u_1, with this holding true for $i = 1, 2, 3$:

12		
		7

	3	
		56

4		
	89	

Table A.6: The cube pattern of the triple v, w, u_1 of the first kind of type 6,6,6

- Now assume the new vertex shares a pair of elements with v that is not a common pair of v and w, without loss of generality, consider $\{1,3\}$. Then element 2 from cell $\{1,2,3\}$ of v would then be placed in another cell of u_2, yielding:

  $$u_2 = \{\{1,3,.\},\{2,.,.\},\{.,.,.\}\}.$$

  Inserting 5, 6, or 7 in the same cell as $\{1,3\}$ results in the absence of a shared pair with any cells of w. However, cells $\{1,3,8\}$, $\{1,3,9\}$, and $\{1,3,4\}$ remain viable.

– Should $\{1,3,4\}$ be a cell of u_2, element 2 must take a place next to a common pair of v and w so its cell would share a pair with a cell of v and a cell of w. It cannot occupy the same cell as either $\{5,6\}$ or $\{8,9\}$. This condition would necessitate $\{7,8,9\}$ or $\{5,6,7\}$ to be a u_2 cell, contravening the $\mathrm{T}(v,u_2)=6$ and $\mathrm{T}(w,u_2)=6$ conditions, respectively. As no pair can satisfactorily complete $\{2,.,.\}$ of u_2, this scenario is infeasible.

– Considering pair $\{8,9\}$ is shared between v and w, the cases where $\{1,3,8\}$ or $\{1,3,9\}$ form a u_2 cell are functionally identical. Without loss of generality, we assume

$$u_2 = \{\{1,3,8\},\{2,.,.\},\{.,.,.\}\}.$$

Here, the $\{7,9\}$ pair from v cell $\{7,8,9\}$ cannot accompany element 2 in u_2 as it would force $\{4,5,6\}$ into being a shared cell between v and u_2, a contradiction. Additionally, placing the pair $\{5,6\}$ in the same cell as element 2 results in a final u_2 cell of $4,7,9$, which does not share a pair with any w cell, another contradiction. The valid pairs shared between u_2 and v, that could accompany element 2, are $\{4,5\}$ and $\{4,6\}$. Since $\{5,6\}$ is a shared pair of v and w, the two possible cases are equivalent. One feasible configuration would be:

$$u_2 = \{\{1,3,8\},\{2,4,5\},\{6,7,9\}\}.$$

Within the cube pattern of the triple v,w,u_2, it is notable that none of the common pairs shared by v and w are duplicated among this triple's vertices. In the following cube pattern which presents the triple v,w,u_2, the union of the i-th rows corresponds to a v cell, the union of the i-th columns matches a w cell, and the union of all units within the i-th grid equates to a u_2 cell.

1	3	
	8	

2		
4		5

		6
	9	7

Table A.7: The cube pattern of the triple v,w,u_2 of the second kind of type 6,6,6

For two triples of the same kind within the type 6,6,6 category, we can modify the cube pattern so that it adheres to the pattern as shown in Table A.7 or A.6. Consequently, the permutation which aligns the corresponding units within their cubes facilitates a mapping from one triple to another.

from Table 4.4 we see the triples of the first kind of type 6,6,6 share 4 neighbours and the triples of the second kind of type 6,6,6 share 1 neighbour. Therefore, the triples from these two classes are not equivalent. ∎

Lemma A.0.4. All the triples of type 5,5,7 are equivalent.

Proof:

Consider a pair of type 7 with their grid pattern as the following:3.7:

123	124
456	357
789	689
v	w

12	3	
4	5	6
	7	89

The grid pattern of v and w of type 7

Table A.8: An example of a type-7 vertex pair

To construct a new vertex u satisfying $\mathrm{T}(v,u)=5$ and $\mathrm{T}(w,u)=5$, it is necessary to identify a common cell between v and u, as well as a common cell between w and u. If either $\{4,5,6\}$ from v or $\{3,5,7\}$ from w were to serve as the common cell, each would share one element with every cell of w or v respectively. This would counter the precondition that $\mathrm{T}(w,u)=5$ and $\mathrm{T}(v,u)=5$. Consequently, neither of these cells can be selected as the mutual cell.

The cells $\{1,2,3\}$ and $\{7,8,9\}$ in v, along with the cells $\{1,2,4\}$ and $\{6,8,9\}$ in w, are each distributed across two cells within w and v, respectively. Any of these could potentially serve as the common cell between their respective vertices and u. However, not all combinations will prove valid.

Given that the cell $\{1,2,3\}$ has empty intersection with the cell $\{6,8,9\}$ of w, they can be chosen as the common cells for u with v and w, respectively. Similarly, the cells $\{7,8,9\}$ of v and the cell $\{1,2,4\}$ of w can be selected as common cells, as they also have empty intersection. Without loss of generality, let $\{1,2,3\}$ and $\{6,8,9\}$ be two cells of u.

This leads to the remaining elements of $\{1,2,\ldots,9\}$ forming the final cell of u, which is represented as follows:

$$u=\{\{1,2,3\},\{4,5,7\},\{6,8,9\}\}.$$

The cube pattern of v,w,u is the following, where each cell of v is the union of the elements of units of the i-th rows of all grids, each cell of w is the union of all the elements of the units of the i-th columns of all grids, and each cell of u is the union of the elements of the units of the i-th grid with $i=1,2,3$:

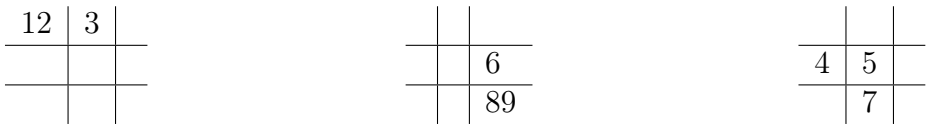

Table A.9: The cube pattern of the triple v, w, u of type 5,5,7

The cube pattern of any triple of type 5,5,7 can be re-arranged so it follows the pattern of this table. Then the permutation that maps the corresponding units to each other, maps the vertices of one triple to the other triple's vertices. ∎

Lemma A.0.5. The vertex triples of type 6,6,7 are classified into two equivalence classes.

Proof:

For a given pair of vertices v and w of type 7 as denoted in Table A.8, a new vertex u is constructed such that it satisfies $\mathrm{T}(v, u) = 6$ and $\mathrm{T}(w, u) = 6$. In this context, each cell of u should share a pair of elements with a cell from both v and w. The shared pairs of v and w can be arranged within the cells of u in three distinct manners:

- In the first scenario, where the mutual pairs $\{1, 2\}$ and $\{8, 9\}$ of v and w exist as separate pairs within two distinct cells of u, as expressed in:

  $$u = \{\{1, 2, .\}, \{8, 9, .\}, \{., ., .\}\}$$

  the only viable element that can be appended to both pairs is 5, as any other element would result in a shared cell between u and v or w, contradicting the conditions $\mathrm{T}(v, u) = 6$ and $\mathrm{T}(w, u) = 6$. Thus, this case is invalid.

- For the second scenario, let u_1 denote the new vertex. In this case, one of v and w's common pairs occupies a single cell, while the other pair is distributed across two cells with one element paired with the other pair as shown:

  $$u_1 = \{\{1, 2, 9\}, \{8, ., .\}, \{., ., .\}\}.$$

  Given that cell $\{7, 8, 9\}$ of v must share a pair with a cell in u_1 and element 9 already exists within a cell of u_1, it must share a pair with cell $\{8, ., .\}$ of u_1. This cell has three possible formations that satisfy this condition, namely, $\{8, 7, 4\}$, $\{8, 7, 5\}$, and $\{8, 7, 6\}$. The first option $\{8, 7, 4\}$ is invalid as it intersects non-trivially with three cells from w. The second option $\{8, 7, 5\}$ is also invalid as it necessitates the final cell of u_1 to be $\{3, 4, 6\}$, which again results in non-trivial

intersection with three cells of w. The only remaining valid configuration is $\{8, 7, 6\}$, hence we define the vertex u_1 as follows:

$$u_1 = \{\{1, 2, 9\}, \{8, 7, 6\}, \{3, 4, 5\}\}.$$

The cube pattern of the triple v, w, u_1 is:

12		
		9

		6
7	8	

	3	
4	5	

Table A.10: The cube pattern of the triple v, w, u_1 of type 6,6,7

- In the final case, one of the two common pairs of v and w is included in a cell of the new vertex u_2, while the other pair's elements are distributed in two different cells that are not shared with the other pair. We represent u_2 as follows:

  $$u_2 = \{\{1, 2, .\}, \{8, ., .\}, \{9, ., .\}\}.$$

  Under these conditions, elements 6 and 7 cannot reside in the same cell. Suppose they were combined in a cell with 8; this would preclude all possible element choices to be placed next to 9. Therefore, u_2 takes the form:

  $$u_2 = \{\{1, 2, .\}, \{8, 7, .\}, \{9, 6, .\}\}$$

  and the only option for the rest of the elements is

  $$u_2 = \{\{1, 2, 5\}, \{8, 7, 3\}, \{9, 6, 4\}\}.$$

  The following is the cube pattern is the triple v, w, u_2:

12		
	5	

	3	
7	8	

4		6
		9

Table A.11: The cube pattern of the triple v, w, u_2 of type 6,6,7

Since the way the common pairs of v and w are arranged in the cells of u_1 and u_2, these two triples are not equivalent. Therefore, all the triples of type 6,6,7 are classified into two classes each following the cube pattern of one of the patterns introduced here. ∎

Lemma A.0.6. The vertices of type 5,6,7 are of two equivalence classes.

Proof:

Given the vertices v and w of type 5 (referenced in Table A.1), we aim to construct a new vertex u satisfying $\mathrm{T}(v,u) = 7$ and $\mathrm{T}(w,u) = 6$. This requires u to share three element pairs with w and two element pairs with v. Further, there must exist a cell in u sharing one element with each cell of v.

Denote this cell as c_1. Considering the cube pattern of v and w, c_1 must share an element pair with a cell of w. The construction of c_1 necessitates an element from $\{1,2,3\}$ and an isolated element from column i combined with an element from the corresponding element pair in the same column for $i = 2,3$. Therefore, we can arbitrarily assign $c_1 = \{1,4,8\}$ without loss of generality.

Given that element 1 is part of cell c_1 in u, elements 2 and 3 must be assigned to another cell in u. Denote this cell as c_2. We cannot include 9 in c_2, as this would result in $\{5,6,7\}$ becoming a shared cell of u and w, which is contradictory to our original conditions. The remaining choices for the third element of c_2 are 5, 6, or 7. However, as $\{5,6\}$ forms a common pair of v and w, the choice of 5 or 6 would not materially alter the configuration of u up to equivalence. Consequently, u could be any of the following:

$$u_1 = \{\{1,4,8\},\{2,3,5\},\{6,7,9\}\}$$
$$u_2 = \{1,4,8\},\{2,3,9\},\{5,6,7\}.$$

So, the vertices of two equivalence classes are of the following cube patterns:

1		
	4	
	8	

23		
		5

		6
9		7

Table A.12: The cube pattern of the triple v, w, u_1 of type 5,6,7

1		
	4	
	8	

23		
	9	

		56
		7

Table A.13: The cube pattern of the triple v, w, u_2 of type 5,6,7

Given that the common pairs of vertices v and w are positioned differently within the cells of u_1 and u_2, it follows that u_1 and u_2 are not equivalent. ∎

Lemma A.0.7. The vertex triples of type 6,7,7 are classified into six equivalence classes.

Proof:

Given the vertices v and w of type 6, as outlined in Table A.4, we aim to construct a new vertex, u, which exhibits a type 7 relationship with both v and w. The cells of u either intersect with all cells of v and w, or only intersect with two of their cells. Accordingly, these cells follow certain configurations, which are as follows:

- Let c_1 denote a cell in u that intersects non-trivially with all cells in both v and w. This cell cannot contain any common pairs of v and w, as this would negate its property of intersecting with all cells of v and w. By referencing the grid pattern of v and w, we can determine there are two non-equivalent possibilities for the configuration of c_1:

  - One feasible configuration for c_1 is to include one element from each common pair of v and w, for instance $\{1, 5, 8\}$. Consequently, the subsequent cell, c_2, must incorporate a pair from both v and w. Reviewing the grid pattern of v and w reveals that the only viable selections for c_2 are $\{2, 3, 4\}$ or $\{6, 7, 9\}$. The adoption of one of these pairs for c_2 necessitates the use of the remaining option for the final cell of u. Let u_1 denote the vertex u under these circumstances:

$$u_1 = \{\{1, 5, 8\}, \{2, 3, 4\}, \{6, 7, 9\}\}.$$

    The cube pattern of the triple v, w, u_1 is:

1		
		5
	8	

2	3	
4		

		6
	9	7

Table A.14: The cube pattern of the triple v, w, u_1 of type 6,7,7

  - If we now assume c_1 to comprise the three elements not included in the common pairs of v and w, then $c_1 = \{3, 4, 7\}$. The subsequent cell of u, denoted as c_2, must share a pair of elements with a cell of v and another pair with a cell of w. Given the grid pattern of v and w, it is clear that c_2 must include a common pair of v and w, in addition to a single element from another common pair, leading to $c_2 = \{1, 2, 5\}$. Let u_2 represent the vertex u in this case, which leads to:

$$u_2 = \{\{3, 4, 7\}, \{1, 2, 5\}, \{6, 8, 9\}\}.$$

The cube pattern of the triple v, w, u_2 is:

	3	
4		
		7

12		
		5

		6
	89	

Table A.15: The cube pattern of the triple v, w, u_2 of type 6,7,7

If we now assume that c_1 intersects non-trivially with three cells of v and only two cells of w, it requires three elements from the three rows of the cube pattern of v and w and from two columns, therefore no common pair of v and w can exist in c_1. There are three non-equivalent possibilities for c_1:

– When $c_1 = \{1, 4, 7\}$, it includes two elements that are not part of v and w's common pairs and one element that is. In this scenario, let c_2 be the cell of u that intersects non-trivially with three cells of w and only two cells of v. The only possible configuration for c_2 in this case would be $c_2 = \{2, 3, 5\}$. Let u_3 denote the vertex u under these conditions, yielding:

$$u_3 = \{\{1, 4, 7\}, \{2, 3, 5\}, \{6, 8, 9\}\}$$

and the cube pattern of v, w, u_3 as:

	3	
4		
		7

2	3	
		5

		6
	89	

Table A.16: The cube pattern of the triple v, w, u_3 of type 6,7,7

– If c_1 comprises two elements each from distinct common pairs of v and w, i.e., $c_1 = \{1, 5, 7\}$, then there exist three non-equivalent options for c_2 which subsequently yield the following vertex configurations:

$$u_4 = \{\{1, 5, 7\}, \{2, 3, 6\}, \{4, 8, 9\}\}$$
$$u_5 = \{\{1, 5, 7\}, \{4, 6, 9\}, \{2, 3, 8\}\}$$
$$u_6 = \{1, 5, 7\}, \{4, 3, 6\}, \{2, 8, 9\}$$

and their cube patterns are the followings:

1		
		5
		7

2	3	
		6

4		
	89	

Table A.17: The cube pattern of the triple v, w, u_4 of type 6,7,7

1		
		5
		7

4		6
	9	

2	3	
	8	

Table A.18: The cube pattern of the triple v, w, u_5 of type 6,7,7

1		
		5
		7

	3	
4		6

2		
	89	

Table A.19: The cube pattern of the triple v, w, u_6 of type 6,7,7

Given that the arrangement of the common pair elements of v and w across the cells of u_i, with $i \in \{1, 2, \ldots, 6\}$, are dissimilar, it can be inferred that the triples v, w, u_i are inequivalent. Subsequent observations made in Table 4.4, where it is noted that some of these triples share differing numbers of common neighbours, further reinforce the assertion of their non-equivalence. ∎

Lemma A.0.8. The vertex triples of type 7,7,7 are categorized into five equivalent classes.

Proof:

Let vertices v and w be of type 7, as outlined in Table A.8, and let u be the third vertex which holds a type 7 relation with both v and w. We will denote the first cell of u as c_1. The plausible arrangements for this cell are:

- In one case, c_1 shares an element with each cell of v. This cell cannot encompass a common pair of v and w because it would not maintain a non-empty intersection with each cell of v. Instead, it can include one element from each of the common pairs, namely $\{1, 2\}$ and $\{8, 9\}$; for instance, $c_1 = \{1, 8, .\}$. Let $s = \{3, 7, 4, 6\}$ designate a set where each element is part of a cell in either v or

w and coexists with a common pair of v and w, according to the grid pattern of v and w. Hence, each element in s can be considered equivalent in this context, whereas the element 5 is distinct. Thus, c_1 could incorporate an element from set s or the element 5, leading to the two non-equivalent configurations for c_1, namely $c_1 = \{1, 8, 4\}$ or $c_1 = \{1, 8, 5\}$ which are analyzed in the following:

- Let $c_1 = \{1, 8, 4\}$ and allow c_2 to represent the cell of u which shares a single element with each cell of w. Consequently, it must also share two elements with a cell of v. In this configuration, the elements of c_2 can take one of the two following arrangements:
  - Let c_2 include an element from each of the common pairs of v and w, in addition to an element from set s. As an example, and representative of other equivalent cases, we could have $c_2 = \{2, 9, 7\}$. Including the element 5 within c_2 is not a feasible option due to $\{2, 9, 5\}$ sharing an element with each cell of v. Under these conditions, we will denote this particular configuration of u as u_1. Therefore, this vertex is arranged as follows:
  $$u_1 = \{\{1, 8, 4\}, \{2, 9, 7\}, \{3, 5, 6\}\}.$$
  The cube pattern of the triple v, w, u_1 is:

1		
4		
		8

2		
	7	9

	3	
	5	6

Table A.20: The cube pattern of the triple v, w, u_1 of type 7,7,7

  - Let c_2 include one element from the common pairs and two elements from set s. Thus, we have $c_2 = \{2, 3, 6\}$ as a feasible configuration. If u_2 represents u under this circumstance, then we have:
  $$u_2 = \{\{1, 8, 4\}, \{2, 3, 6\}, \{5, 7, 9\}\}$$
  and the cube pattern of the triple v, w, u_2 is:

1		
4		
		8

2	3	
		6

	5	
	7	9

Table A.21: The cube pattern of the triple v, w, u_2 of type 7,7,7

∗ Alternatively, c_2 can take one element from s and the element 5, resulting in $c_2 = \{2, 5, 6\}$. If u_3 represents u under this arrangement, we derive the following vertex configurations:

$$u_3 = \{1, 8, 4\}, \{2, 5, 6\}, \{3, 7, 9\}\}$$

with the cube pattern of v, w, u_3 as follows:

1		
4		
		8

2		
	5	6

	3	
	7	9

Table A.22: The cube pattern of the triple v, w, u_3 of type 7,7,7

– For the case where $c_1 = \{1, 8, 5\}$, the cell c_1 intersects with each cell of both v and w. Therefore, cell c_2 must share two elements with one cell of v, two elements with one cell of w, one element with another cell of v, and one element with another cell of w. By utilizing the grid pattern of v and w, it is clear that the only feasible construction for c_2 is to select one element from a common pair and two elements from the set s from two rows and two columns. For instance, let $c_2 = \{9, 4, 6\}$. We will represent u in this case as u_4. The vertex then becomes:

$$u_4 = \{\{1, 8, 5\}, \{4, 6, 9\}, \{2, 3, 7\}\}.$$

The corresponding cube pattern for v, w, u_4 is as follows:

1		
	5	
		8

4		6
		9

2	3	
	7	

Table A.23: The cube pattern of the triple v, w, u_4 of type 7,7,7

- When none of the elements in c_1 are sourced from the common pairs of v and w, two of its elements must necessarily be 3 and 7. Given that $\{3, 5, 7\}$ constitutes a cell of w, 5 cannot be the third element of c_1. As such, the third element of c_1 must be an element from the set s. As an example, consider $c_1 = \{3, 7, 4\}$.

  Now, let c_2 share a single element with each cell of w. Given that $\{3, 5, 7\}$ is a cell of w and elements 3 and 7 are already included in cell c_1, element 5 must be included in c_2, alongside two other elements - each originating from a distinct cell of w. From the cell $\{1, 2, 3\}$ of w, c_1 can incorporate an element from the

common pair $\{1, 2\}$. Meanwhile, from the cell $\{6, 8, 9\}$, it can only incorporate 6. If it incorporates either 8 or 9, c_2 will end up sharing one element with each cell of v, but we already know in this instance that c_2 intersects with only two cells of v. Therefore, $c_2 = \{5, 1, 6\}$.

Represent the vertex u in this scenario as u_5. As such, the configuration is:

$$u_5 = \{\{3, 7, 4\}, \{5, 1, 6\}, \{2, 8, 9\}\}.$$

The corresponding cube pattern for the triple v, w, u_5 will be as follows: v, w, u_5:

	3	
4		5
	7	

1		
	5	6

2		
		89

Table A.24: The cube pattern of the triple v, w, u_5 of type 7,7,7

Thus, every vertex triple of type 7,7,7 is equivalent to one of the triples v, w, u_i where $i \in \{1, 2, 3, 4, 5\}$. These triples are not equivalent due to the varying placement of the common element pairs between vertices v and w within the cube patterns of the third vertex u. As shown in Table 4.4, the count of shared neighbors for some of these triples differs, further substantiating their non-equivalence. ∎

Lemma A.0.9. The vertex triples of type 5,7,7 are classified into five equivalence classes.

Proof:

Let v and w represent the vertices of type 5 as detailed in Table A.1. We aim to construct a third vertex, u, such that $\mathrm{T}(v, u) = \mathrm{T}(w, u) = 7$. Denote the first cell of u as c_1 and assume it shares a single element with each cell of v. The potential scenarios for this cell are:

- One component of c_1 is taken from the cell $\{1, 2, 3\}$. The remaining two elements of c_1 originate from two distinct common pairs of v and w. An equivalent possibility for c_1 is $\{1, 5, 8\}$, as it shares one element with each cell of v and w. Consequently, the remaining cells of u share two elements with a cell of v and one element with another cell of v, and the situation is analogous for w.

  Let $s = \{4, 7\}$. The elements of s are interchangeable, as they are the sole elements that sit alongside the common pairs of v and w in the cells of these vertices. The following scenarios are feasible for the cell c_2 of u:

– The cell c_2 includes two elements, each from a distinct common pair of v and w, and a single element from the set s. For instance, $c_2 = \{9, 6, 7\}$. If u is denoted as u_1 in this case, it can be represented as:

$$u_1 = \{\{1, 5, 8\}, \{9, 6, 7\}, \{2, 3, 4\}\}.$$

The corresponding cube pattern for v, w, u_1 is then:

1		
		5
	8	

		6
9	7	

23		
	4	

Table A.25: The cube pattern of the triple v, w, u_1 of type 5,7,7

– If the cell c_2 takes two elements from the cell $\{1, 2, 3\}$ and one element from the set s, it leads to an equivalent vertex to u_1.

– The cell c_2 takes two elements from the set $\{1, 2, 3\}$ and one element from a common pair of v and w. For instance, $c_2 = \{2, 3, 6\}$. If u_2 represents u in this case, it is expressed as:

$$u_2 = \{\{1, 5, 8\}, \{2, 3, 6\}, \{4, 7, 9\}\}.$$

The cube pattern of the triple v, w, u_2 is subsequently:

1		
		5
	8	

23		
		6

	4	
9	7	

Table A.26: The cube pattern of the triple v, w, u_2 of type 5,7,7

- The cell c_1 contains one element from the common pairs, one element from the set $\{1, 2, 3\}$, and one element from the set s. A potential combination for c_1 could be $\{1, 4, 8\}$. It intersects with each cell of v at exactly one point and shares two elements with a cell of w.

  For the cell c_2, it intersects with each cell of w at one point and shares two elements with a cell of v. Given that $\{4, 8, 9\}$ is a cell of w and the elements 4 and 8 are included in c_1, the cell u_2 must contain 9. Furthermore, it requires an element from $\{1, 2, 3\}$. Consequently, the last element of c_2 has to be 7, yielding $c_2 = \{9, 7, 2\}$.

  Denoting this representation of u as u_3, we can express it as:

$$u_3 = \{\{1, 4, 8\}, \{9, 7, 2\}, \{3, 5, 6\}\}.$$

The cube pattern for the vertex triple v, w, u_3 is subsequently:

1		
	4	
	8	

2		
	9	7

3		
		56

Table A.27: The cube pattern of the triple v, w, u_3 of type 5,7,7

- If c_1 takes on the elements 1, 4, and 7, it shares a single element with each cell of both v and w. As a result, the remaining cells of u each intersect with two elements of a cell from v, and a single element of another cell from v. The same pattern holds true with respect to w. For c_2, we identify two potential, non-equivalent arrangements:
  - In the scenario where c_2 draws one element from $\{1, 2, 3\}$ and two elements from a common pair of v and w, one possibility for this cell is $c_2 = \{2, 5, 6\}$. We will denote u as u_4 in this case. Under this configuration, u_4 would be:

    $$u_4 = \{\{1, 4, 7\}, \{2, 5, 6\}, \{3, 8, 9\}\}.$$

    Consequently, the cube pattern for v, w, u_4 appears as follows:

1		
	4	
		7

2		
		56

3		
	89	

Table A.28: The cube pattern of the triple v, w, u_4 of type 5,7,7

  - For another feasible configuration of c_2, two elements can be selected from $\{1, 2, 3\}$ along with a single element from a common pair of v and w. Consider the example $c_2 = \{2, 3, 9\}$. In this circumstance, represent u as u_5. Consequently, u_5 is structured as follows:

    $$u_5 = \{\{1, 4, 7\}, \{2, 3, 9\}, \{5, 6, 8\}\}.$$

    As a result, the cube pattern for the v, w, u_5 triple emerges as follows:

1		
	4	
		7

23		
	9	

		56
	8	

Table A.29: The cube pattern of the triple v, w, u_5 of type 5,7,7

Considering the distinct arrangement of elements pertaining to the common cell and common pairs of vertices v and w within the cells of u, it is clear that the triples v, w, u_i for $i \in \{1, 2, 3, 4, 5\}$ are not equivalent. As a result, vertex triples of type 5,7,7 are categorised into five distinct equivalence classes. As evidenced in Table 4.4, triples from certain different classes share varying quantities of common neighbours. ∎

Appendix B

Inclusion of Vertex Quadruples

The analysis that follows will produce the results depicted in the final column of Table 4.5. We fix the type of the triple, u, v, w, in each of the subsequent bullet points and investigate the possible scenarios for the fourth vertex, p. Consequently, we ascertain the maximal complete bipartite subgraph which results from applying the method outlined in Remark 4.1.1 to the quadruple.

- The triple u, v, w is of type 5,5,5:

  We recall Table 4.4 where we demonstrated that triples of type 5,5,5 can be classified into two classes, namely the first kind and the second kind. Also, we observed that triples of the first kind share 6 neighbours, while triples of the second kind have no common neighbours.

  Assuming that the triple u, v, w belongs to the second kind of 5,5,5, it follows that the vertices of the quadruple do not share any neighbours because the vertices of the triple do not have any common neighbours.

  Consider a triple of the first kind of type 5,5,5 as follows:

$$\begin{array}{ccc} 123 & 123 & 123 \\ 456 & 489 & 468 \\ 789 & 756 & 579 \\ v & w & u \end{array} \tag{B.1}$$

  From the same table, we observe that the maximal complete bipartite subgraph derived from this triple by the method outlined in Remark 4.1.1 is a $K_{4,6}$:

$$\Big(\mathrm{CN}\big(\mathrm{CN}(v,w,u)\big), \mathrm{CN}(v,w,u)\Big) = K_{4,6}. \tag{B.2}$$

  For this triple of type 5,5,5 we study the cases number 5 and 6 of Table 4.5:

3. The four triples of the quadruple v, w, u, p are of type 5,5,5. If one of them is of the second kind, then the quadruple does not share any neighbours. Suppose all of them are of the first kind. Since all the pairs of this quadruple are of type 5, by Lemma 4.1.9, the common cell of p with the rest of the vertices of the quadruple is $\{1, 2, 3\}$. Our objective is to identify a possible fourth vertex in a way that every triple of the quadruple is of the first kind of type 5,5,5. To accomplish this, each element from the pairs of common elements shared by the vertex pairs v, w and v, u and w, u should be allocated to distinct cells within vertex p. The common pairs of v, w are $\{5, 6\}$ and $\{8, 9\}$. Then,

$$p = \{\{1, 2, 3\}, \{5, 8, .\}, \{6, 9, .\} \quad \text{or} \tag{B.3}$$
$$p = \{\{1, 2, 3\}, \{5, 9, .\}, \{6, 8, .\}\}. \tag{B.4}$$

   Also, one of the common pairs of w, u and v, u is $\{5, 7\}$ and $\{7, 9\}$ respectively, which means 7 cannot be in the same cell with 5 and 9. It is not possible unless 5 and 9 are in the same cell. Thus, the vertex p in (B.3) is not a valid candidate. Using p in (B.4), we have:

$$p = \{\{1, 2, 3\}, \{5, 9, 4\}, \{6, 8, 7\}\}. \tag{B.5}$$

   In Figure 4.9, we have listed all the common neighbours of vertices v, w, and u. Upon examining the adjacency relations of these common neighbours with vertex p, it is evident that p shares an edge with each of these common neighbours. Therefore, $\{v, w, u, p\} \subseteq \mathrm{CN}(\mathrm{CN}(v, w, u))$. Similar to previous cases, the maximal complete bipartite subgraph derived from the quadruple v, w, u, p is equal to the $K_{4,6}$ in equation B.2:

$$\Big(\mathrm{CN}\big(\mathrm{CN}(v, w, u, p)\big), \mathrm{CN}(v, w, u, p)\Big) = K_{4,6}.$$

4. Since the triple p, w, u is of type 5,5,5, all the vertices of this triple share a cell which is $\{1, 2, 3\}$. However, if p has the cell $\{1, 2, 3\}$, it cannot be in type 7 with v. As a result, it can be concluded that a quadruple with the pair types as outlined in case number 6 does not exist.

- The triple v, w, u is of type 6,6,6:

  If any triple within the quadruple v, w, u, p falls into the equivalence class of type 6,6,6 that does not share any neighbours (refer to Table 4.4), the quadruple can either have one common neighbour or none. This scenario results in a $K_{1,36}$ or it may not form a complete bipartite subgraph.

Let the following triple v, w, u belong to the equivalence class of vertices of type 6,6,6 that share four neighbours.

$$\begin{array}{ccc} 123 & 124 & 127 \\ 456 & 389 & 356 \\ 789 & 567 & 489 \\ v & w & u \end{array} \tag{B.6}$$

As observed in Table 4.4, the maximal complete bipartite subgraph that can be constructed from this triple, using the method outlined in Remark 4.1.1, forms a $K_{6,4}$:

$$\Big(\mathrm{CN}\big(\mathrm{CN}(v,w,u)\big), \mathrm{CN}(v,w,u)\Big) = K_{6,4}$$

The common neighbours of this triple coincide with the common neighbours of the vertex pair v, w, as previously illustrated in Figure 4.4.

Now we study cases number 7 and 8 of Table 4.5:

5. Since p is in a type 5 relationship with v, w, and u, it necessitates a common cell with each. There are three possible cells to choose from in v as the common cell of v and p. It is known that each cell of v has an empty intersection with exactly one cell of w and one cell of u. Upon choosing one cell of v, these respective cells of w and u are designated as the common cells with p. Consequently, p could represent any of the following vertices, namely p, r, and t:

$$\begin{array}{ccc} 123 & 124 & 127 \\ 489 & 356 & 389 \\ 567 & 789 & 456 \\ p & r & t \end{array}$$

   It can be readily confirmed that the vertices p, r, and t are adjacent to all the common neighbours of v, w, and u depicted in Figure 4.4. As a result, we can ascertain that $\{v, w, u, p, r, t\} \subseteq \mathrm{CN}(\mathrm{CN}(v, w, u))$. Analogous to previous cases, we can conclude that the maximal complete bipartite subgraph derived from the quadruple v, w, u, p corresponds to a $K_{6,4}$:

$$\big(\,\mathrm{CN}(\mathrm{CN}(v,w,u,p)), \mathrm{CN}(v,w,u,p)\big) = K_{6,4}.$$

6. Each triple of the quadruple v, w, u, p is of type 6,6,6. We will assume all triples belong to the class of triples of type 6,6,6 that share four neighbours, as the alternative would result in the quadruple sharing only one common neighbour or none at all. Referring to the cube pattern in Table A.6, we observe that each triple's vertices share three pairs of elements from

$\{1, 2, \ldots, 9\}$. For the triple v, w, u in (B.6), the shared pairs are $\{1, 2\}$, $\{5, 6\}$, and $\{8, 9\}$. Therefore, p must also share these same pairs, indicating that p must have the form $p = \{\{1, 2, .\}, \{5, 6, .\}, \{8, 9, .\}\}$.

However, there is no valid placement for elements 3, 4, and 7 as they are in the same cell with a shared pair in each vertex of the triple v, w, u. Placing 3 in one of the empty spots in p would result in a shared cell with a vertex of the triple v, w, u. The same issue arises for elements 4 and 7.

Therefore, we conclude that there is no vertex that can be in a type 6 relationship with v, w, and u.

- The triple v, w, u is of type $5, 5, 7$:

  Consider the following vertex triple of this type:

$$\begin{array}{ccc} 123 & 124 & 123 \\ 456 & 357 & 689 \\ 789 & 689 & 457 \\ v & w & u \end{array} \tag{B.7}$$

  The common neighbours of these vertices can be identified in the same manner as was done for vertices v and w in the diagram provided in Figure 4.6. As per Table 4.4, the complete bipartite subgraph constructed from such a triple yields a $K_{4,4}$:

$$\Big(\mathrm{CN}\big(\mathrm{CN}(v, w, u)\big), \mathrm{CN}(v, w, u)\Big) = K_{4,4}. \tag{B.8}$$

  Now we examine case number 9 of Table 4.5:

  7. In this scenario, all triples are of type 5,5,7 relationship. Given that $\mathrm{T}(p, v) = \mathrm{T}(p, w) = 5$, vertex p must share one cell with v and one with w. However, the common cell with w cannot be $\{6, 8, 9\}$ and the common cell with v cannot be $\{1, 2, 3\}$, as these would conflict with $\mathrm{T}(p, u) = 7$. Also, the common cell of p and v cannot be $\{4, 5, 6\}$ as it contradicts $\mathrm{T}(p, w) = 5$, and the common cell of p and w cannot be $\{3, 5, 7\}$ as this contradicts with $\mathrm{T}(p, v) = 5$. Hence, the only viable option for p is the following configuration:

$$p = \{\{1, 2, 4\}, \{3, 5, 6\}, \{7, 8, 9\}.$$

     It can be easily verified that this vertex is adjacent to all the common neighbours of the triple v, w, u depicted in Figure 4.6. Consequently, $\{v, w, u, p\} \subseteq \mathrm{CN}(\mathrm{CN}(v, w, u))$. Similar to previous cases we deduce:

$$\Big(\mathrm{CN}\big(\mathrm{CN}(v, w, u, p)\big), \mathrm{CN}(v, w, u, p)\Big) = K_{4,4}.$$

Bibliography

[1] R. Mathon, A. Rosa, *A new Strongly Regular Graph*, Journal Of Combinatorial Theory, Series A 38, 84-86, 1985.

[2] L. Lovász, *Kneser's Conjecture, Chromatic Number, and Homotopy*, Journal of Combinatorial Theory, Series A, 25(3):319–324, 1978.

[3] J. Matoušek, G. M.Ziegler, *Topological Lower Bound for the Chromatic Number: A Hierarchy*, ArXiv, 2003.

[4] J. Matoušek, *Using the Borsuk–Ulam Theorem: Lectures on Topological Methods in Combinatorics and Geometry*, Springer, 2008.

[5] A. Hatcher, *Algebraic Topology*, Cambridge University Press, 2002.

[6] J. Milnor, *Morse Theory*, Princeton University Press, 1963.

[7] J. W. Walker, *From Graphs to Ortholattices and Equivariant Maps*, Journal of Combinatorial Theory, Series B 35, 171-192, 1983.

[8] R. Forman, *A User's Guide to Discrete Morse Theory*, Séminaire Lotharingien de Combinatoire 48, Article B48c, 2002.

[9] R. Forman, *Morse Theory for Cell Complexes*, Adv. Math. 134, pp. 90-145, 1998.

[10] R. Green, *Morse matchings on polytopes and their subcomplexes*, University of Colorado Boulder, 2011.

[11] V. Robins, P. J. Wood, A. P. Sheppard, *Theory and Algorithms for Constructing Discrete Morse Complexes from Grayscale Digital Images*. IEEE Transactions on Pattern Analysis and Machine Intelligence, 33(8), 1646-1658, 2011.

[12] K. Mischaikow, V. Nanda, *Morse Theory for Filtrations and Efficient Computation of Persistent Homology*, Discrete and Computational Geometry, 50(2), 330-353, 2013.

[13] H. Edelsbrunner, D. Letscher, A. Zomorodian, *Topological Persistence and Simplification*, Discrete and Computational Geometry, 28(4), 511-533, 2002.

[14] T. Lewiner, H. Lopes, A. W. Vieira, *Efficient Implementation of Marching Cubes' Cases with Topological Guarantees*, Journal of Graphics Tools, 8(2), 1-15, 2003.

[15] T. Lewiner, H. Lopes, G. Tavares, *Applications of Forman's discrete Morse theory to topology visualization and mesh compression*, IEEE Transactions on Visualization and Computer Graphics. 10 (5): 499–508, 2004.

[16] U. Bauer, C. Lange, M. Wardetzky, *Optimal Topological Simplification of Discrete Functions on Surfaces*, Discrete and Computational Geometry. 47 (2): 347–377, 2012.

[17] N. Deo, *Graph Theory with Applications to Engineering and Computer Science*, Prentice Hall, 1974.

[18] R. Fritsch, G. Fritsch, *The Four-Color Theorem: History, Topological Foundations, and Idea of Proof*, Springer, 1998.

[19] F. Leighton, *A Graph Coloring Algorithm for Large Scheduling Problems*, Journal of Research of the National Bureau of Standards, vol. 84, 1979.

[20] M.R. Garey, D.S. Johnson, *The complexity of near-optimal graph colouring*, Journal of the ACM (JACM), 23(1), 43-49, 1976.

[21] R. Beutler, *Frequency Assignment and Network Planning for Digital Terrestrial Broadcasting Systems*, Kluwer Academic Publishers, 2004.

[22] A. W. Appel, *Modern Compiler Implementation in Java, Second Edition*, Cambridge University Press, 2002.

[23] M. van Steen, *Graph Theory and Complex Networks: An Introduction*, M. van Steen (publisher), 2010.